

PALEOBATHYMETRIC EVOLUTION OF THE MIOCENE DEPOSITS OF  
GÖMBE AND AKSU BASINS, ANTALYA, TURKEY

A THESIS SUBMITTED TO  
THE GRADUATE SCHOOL OF NATURAL AND APPLIED SCIENCES  
OF  
MIDDLE EAST TECHNICAL UNIVERSITY

BY  
FATİH SEÇKİN ŞİŞ

IN PARTIAL FULFILLMENT FOR THE REQUIREMENTS  
FOR  
THE DEGREE OF MASTER OF SCIENCE  
IN  
GEOLOGICAL ENGINEERING

JANUARY 2018



Approval of the thesis:

**PALEOBATHYMETRIC EVOLUTION OF THE MIOCENE DEPOSITS OF  
GÖMBE AND AKSU BASINS, ANTALYA, TURKEY**

Submitted by **FATİH SEÇKİN ŞİŞ** in partial fulfillment of the requirements for the degree of **Master of Science in Geological Engineering Department, Middle East Technical University** by,

Prof. Dr. Gülbin Dural  
Dean, Graduate School of **Natural and Applied Sciences**

Prof. Dr. Erdin Bozkurt  
Head of Department, **Geological Engineering**

Prof. Dr. Nuretdin Kaymakcı  
Supervisor, **Geological Engineering Dept., METU**

**Examining Committee Members:**

Prof. Dr. Erdin Bozkurt  
Geological Engineering Dept., METU

Prof. Dr. Ercan Özcan  
Geological Engineering Dept., İTÜ

Prof. Dr. Nuretdin Kaymakcı  
Geological Engineering Dept., METU

Prof. Dr. M. Cihat Alçıçek  
Geological Engineering Dept., Pamukkale University

Yrd. Doç. Dr. Ulaş Avşar  
Geological Engineering Dept., METU

**Date:** 30.01.2018

**I hereby declare that all information in this document has been obtained and presented in accordance with academic rules and ethical conduct. I also declare that, as required by these rules and conduct, I have fully cited and referenced all material and results that are not original to this work.**

Name, Last Name: Fatih Sekin ŐİŐ

Signature:

## ABSTRACT

### PALEOBATHYMETRIC EVOLUTION OF THE MIOCENE DEPOSITS OF GÖMBE AND AKSU BASINS, ANTALYA, TURKEY

Fatih Seçkin ŞİŞ  
M.Sc., Department of Geological Engineering  
Supervisor: Prof. Dr. Nuretdin KAYMAKÇI

January 2018, 105 pages

The Late Cenozoic Antalya Basins, located at the eastern part of the Beydağları Platform, within the Isparta Angle, unconformably developed on Mesozoic autochthonous carbonate platforms in the western Taurides. Aksu Basin developed in the inner part of the Isparta Angle and bounded by Aksu Thrust at the east. Gömbe Basin located at the western limb of the Isparta Angle and developed as a foreland basin in front of the Lycian Nappes on the Beydağları Platform. During their evolution, these basins experienced important bathymetric changes possibly due to vertical motions and variation in the sediment supply. This study provides a detailed analysis of paleobathymetric evolution of these basins.

The conducted paleobathymetric study involves determination of the depositional depth of these basins by using foraminiferal fauna. It is based on the ratio of abundance of planktonic versus benthic foraminifera, which is related to the water depth. Percentage of planktonic foraminifera to total foraminifer population (%P) increases from shallow to deep water. However, some of the benthic foraminifera species are directly affected by the oxygen level of the bottom waters, rather than paleobathymetry, and are regarded as stress markers, hence they are discarded in the calculations of %P. In

addition, carbonate dissolution of the foraminifera has the potential for miscalculations, since planktonic foraminifera are more prone to dissolution than the benthic ones. Nevertheless, recognition and determination of benthic species would be adequate for overcoming this complication. At the end, the obtained quantitative results must be verified and validated qualitatively using specific benthic depth markers.

Depositional depth of the Aksu Basin were shallowing as a general trend, and rate of sedimentation exceeded the rate of subsidence in the middle part of the section. For most levels, calculated depths of Gömbe basins indicated depositional depths around thousand meters, contrary to the high sedimentation rates as indicated by turbiditic facies of the basin infills.

Keywords: Paleobathymetry, Benthic Foraminifera, Foreland, Gömbe Basin, Aksu Basin

## ÖZ

### GÖMBE VE AKSU HAVZALARINA AİT MİYOSEN ÇÖKELLERİNİN PALEOBATİMETRİK EVRİMİ, ANTALYA, TURKEY

Fatih Seçkin ŞİŞ  
Yüksek Lisans, Jeoloji Mühendisliği Bölümü  
Tez Yöneticisi: Prof. Dr. Nuretdin KAYMAKÇI

Ocak 2018, 105 sayfa

Geç Senozoik Antalya Havzası, Beydağları Platformunun doğusunda, Isparta Büklümü içerisindeki Batı Toroslar Mesozoik otokton karbonat platformunun üzerinde uyumsuz olarak gelişmiştir. Aksu Havzası Isparta Büklümü'nün iç kısmında gelişmiş olup doğuda Aksu Fayı ile sınırlanmıştır. Gömbe Havzası ise, Isparta Büklümü'nün batı kanadında yer alır ve Beydağları Platformu üstünde, Likya Napları'nın doğusunda bir önülke havzası olarak gelişmiştir. Bu havzalar evrimleri sırasında düşey hareketler ve çökelme miktarındaki değişime bağlı olarak önemli batimetrik değişiklikler gösterir. Bu çalışma, bu havzaların paleobatimetrik evriminin detaylı bir incelemesini kapsar.

Yapılan paleobatimetrik çalışma, foraminifer faunasını kullanarak bu havzaların çökelme derinliğinin belirlenmesini içerir. Uygulanan yöntem, su derinliği ile ilişkili olan bentik foraminifer miktarı ile planktonik foraminifer miktarının oranlanmasına dayanır. Planktonik foraminiferlerin toplam foraminifer popülasyonuna oranı (%P) sığdan derine doğru artar. Bununla birlikte, bazı bentik foraminiferler, oksijen seviyesinden doğrudan etkilenir ve stres belirteçleri olarak kabul edilirler ve bu nedenle popülasyon oranı hesaplamasına dahil edilmezler. Buna ek olarak, karbonat

kabuk çözünmesi planktonik foraminiferlerde bentik olanlara göre daha yaygındır. Bu durum yanlış hesaplamalara neden olabilir. Fakat yine de, bentik türlerin belirlenmesi ve tanınması bile bu komplikasyonun üstesinden gelmek için yeterlidir. Ayrıca, elde edilen niceliksel verileri, derinlik belirteçleri olan bentik foraminifer türleri kullanarak, nitel olarak doğrulamak mümkündür.

Aksu havzasının depolanma derinliğindeki genel eğilime bakıldığında sığlaştığı görülmektedir ve kesitin orta seviyelerinde sedimantasyon oranı çökme oranını geçmektedir. Gömbe havzasının türbiditik fasiyeslerinin işaret ettiği hızlı depolanmaya rağmen, birçok seviyede hesaplanan sonuçlar çökmenin bin metre kadar derinlikte gerçekleştiğini göstermektedir.

Anahtar Kelimeler: Paleobatimetri, Bentik Foraminifer, Önülke, Gömbe Havzası, Aksu Havzası

*To my mother*

## ACKNOWLEDGEMENT

I would like to thank my supervisor Prof. Dr. Nuretdin KAYMAKCI for his encouragements and support during my M. Sc. study. His immense knowledge guided me in all the time of research and it was a great experience to learn more about not only geology but also life. It is an honor to work with him.

I would like to express my sincere gratitude Dr. Tanja KOUWENHOVEN, for her advice and guidance in foraminifera identifications and paleobathymetric interpretations. Without her, this study could not be concluded easily.

I am grateful to Prof. Dr. Erdin BOZKURT, Prof. Dr. Ercan ÖZCAN, Prof. Dr. M. Cihat ALÇIÇEK and Assis. Prof. Dr. Ulaş AVŞAR for their constructive reviews that significantly improved this study.

I would like to thank Ayten KOÇ for her considerable time and efforts during fieldwork. I am grateful to Dr. Cor LANGEREIS and Nora HUGENHOLTZ for their hosting in the Utrecht. Also many thanks to Dr. Jan Willem ZACHARIASSE for his guidance in the Utrecht. Also, many thanks to Prof. Dr. Demir ALTINER and Prof. Dr. Sevinç ÖZKAN ALTINER for their motivation and knowledge.

I would like to thank Serkan YILMAZ for his hours of time in the SEM laboratory. Moreover, I would like to thank TÜBİTAK for giving financial support for this study (Grant Number 111Y239). I am grateful to my friends Levent TOSUN, Gamze TANIK, Serdar Görkem ATASOY, Zehra DEVECİ, Mustafa Yücel KAYA, Hakan TANYAŞ, Gökhan GÜLER and Mehtap ADIGÜZEL for their friendship and encouragements.

At last but definitely not the least, I would like to give my sincere thanks to my mother Selime Nursel KUŞ for her patience and endless support before and during this study. This thesis could only be narrated as a section of share a life; I would like to thank my darling Elif YAMAN. Thanks to the people who make my life meaningful. This thesis belongs to them as much as belongs to me.

## TABLE OF CONTENTS

ABSTRACT .....	v
ÖZ .....	vii
ACKNOWLEDGEMENT .....	x
TABLE OF CONTENTS .....	xi
LIST OF FIGURES .....	xiv
LIST OF TABLES .....	xvii
ABBREVIATIONS .....	xviii
CHAPTERS	
1. INTRODUCTION .....	1
1.1 Purpose and Scope .....	1
1.2 Study Area.....	4
1.3 Method of Study.....	5
1.4 Previous Studies .....	6
1.5 Regional Geology.....	10
2. STRATIGRAPHY .....	13
2.1 Basement Units .....	13
2.1.1 Beydağları Platform Carbonates .....	13
2.1.2 Lycian Nappes.....	14
2.1.3 Antalya Nappes .....	14
2.2 Gömbe Basin.....	15
2.2.1 Elmalı Formation .....	16

2.2.2 Uçarsu Formation .....	17
2.3 Aksu Basın .....	19
2.3.1 Aksu Formation.....	19
2.3.1.1 Kapıkaya Conglomerate.....	20
2.3.1.2 Karadağ Conglomerate.....	21
2.3.1.3 Kargı Conglomerate .....	21
2.3.2 Karpuzçay Formation.....	21
2.3.3 Gebiz Limestone .....	23
2.3.4 Post-Miocene Units .....	23
3. PALEOBATHYMETRY .....	25
3.1 History of P/B and Depth Relation .....	26
3.2 Sample Collection and Preparation .....	31
3.2.1 Sample Preparation .....	34
3.3 Suitability of Samples .....	36
3.4 Stress Markers .....	38
3.5 %P and Depth Results .....	40
3.6 Taxonomic check .....	40
4. DISCUSSION .....	47
5. CONCLUSIONS.....	51
REFERENCES.....	53
APPENDICES	
A. EDS ANALYSES RESULTS OF SEVERAL GRAINS .....	65
B. QUANTITATIVE DATA ANALYSES .....	71
C. TAXONOMIC NOTES.....	73
D. PLATES AND EXPLANATIONS .....	89

PLATE 1 .....	90
PLATE 2 .....	92
PLATE 3 .....	94
PLATE 4 .....	96
PLATE 5 .....	98
PLATE 6 .....	100
PLATE 7 .....	102
PLATE 8 .....	104

## LIST OF FIGURES

- Figure 1:** a) Outline tectonic scheme of Eastern Mediterranean region. b) Major tectonic units and Neogene sedimentary basins in the Isparta Angle (the sources of the figures are mentioned in the text)..... 3
- Figure 2:** Position of Neogene Gömbe and Aksu Basins within the Eocene to recent configurations of the central and the western Taurides (SW Anatolia) (simplified from 1/500.000 scale geological map of Turkey, MTA 2002) ..... 4
- Figure 3:** Generalized columnar section Lycian Foreland Basin, LN: Lycian Nappes; BP: Beydağları Platform (Modified from Collins and Robertson, 1998; Şenel, 2004) ..... 15
- Figure 4:** Geological map of the Gömbe Basin. Measured sections are indicated. A-A' (GB) includes the turbidites of of Uçarsu Formation and B-B' (GÖM) includes Elmalı Formation (Modified from Şenel, 2004) ..... 16
- Figure 5:** Measured section from Uçarsu formation in the Gömbe Basin..... 18
- Figure 6:** General view of turbidites of the Gömbe Basin, Section GB..... 18
- Figure 7:** Generalized columnar section of Aksu Basin, LN: Lycian Nappes; BP: Beydağları Platform; AN: Antalya Nappes (Modified from Çiner et al., 2008)..... 19
- Figure 8:** Geological map of the Aksu Basin. Measured section, coded as IS, is indicated as A-A'. (Modified from Deynoux, 2005 and Çiner et al. 2008).P: Pliocene, Q: Quaternary..... 20
- Figure 9:** Sandstone and mudstone alternation of Karpuzçay Formation with reverse faults in Aksu Basin ..... 21
- Figure 10:** Measured section from Karpuzçay Formation, Aksu Basin. .... 22
- Figure 11:** First (I) line is the regional model of the Van Marle et al. (1987) and second (II) line is the model of Wright (1977) (as cited in Van Marle et al., 1987)..... 27

<b>Figure 12:</b> Observed versus predicted depth plots (Van der Zwaan et al., 1990).....	29
<b>Figure 13:</b> %P versus depth graphic based on Equation (1) (Van der Zwaan et al., 1990). .....	31
<b>Figure 14:</b> Sample collection from (a) Turbidites from the Gömbe Basin, coded as GB, (b) from the Gömbe Basin, coded as GÖM, (c) from Aksu Basin, coded as IS. 32	
<b>Figure 15:</b> (a) Quartz grains (See EDS analyses APPENDIX A, Figure 25); (a) Black rock fragments (See EDS analyses in APPENDIX A, Figure 26) from GB section, GB-30; (b) Rock grains with calcite matrix (See EDS analyses APPENDIX A, Figure 24) form GÖM section, GÖM-12; (c) Rock grains with calcite matrix from Aksu (IS) section, IS-36 (See EDS analyses APPENDIX A, Figure 22; (d) Rock grains with calcite matrix from Aksu (IS) section, IS-56 (See EDS analyses Appendix B, Figure 23) .....	33
<b>Figure 16:</b> Steps 1-7 are the freeze thaw method (Kennedy and Coe, 2014) and step 8 was applied for analyses (Van Hinsbergen et al., 2005). .....	35
<b>Figure 17:</b> Overview of processes affecting the generation of the benthic foraminiferal assemblage (De Stigter et al., 1996).....	37
<b>Figure 18:</b> Living depth of the benthic foraminiferal in terms of food availability and oxygen concentration. (Jorissen et al., 1995; Van der Zwaan et al., 1999) .....	39
<b>Figure 19:</b> %P and depth graphics with the stratigraphic sections from GÖM section (see also Appendix B for calculated values) .....	41
<b>Figure 20:</b> %P and depth graphics with the stratigraphic sections from IS section (see also Appendix B for calculated values) .....	42
<b>Figure 21:</b> Depth range of the marker species (Modified from Van Hinsbergen et al.2005). (See also Chapter 4) .....	43
<b>Figure 22:</b> Depth ranges, indicated with blue color, according to depth markers from Gömbe Basin. ....	44
<b>Figure 23:</b> Depth ranges, indicated with blue color, according to depth markers from Aksu Basin. ....	45

**Figure 24:** Global eustatic sea level change in Miocene (Haq et al., 1988). Red line is short term, orange line is long term sea level change (Modified from Haq et al., 1988) Paleobathymetry curves of the Gömbe (purple line) and Aksu (green line) Basins. . 49

**Figure 25:** Rock grains with calcite matrix from AK-36, Figure 13 (c) ..... 66

**Figure 26:** Rock grains with calcite matrix from AK-56, Figure 13 (d) ..... 67

**Figure 27:** Rock grains with calcite matrix from GÖM-12, Figure 13 (b)..... 68

**Figure 28:** Black rock fragments from GB-30, Figure (a) ..... 69

**Figure 29:** Quartz grain from GB-30, Figure (a)..... 70

**Figure 30:** Principles types of chamber arrangement. a. single chambered; b. uniserial; c. biserial; d. triserial; e. palnispiral to biserial; f. milioline; g. planispiral evolute; h. planispiral involute; i. streptospiral; j-k-l. trochospiral (Spiral view; side view; umbilical view) (Modified from Loeblich and Tappan, 1964 as cited in Ucl.ac.uk, 2018)..... 74

**Figure 31:** Principles types of aperture. a. open end of tube; b. terminal radiate; c. terminal slit; d. umbilical; e. loop shaped; f. interiomarginal; g.interiomarginal multiple; h. areal crbrate; i. with phialine lip; j. with bifid tooth; k. with umbilical teeth; with umbilical bulla (Modified from Loeblich and Tappan, 1964 as cited in Ucl.ac.uk, 2018)..... 74

## LIST OF TABLES

<b>Table 1:</b> Geographic positions of the bottom and the top of the measured sections (UTM 35S).....	5
<b>Table 2:</b> Authors of studies and their claims about P/B and depth relations in a chronological order. ....	30
<b>Table 3:</b> Number of planktonic and benthic foraminifera in Gömbe section with %P and calculated depth based on Equation (1).....	71
<b>Table 4:</b> Number of planktonic and benthic foraminifera in Aksu section with %P and calculated depth based on Equation (1) .....	72

## ABBREVIATIONS

- D : Depth
- P : Planktonic foraminifera
- B : Benthic foraminifera
- S : Stress markers
- P/B : Ratio of planktonic foraminifers to benthic foraminifers
- %P : Percentage of planktonic foraminifers to total foraminifera population
- IN : Inner neritic
- MN : Middle neritic
- LN : Lower neritic
- UB : Upper bathyal
- MB : Middle bathyal
- LB : Lower bathyal
- ULM : Upper Light Microscope
- EDS : Energy Dispersive Spectroscopy
- SEM : Scanning Electron Microscopy

## CHAPTER 1

### INTRODUCTION

#### 1.1 Purpose and Scope

The Late Cenozoic Antalya Basins, located within the Isparta Angle, was formed on the Mesozoic autochthonous carbonate platform in the western Taurides. The Isparta Angle has a triangular geometry (Figure 1a), defined with morpho-tectonic structural units connected to the Aegean Arc in the southwest and to the Cyprus Arc in the southeast (Blumenthal, 1963). Terminal closure of the Neotethyan Ocean signifies the deformation history from Mesozoic to Early Cenozoic, which comprises thrusting of the Lycian Nappes and associated ophiolitic units over the Beydağları and Geyikdağı para-autochthonous units (Özgül 1976 and 1984, Poisson et al., 2003a; Van Hinsbergen et al. 2010).

Antalya Basins comprises three sub-basins, namely; Aksu, Köprüçay and Manavgat basins. They are located at the eastern part of the Beydağları Platform (Akay et al., 1985; Flecker et al., 1998 and 2005, Glover and Robertson, 1998; Poisson et al. 2003a and 2011; Üner et al., 2015), in the core of the Isparta Angle. These basins are associated with the evolution of the Central Taurides (Özgül, 1984) and developed in response to the development of Aksu and Kırıkkavak Faults (Koç et al., 2016).

The main emplacement and stacking of Taurides within the eastern limb of the Isparta Angle took place during the Late Cretaceous to Oligocene time interval (Özgül, 1984;

Poisson et al., 2003a). However, recent studies provided plausible evidence that in the inner part of the Isparta Angle, in Aksu, Köprüçay and Manavgat basins, thrusting continued until Pliocene (Çiner et al., 2008; Koç et al., 2016).

The Lycian Foreland basin, on the other hand, is located at the west of Beydağları Platform (Figure 1b), which constitutes the western limb of the Isparta Angle, and is related to emplacement of Lycian Nappes. The Lycian Nappes thrust from northwest to southeast over the Beydağları platform by the end of Middle Miocene and developed the Gömbe Foreland basin which is referred to as Lycian Basin in this study as proposed by Hayward (1984) and Flecker et al. (2005) (Figure 1 and 2).

The Lycian Foreland basin was previously treated as three geographically and lithostratigraphically distinct basins, namely Beydağları Miocene Basin, Darıören basin and Kasaba basin; however, the common tectonic control for these three basins was later combined in to Lycian Foreland basin (Flecker et al., 2005).

Miocene to Pliocene stratigraphy and kinematic evolution of the Antalya Basins and Lycian Foreland Basin within the Isparta Angle have been widely studied and relatively well known. However, there is no published study on the paleobathymetric evolution of these. In other words, there is no information about the change in the accommodation space and vertical block movements in the region. In this regard, the main purpose of this thesis work is to study the paleobathymetry of the Gömbe and Aksu Basins by using planktonic and benthic foraminiferal ratio within the infill of these basins. In this context, this study will shed some light on the development history of Aksu Basin and Gömbe sector of Lycian Basin (Figure 2) especially on how the accommodation space and water depth changed in these during their evolution.

The evolution of the these basins within the Isparta Angle is closely linked with the Africa - Eurasia convergence and collision of intervening continental blocks (Flecker et al., 2005; Çiner et al., 2008; Üner et al. 2015; Koç et al., 2016). In this regard, information obtained from these basins will provide constraints on the evolution of the eastern Mediterranean basins over the last ~15 My.

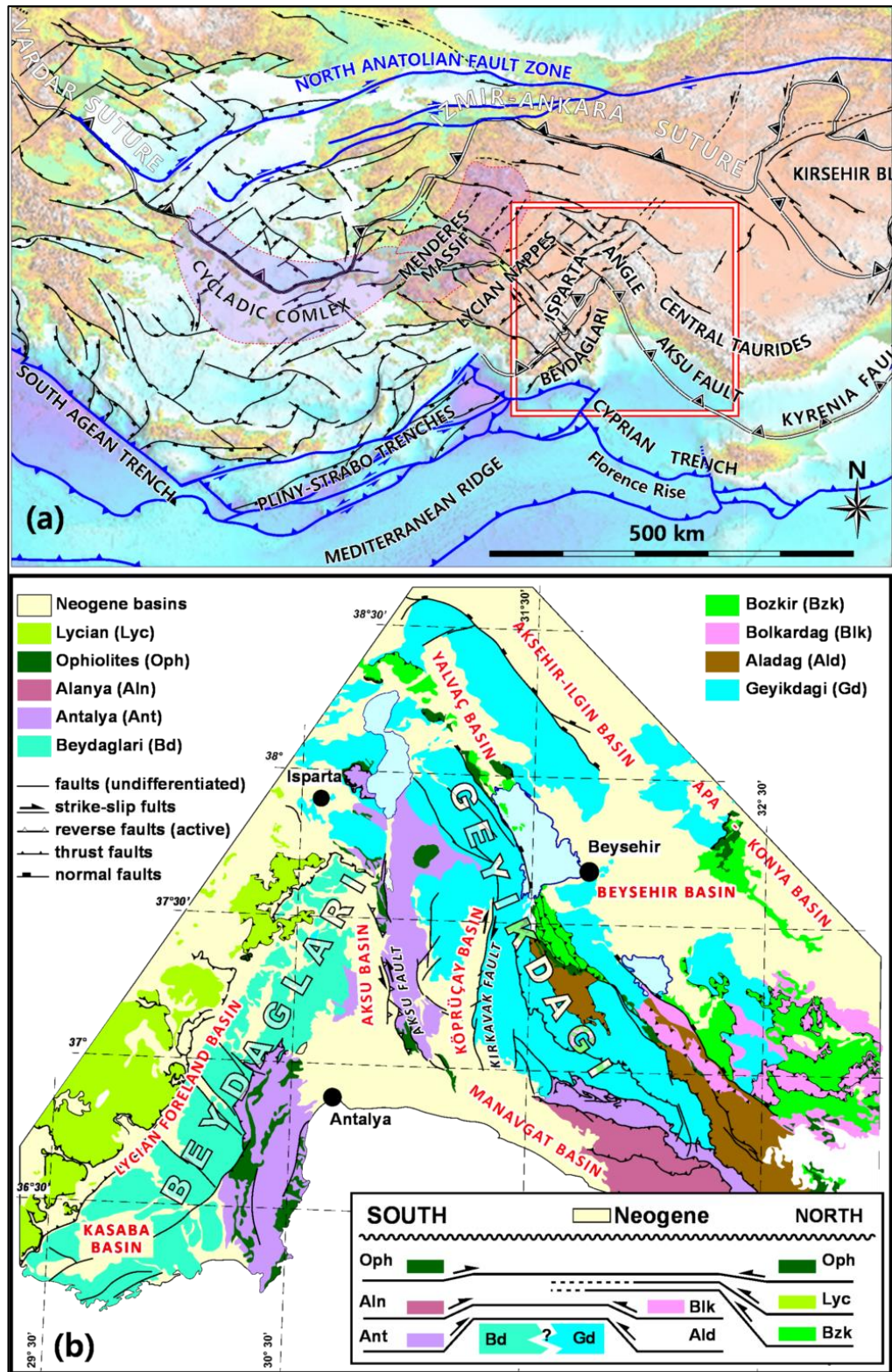


**Figure 1:** a) Outline tectonic scheme of Eastern Mediterranean region. b) Major tectonic units and Neogene sedimentary basins in the Isparta Angle (the sources of the figures are mentioned in the text).

## 1.2 Study Area

This study was conducted on two locations; on the Gömbe Basin and the Aksu Basin. Two sections are measured in the Gömbe Basin. One of the sections is located near Gömbe Village and coded as GB. It is located along the old road connecting Gömbe to Kalkan next to the Çayboğazı Dam. The second section is coded as GÖM, and located along the Akçay – Kalkan Road, south of the Çayboğazı Dam (Figure 2).

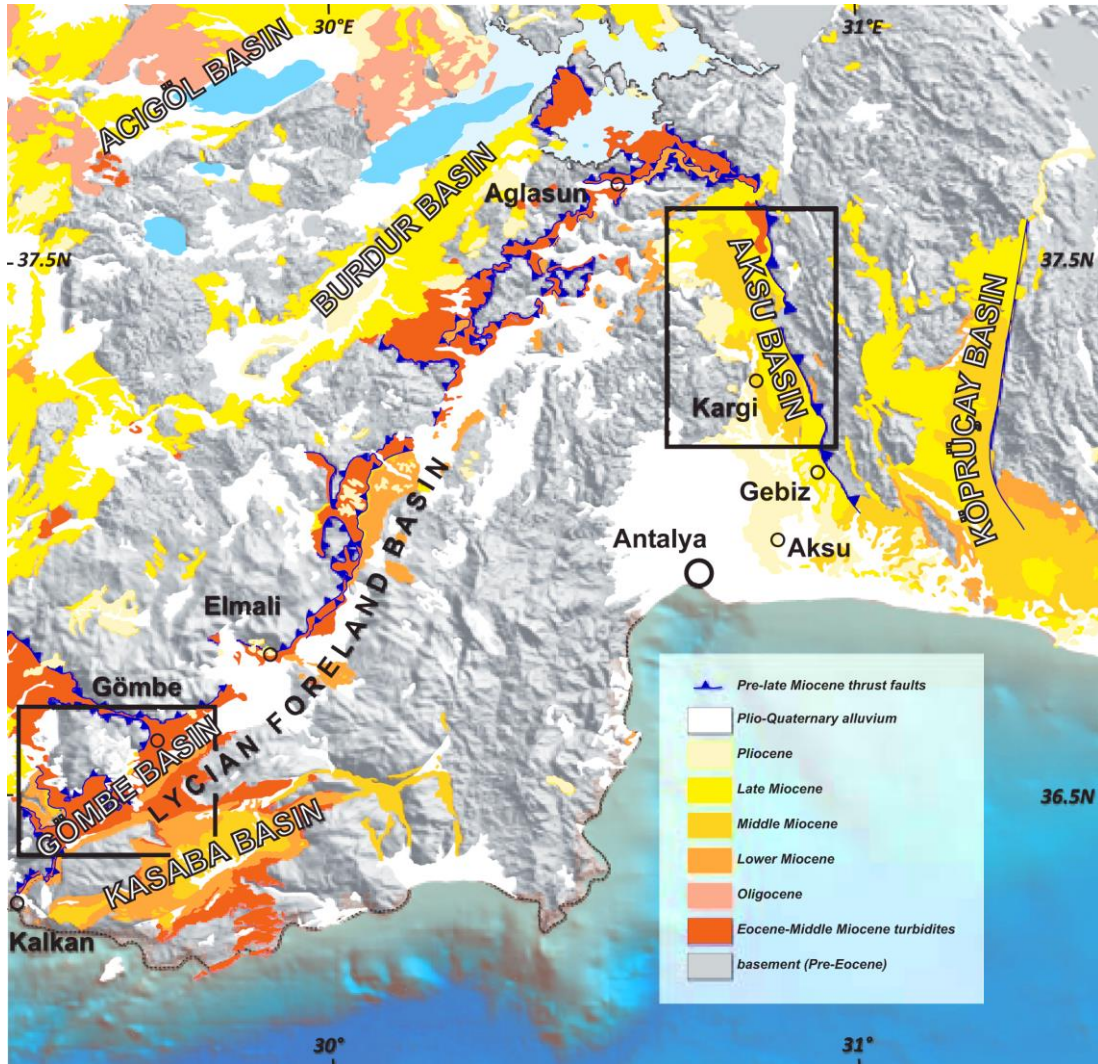


**Figure 2:** Position of Neogene Gömbe and Aksu Basins within the Eocene to recent configurations of the central and the western Taurides (SW Anatolia) (simplified from 1/500.000 scale geological map of Turkey, MTA 2002)

The section in the Aksu Basin is coded as IS and geographically it is located on the Antalya – Isparta Highway (Figure 2). The coordinates of the top and bottom of the measured sections are given below (Table 1).

**Table 1:** Geographic positions of the bottom and the top of the measured sections (UTM 35S)

<b>Sections</b>	<b>Bottom</b>		<b>Top</b>	
<b>GB</b>	29.65832°E	36.50285°N	29.65602°E	36.53072°N
<b>GÖM</b>	29.66575°E	36.53047°N	29.65888°E	36.50697°N
<b>IS</b>	30.76404°E	37.4975°N	30.76425°E	37.55128°N

### **1.3 Method of Study**

This study is carried out through three successive phases. These include literature survey, field studies and laboratory work. Literature survey includes the collection of an available information about the paleobathymetry related studies in the region and elsewhere. It also includes collection of and studies of foraminifera of late Cenozoic, and literature about the tectonic evolution of the Eastern Mediterranean region and SW Turkey.

The field studies include measurement of stratigraphic sections and collection of samples for paleobathymetric purpose. Along the section, the sample interval is predetermined as 10 meters, which is large enough for the desired precision of the bathymetric change with respect to sedimentation rate. From Aksu and Gömbe basins, 175 samples were collected in total.

The laboratory studies included the sample preparation, micropaleontological analyses and imaging of the identified foraminifera species or genera. Sample preparation was performed by washing the samples in the geochemistry laboratory of the Geological Engineering Department Middle East Technical University. Washing and sample preparation elaborated in the next section. Micropaleontological analyses and

identifications were done by studying the morphology of the benthic and planktonic foraminifera in the micropaleontology laboratory of the Geology Department, Utrecht University. At the latest stage, the foraminifer species were imaged in the Scanning Electron Microscopy Laboratory the Metallurgical and Materials Engineering Department Middle East Technical University.

#### **1.4 Previous Studies**

The previous studies related to the content of this thesis include only that papers related to the tectonics, paleogeography, stratigraphy and sedimentology of the SW Turkey, Beydağları region and Antalya basins. Other topics are omitted for the sake of clarity and coherence. A summary of these studies are given below in chronological order.

Özgül (1976) is one of the most important papers on the basic characteristics and tectonics of Taurides in southern Turkey. In this paper and its updated version (Özgül 1984) summarizes the key elements of Taurides and Beydağları platform and provide a very simple but outstanding evolutionary scenario for the Taurides during much of Mesozoic era.

Akay et al. (1985) carried out one of the oldest comprehensive study related to the stratigraphy and tectonic characteristics of Neogene deposits within the Isparta Angle. They studied the Neogene biostratigraphy of the Antalya Basins based on planktonic foraminifera and nannoplanktons. They classified the Antalya Basins into three sub-basins, which were the Beydağları Miocene basin, Antalya Miocene basin and Antalya Upper Miocene-Pliocene basin. They proposed for the first time a lithostratigraphic scheme that established the basic lithostratigraphy of the Neogene units. They also defined various formations and delineated their boundaries.

Akay and Uysal (1988) provided new tectonic information and new scenarios for the evolution of Antalya Basins during post Eocene times. They proposed four tectonic phases; 1) Upper Eocene -Lower Oligocene, 2) Langhian, 3) Upper Tortonian, and 4) Upper Pliocene to recent compressional-contractonal tectonic phases. They claimed that Antalya Basins were evolved with the convergence of the post-Eocene tectonic regime.

Flecker et al. (1998) studied the Miocene basins of Antalya within the Isparta Angle. They defined four sub-basins; these are the Dariören foreland basin on the western margin of Isparta Angle (Lycian Basin), and the other three of them are the Aksu, Köprü and Manavgat basins. They used Sr isotope ratios for dating the neritic limestone and measured paleocurrent directions from conglomerates underlying the limestone. They stated that basin development in all Antalya basins, including Aksu, Manavgat and Köprüçay basins, by the early Burdigalian.

Glover and Robertson (1998) studied the tectonic evolution of Plio-Pleistocene configuration of Aksu Basin in detail and they argued that sedimentation in the Aksu Basin commenced by the Late Miocene, developed under the direct control of the Late Miocene compression. They also proposed that the region was subjected to transtensional deformation and associated differential subsidence that continued until the early Pliocene. Then the region subjected to rifting and marginal uplift (rift shoulder uplift) occurred during between the late Pliocene to early Pleistocene time interval. According to these authors, supra-subduction zone extension and tectonic 'escape' of Anatolia (Şengör et al., 1985) were westwards towards the Aegean are the main factors that controlled the regional tectonic configuration.

İslamoğlu (2002) studied eight sections of the Antalya basins for their molluscan fauna. This study established chronostratigraphic ranges of molluscan fauna and suggested an alternative lithostratigraphic division of the basins. According to this author, Aksu Formation, which is one of the main concern of this thesis, is dated as Lower Tortonian and overlies unconformably the Altınkaya formation, which is containing Upper Burdigalian - Langhian molluscan fauna.

Poisson et al. (2003) studied the Aksu Basin and updated the stratigraphic positions of various units based on molluscs, foraminifera and nannoplanktons. They also provided one of the first fault kinematic data using fault slip data sets from the basin. This study argued also that Aksu Thrust emerged during the Pliocene and translated from east to west during that time interval.

Şenel (2004) studied Lycian foreland basin and their relationship with the Lycian Nappes and coined the name Yeşilbarrak Nappe as the leading thrust of the Lycian Nappes. This study provided new structural and tectonostratigraphic information and

modified the lithostratigraphy of the region and combined Elmalı and Uçarsu formation under the single name; Gömbe Unit.

Flecker et al. (2005) conducted a very detailed sedimentological study on the Miocene Antalya basins that include, Lycian forland, Aksu, Köprüçay and Manavgat basins. They also conducted analysis of facies associations and biostratigraphy of the basin in-fill and proposed a paleogeographic development scenario for the evolution of these basins during the Miocene to Pliocene. They also concluded that the development and evolution of these basins are responded by tectonic regime. Other factors, such as sea level changes and sedimentary processes played minor role in the establishment of basin architecture.

İşler et al. (2005) provided first comprehensive study on the off-shore parts of Antalya basins based on 2D seismic reflection data. They proposed two major phases of deformation in the basins. The middle – late Miocene and Pliocene to Recent non-coaxial compressional deformation. The first phase is characterized by development of a fold-n-thrust belt in the basin during Miocene and the second phase is characterized by early Pliocene to recent transcurrent tectonics manifested by local transtension and transpression associated with basin-wide halokinesis related to Messinian evaporates present in the basin.

Karabıyıkoglu et al. (2005) studied the Miocene reefs in the Aksu basin in terms of their stratigraphy, paleoenvironmental characteristics and their bearing on the basin development. They concluded that the coral reefs are developed on the alluvial fan/fan-delta complexes and shallow marine shelf carbonates during the late Miocene in the Aksu basin.

Çiner et al. (2008) is one of the most complete studies in terms of tectonostratigraphical evolution of Antalya Basins at the core of the Istarta Angle. They refined the Miocene lithostratigraphy and chronostratigraphy of these basins. They argued that the Miocene units comprises various units belonging to diverse depositional settings extending from continental to marine coarse to fine clastics, partly coral reefs, and reefal shelf carbonates. They revised the stratigraphy of the basins and proposed nine formations and twelve members for the Miocene units of

Antalya basins. They made a remark that structural styles in the basins are in contrast with the previously proposed evolutionary scheme of the Isparta Angle.

Sagular (2009) studied the Late to Early Pleistocene of Aksu Basin and eastern margin of Manavgat Basin around Manavgat-Oymapinar area and the outcrops along the Antalya-Akseki road. They calibrated fossil ascidian spicules with nannoplanktons. Later, Sagular and Çoban (2009) conducted mineralogical and rock chemical analyses of the samples from the same area.

Poisson et al (2011) studied the stratigraphy and paleogeography of Miocene Aksu Basin in its relationship with the pre-Neogene paleogeography and the emplacement of Lycian nappes into the region. They also provided an evolutionary scenario for the evolution of the Aksu Basin mainly during the Messinian.

Hall et al. (2014) studied the off-shore SW Turkey, including a part of off-shore Antalya Basins using very high resolution multichannel 2D seismic profiles combined with on-land exploration wells drilled by Turkish Petroleum Company over the last 40 years and the Deep Sea Drilling Project (DSDP) wells. They established a seismic stratigraphical scheme and correlated the established seismic horizons with the DSDP wells. They provided very detailed geometry of most of the structures in the Finike Basin and a part of Pliny-Strabo Trench. They claimed that the Pliny-Strabo Trench corresponds to a slab tear at the northern edge of northwards subducting African Oceanic Slab and it continues on-land. They further claimed that the alleged Fethiye-Burdur Fault Zone is the on-land continuation of this tear without providing any tangible evidence.

Üner et al. (2015) conducted kinematic analyses and sedimentological studies on the Aksu Basin. They indicated that Aksu Basin started to develop by the middle Miocene and has experienced four tectonic deformation phases until today. They claimed that these deformation phases are also valid for the development and evolution of Isparta Angle.

Koç et al. (2016) carried out a comprehensive paleomagnetic study on the Antalya Basins within the Isparta Angle, namely Aksu, Köprüçay and Manavgat basins. They claimed that Aksu Basin has not been rotated over the last 15 Ma while Köprüçay

basin rotated clockwise, Manavgat Basin rotated counter-clockwise owing to thrusting, and propagation of deep seated Kırkkavak and Aksu thrusts. They further implied that the Aksu Basin is passively carried piggy-back on the Bucak thrust which accommodated at least 20° counter-clockwise rotation Beydağları during the Middle Miocene to recent.

### **1.5 Regional Geology**

Convergence between African and Eurasian plates resulted in partial closure of the different branches of Neotethyan oceanic basin and resulted in present tectonic scheme of Eastern Mediterranean region (Flecker et al., 1998). The South Aegean and Cyprus arcs are two subduction systems along which oceanic crust at the northern edge of the African Plate, which constitutes the remnant oceanic crust of the eastern subducting below Anatolia at the southern edge of Eurasia (Figure 1a). Various slab-edge processes during the late Cretaceous and onwards gave way to the formation and total destruction of various sedimentary basins on the overriding plate. The remnants of these basins are exposed partly in various locations in SW Anatolia. These basins include very thick Eocene to recent marine to continental deposits (Hayward and Robertson, 1982; Hayward, 1984; Glover and Robertson, 1998; Flecker et al., 2005; İşler et al., 2005; Alçiçek et al., 2006 and 2013; Faccenna et al., 2006; Çiner et al., 2008; Mackintosh and Robertson, 2009; Ten Veen et al., 2009; Hall et al., 2014).

The basement of most of these basins belongs to Mesozoic autochthonous carbonate platform units composed of various accreted and stacked nappes most of which derived from north, from the Izmir Ankara-Erzincan Suture zone while the source of the other nappes are still under debate (Figure 1 and 2). Three contrasting source has been proposed for the origin of these nappes. According to the first scenario all of the Tauride nappes (Figure 1) are derived from a northerly located oceanic basin (Ricou et al. 1975), which is most probably the northern branch of the Neotethys ocean (Şengör et al., 1984). The second scenario is proposed by Ricou et al. (1979) which is the modified version of the first scenario. They consider that all the nappes were derived from north but the Antalya Nappe on the eastern margin of the Beydağları Platform first emplaced during the Late Cretaceous and moved northwards along a

sinistral strike-slip fault zone and thrust over the central Tauride autochthon. According to the third scenario, the nappes located at the north of the Taurides are derived from north while the nappes located at the south of the Taurides are derived from south as illustrated in Figure 1 (Dumont et al. 1972). The last scenario implicitly requires more than one Mesozoic basin south of the Taurides.

The Antalya basins, which are the main concern of this thesis, are developed mainly on the Antalya and Alanya Nappes and onlap on to the Beydağları Platform in the west by the Lower Miocene. However, Gömbe sector of the Lycian Basin developed progressively on the Beydağları Platform as the Lycian Nappes advanced eastwards and thrust over the , Beydağları platform from the west during the Eocene to Middle Miocene time interval (Hayward, 1984).

The Beydağları Platform together with the Geyikdağı Unit constitutes the main axis of the Taurides since they are the structurally lowest units in the belt. They are considered as para-autochthonous units and comprises thick Mesozoic carbonates spanning from Paleozoic to late Cretaceous. Carbonate deposition on the Beydağları Platform continued until early Miocene in Places (Hayward, 1984).

Alanya Nappes contains Permian and Triassic high pressure metamorphic rocks with peak metamorphism took place around Santonian and characterized by eclogite to blueschist facies rocks overprinted by younger medium grade greenschist facies metamorphism (Çetinkaplan et al., 2016).

Antalya Nappes, contain various volcanic and volcanoclastic rocks, various ophiolitic fragments belonging to different depths of an oceanic crust, as well as various sedimentary units belong to different tectonic and depositional environment typical for coloured melanges implying that it is developed in an accretionary wedge environment possible at the southern margin of northward subducting Pamphylia Ocean of Şengör and Yılmaz (1981) (Çetinkaplan et al., 2016). It is thrust over, during the late Cretaceous, by the Alanya Nappes and both of them together thrust over the Geyikdağı Unit (Figure 1b).



## CHAPTER 2

### STRATIGRAPHY

The rock units exposed in the region are classified into two groups: basement rocks and basin infill. The basement units comprise Beydağları platform, Lycian Nappes and Antalya Nappes (Figure 1). The second group, include the Neogene marine successions in the Gömbe and Aksu basins, which are the main the concern of the thesis (Figure 2).

#### **2.1 Basement Units**

The basement units comprise the western Taurides and the western margin of the central Taurides that include three isopic zones, namely 1) Beydağları Platform, 2) Lycian Nappes, 3) Antalya Nappes (Figure 1). Although, the basement units are not the subject of this study, nevertheless, brief information about them is given below.

##### **2.1.1 Beydağları Platform Carbonates**

Beydağları Platform, as mentioned previously, is structurally the lowest and para-autochthonous unit (Özgül 1976 and 1984). It comprises Triassic to Late Cretaceous shallow marine carbonate platform carbonates (Robertson and Woodstock, 1982; Hayward, 1984; Poisson et al., 2003b) which succeed into Eocene to Early Miocene carbonates and clastics deposited during the emplacement of Lycian Nappes as the Platform subsided in response to flexural loading of the Lycian Nappes. This

subsidence facilitated the deposition of deep marine facies characterized by marls indicating of very low sedimentation rate (Poisson et al., 2003b).

### **2.1.2 Lycian Nappes**

The Lycian Nappe are located at the western limb of the northwestern margin of the Isparta Angle as an allochthonous unit (Collins and Robertson, 1998). Lycian Nappes comprises a series of sheets from Mesozoic to Tertiary. General acceptance concerning the origin of Lycian Nappe is that it originated from northern margin of the Neotethyan ocean, translated southward over the Menderes Massif, thus causing its regional main Menderes Massif during the Eocene (Hayward, 1984; Collins and Robertson, 1998); on the other hand, it is also considered to be originated from near the Beydağları platform (Poisson et al., 2003b). Lycian Nappes comprises Mesozoic shallow water carbonates, cherts, and clastic sediments of Eocene age. Moreover, ophiolites developed, consisting of serpentinized peridotite and amphibolitic metamorphic sole, during the late Cretaceous to early Tertiary (Harward, 1984; Collins and Robertson, 1998). Overthrusting on the Beydağları platform ended in the Langhian (Poisson et al., 2003b).

### **2.1.3 Antalya Nappes**

Antalya Nappe was named by Lefevre (1967) and later Woodcock and Robertson (1977) suggested the “Antalya Complex” term instead, which is more neutral and descriptive. According to Poisson et al. (2003b), two terms can be differentiated with respect to the timing of emplacement; “Antalya Complex” includes the Paleozoic basement while “Antalya Nappes” includes only the allochthonous thrust sheets. Although the origin of the Antalya Nappes has been debated, Çetinkaplan et al. (2016) provided a convincing evidence that it was derived from the Pamphalian Basin, which is located that at the southern branch of the Neotethys ocean (Poisson et al., 2003b and 2011). Antalya Nappes contains very diverse rocks assemblages from Mesozoic deep and shallow marine sedimentary rocks to mainly turbiditic, pelagic limestones, and radiolarites (Hayward, 1984). They also include pillow lavas, dolerites, gabbros, and peridotites belonging to the ophiolite suite (Woodcock and Robertson, 1982; Morris and Robertson, 1993). Antalya Nappes were emplaced onto the Beydağları Platform

during Late Cretaceous to Paleocene (Hayward 1984), although, they were partly remobilized during the Neogene (Koç et al. 2016).

## 2.2 Gömbe Basin

Gömbe Basin, constituting an integral part of the Lycian Foreland Basin, is exposed in the southeastern front of the Lycian Nappes (Figure 1b and 2). Generalized columnar section is presented below (Figure 3) It comprises two lithostratigraphic units; namely Elmalı and Uçarsu formations (Şenel, 2004).

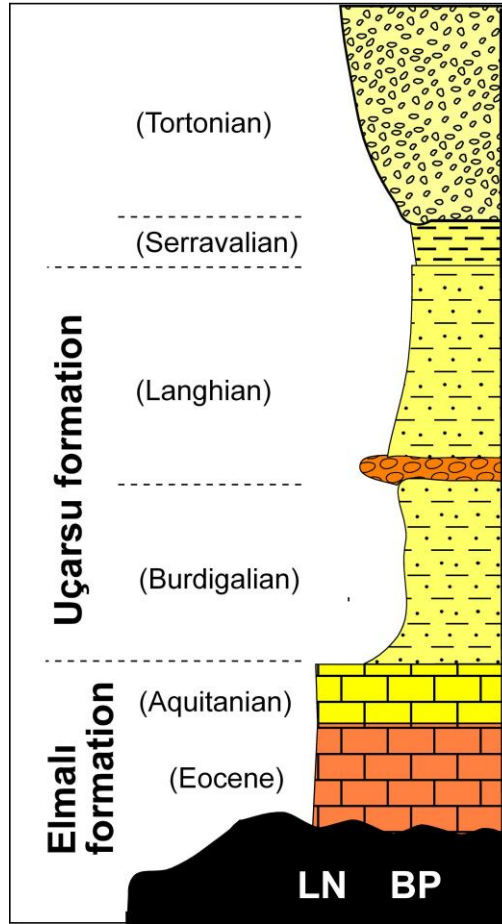


**Figure 3:** Generalized columnar section Lycian Foreland Basin, LN: Lycian Nappes; BP: Beydağları Platform (Modified from Collins and Robertson, 1998; Şenel, 2004)

Two composite sections were measured in Gömbe Basin. The Uçarsu Formation, is coded as GÖM (BB' in Figure 4). The other is the overlying turbidites (Figure 6) are coded as GB (AA' in Figure 4).

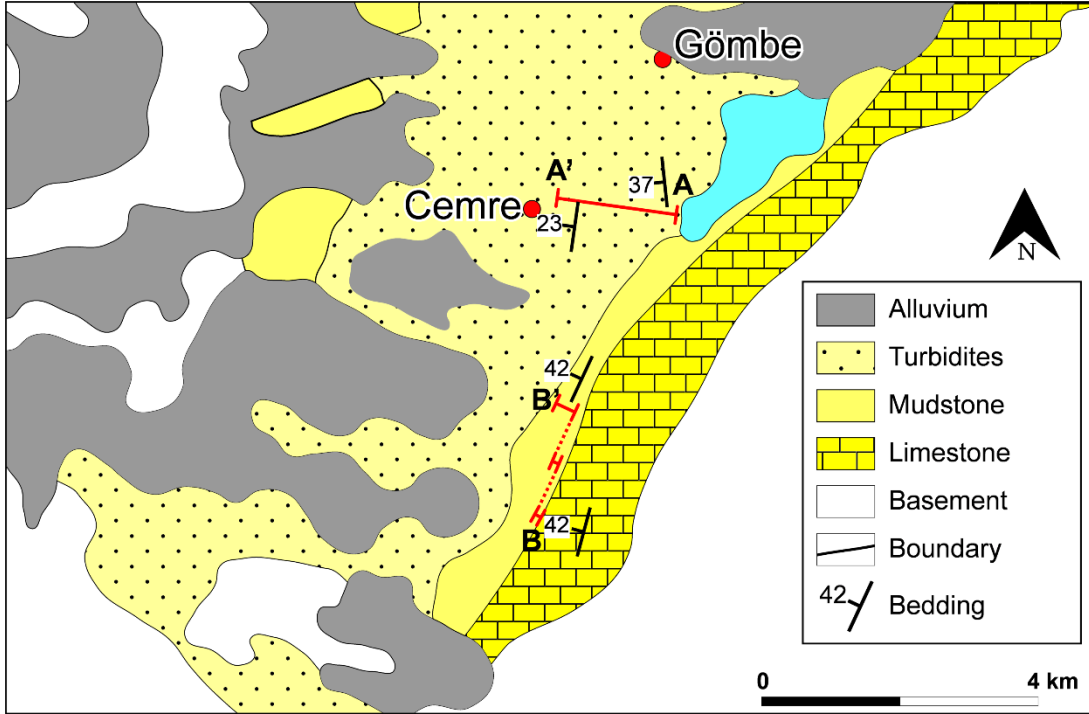


**Figure 4:** Geological map of the Gömbe Basin. Measured sections are indicated. A-A' (GB) includes the turbidites of of Uçarsu Formation and B-B' (GÖM) includes Elmalı Formation (Modified from Şenel, 2004)

### 2.2.1 Elmalı Formation

It was named first by Önalın (1979). It is extensively exposed on the Lycian Foreland Basin. Except the Gebeler district, Elmalı Formation overlies the Beydağları Platform and it is overlain by Uçarsu Formation, between Elmalı and Fethiye. The thickness of the unit is more than 1000 m (Şenel, 2004).

Elmalı Formation is characterized by gray, green, dark gray, light brown thinly to thick bedded sandstones, siltstones and claystones with limestone intercalations. It also includes polygenic conglomerates, debris flow and turbiditic facies dominated by sandstones. Coarse to fine grained pebble bearing sandstones are observed with both well and poor grading. Siltstone and claystone are dark colored and thin bedded. Several limestone beds are interbedded with sandstones at lower levels with 7-8 m

thickness. Carbonate beds are characterized by sandy limestone, calcarenite, micrite and clayey micrite (Şenel, 2004).

The formation includes foraminifera and nannoplanktons. The age of this formation is Late Lutetian to Early Miocene. (Şenel, 2004).

It is correlated with the Varşakyayla formation and Küçükköy formation on the upper level of the Beydağları autochthon (Şenel, 2004).

### **2.2.2 Uçarsu Formation**

It was named by Şenel (2004) and it is exposed between Kalkan, Elmalı, Korkuteli and around Ağlasun. It is tectonically overlain by the Lycian Nappes from west and its thickness reaches up to 220 m (Figure 5).

Uçarsu Formation is characterized by green, greenish gray mudstone, siltstone, sandstone and conglomerate alternations, and sandy limestone intercalations. It is differentiated from the Elmalı Formation by its overall coarser grain size and presence of macrofossils. At the bottom it contains light grey to green, poorly sorted, coarse grained, thick-bedded sandstone. The unit continuous with thick bedded, well-sorted conglomerates thick bedded sandy limestone alternation and shale intercalations. Towards the top, the sequence becomes coarser and thicker. At the top levels, coarser grained sandstones is overlain by thick-bedded conglomerate; the thickness of individual conglomerate bed may reached up to 70 cm. The uppermost parts of the sequence is characterized by very thick-bedded boulder conglomerates with subrounded to subangular pebbles. The sorting and roundness become poorer upward in the section (Şenel, 2004).

The section includes gastropoda, corals fragments, echinoids and foraminifera. The age of this formation is Late Burdigalian to Early Langhian (Şenel, 2004).

It correlated with the Kasaba formation on the Beydağları Platform and is transgressive over the Lycian Nappes in places (Şenel, 2004).

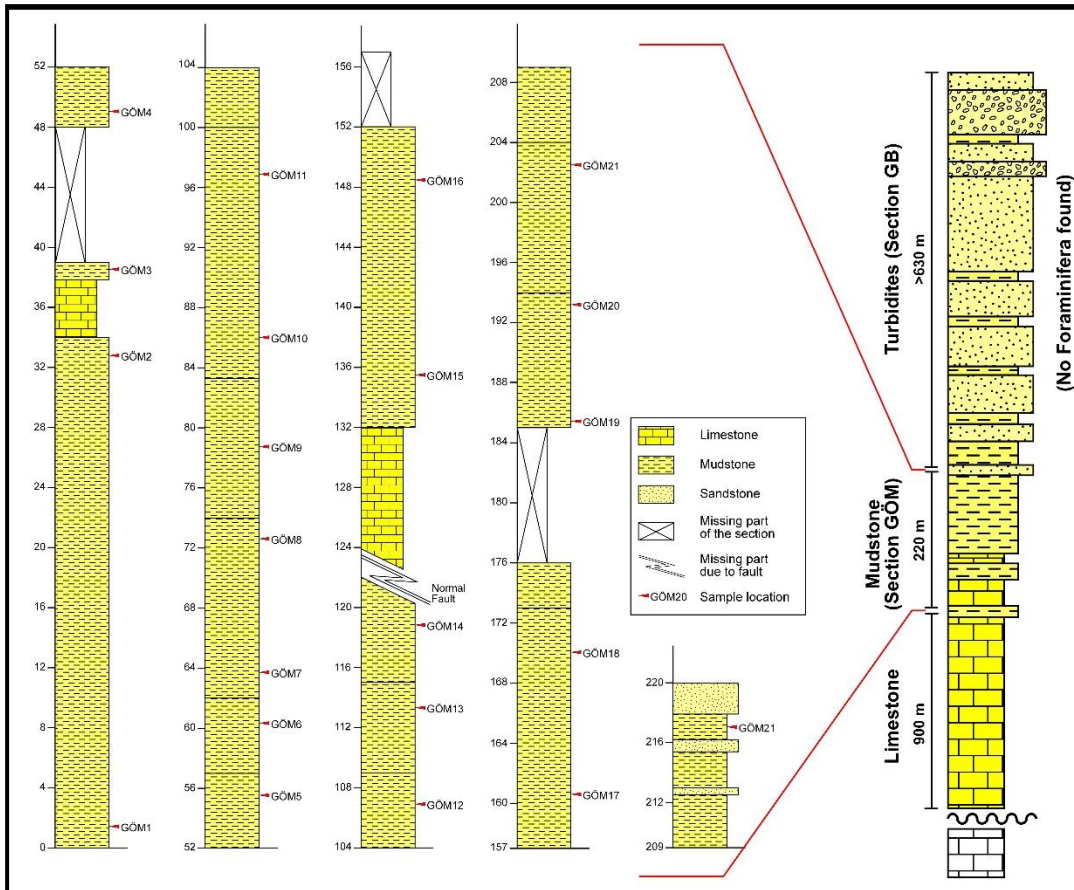


**Figure 5:** Measured section from Uçarsu formation in the Gömbe Basin

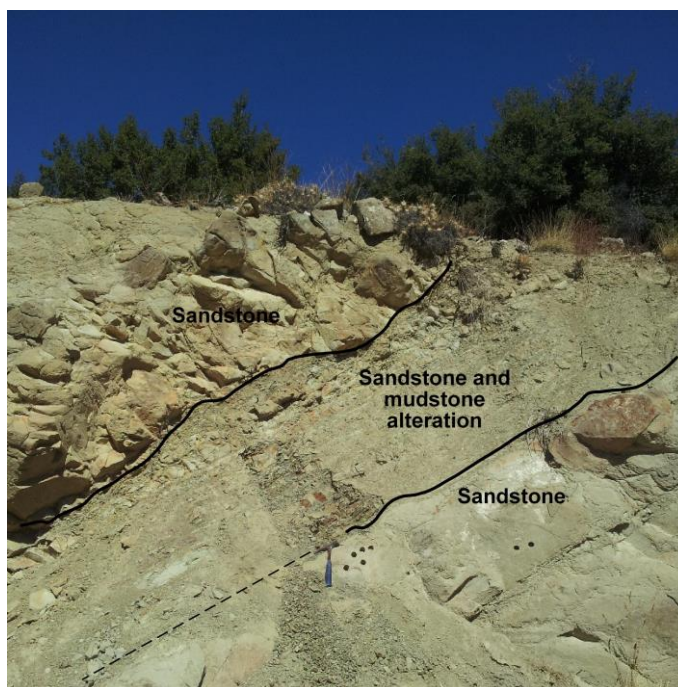


**Figure 6:** General view of turbidites of the Gömbe Basin, Section GB.

### 2.3 Aksu Basin

Aksu Basin was developed within the Isparta Angle. Generalized columnar section of the basin presented in Figure 7. It is delimited in the east with the Aksu thrust and onlaps on to the eastern margin of the Beydağları Platform (Figure 8). It comprises three Miocene formations, namely 1) Aksu Formation, 2) Karpuzçay Formation, and 3) Gebiz Limestone. Pliocene and Quaternary units overlies these units in various places.

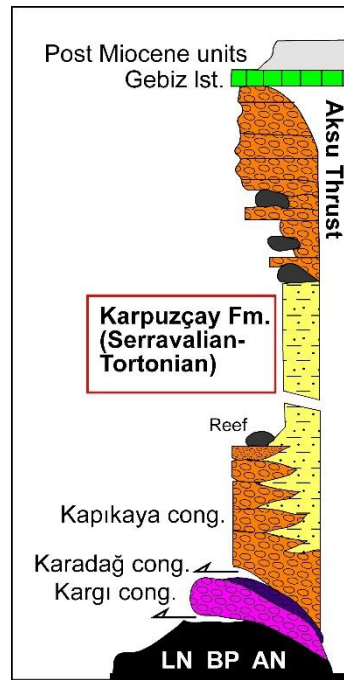


**Figure 7:** Generalized columnar section of Aksu Basin, LN: Lycian Nappes; BP: Beydağları Platform; AN: Antalya Nappes (Modified from Çiner et al., 2008).

#### 2.3.1 Aksu Formation

It was named by Akay et al. (1985) and is exposed in the northern part and eastern margin of the basin. Aksu Formation unconformably overlies the basement units and laterally grades into the Karpuzçay Formation. Its thickness reaches upto 1280 m (Akay et al., 1985). Aksu Formation is characterized mainly by conglomerates, and thinly bedded sandstones, mudstones and marl intercalations with occasional

limestone blocks. Çiner et al. (2008) divided Aksu Formation into three sub units as Kapıkaya Conglomerate, Karada Conglomerate and Kargı Conglomerate.

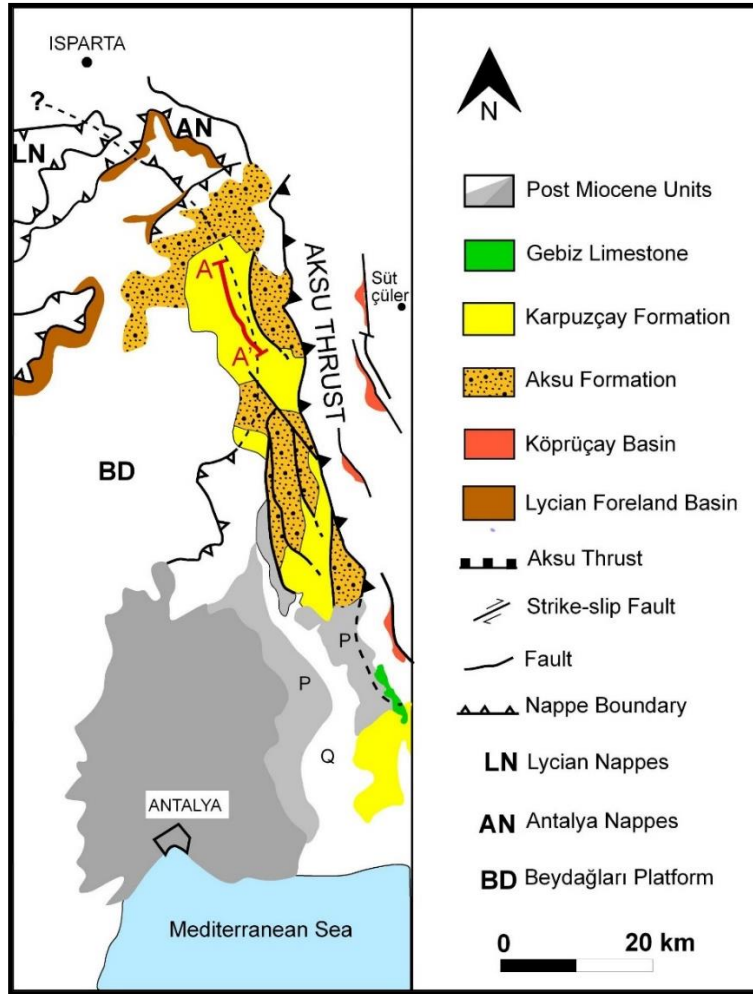


**Figure 8:** Geological map of the Aksu Basin. Measured section, coded as IS, is indicated as A-A'. (Modified from Deynoux, 2005 and Çiner et al. 2008).P: Pliocene, Q: Quaternary.

### 2.3.1.1 Kapıkaya Conglomerate

It is exposed near the Taşyayla Village. Lower part of the unit is composed of coastal alluvial fan deposits, and upper levels are shallow marine deposits with marl intercalations (Çiner et al., 2008) According to the nannofossil content of the intercalations, the age of the unit is Serravalian to Tortonian (Akay et al., 1985).

### 2.3.1.2 Karadağ Conglomerate

It is exposed in the middle part of the Aksu Basin. Its thickness is higher than 1000 m and characterized by occasional sandy beds intercalated with marls and at higher levels with reefal limestones. Intercalated conglomerates are derived from white to grey Mesozoic limestones, dark colored sandstones, reddish to greenish radiolarites and ultramafics. The age of the unit is Burdigalian to Langhian (Çiner et al., 2008)

### 2.3.1.3 Kargı Conglomerate

It is well exposed along the Antalya-Isparta Road, near the Kargı Tunnel close to the northernmost edge of the basin. It is composed of reddish conglomerates with red mudstone and sandstone intercalations (Çiner et al., 2008). It includes coral-algal reef buildups. The age of the unit is Tortonian (Karabıyıköglü et al, 2005).

### 2.3.2 Karpuzçay Formation

It was firstly named by Akay et al. (1985) and widely exposed in the basin. Best outcrops are observed along road cuts along the Antalya Isparta Highway. It laterally grades into the Aksu and Karpuzçay and is overlain by Pliocene deposits. Its thickness is measured 2050 m (Akay et al., 1985).



**Figure 9:** Sandstone and mudstone alternation of Karpuzçay Formation with reverse faults in Aksu Basin

The formation is characterized by sandstone and mudstone alternation with coarse conglomerate intercalations at the upper levels. Mudstones are grey, green and yellow colored, and sandstones are generally lighter colored (Figure 9). Thin to thick sandstone beds, which show fining and coarsening upwards sequences, alternated with laminated and thinly bedded mudstones (Akay et al., 1985, Çiner et al., 2008). The measured section of the formation is presented in Figure 10.

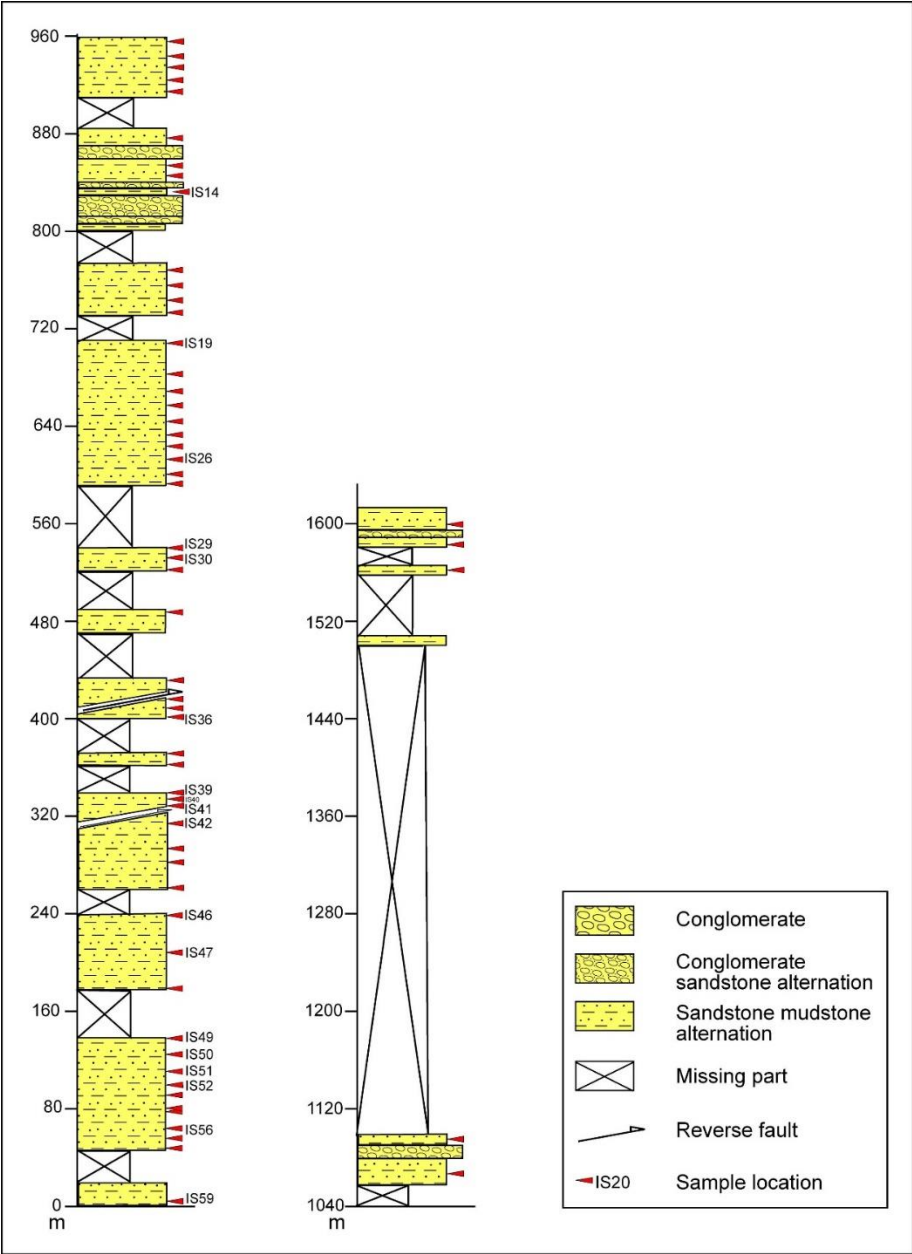


**Figure 10:** Measured section from Karpuzçay Formation, Aksu Basin.

It includes foraminifera and nannofossil. The age of the formation is assigned as Serravalian to Tortonian (Çiner et al., 2008).

### **2.3.3 Gebiz Limestone**

It was firstly named by Poisson (1977) type section is at the southern part of the Aksu Basin. It unconformably overlies Antalya Nappes and Karpuzçay Formation. Its thickness is 40 m (Akay et al., 1985).

From bottom to top, it is composed of loosely consolidated sandstone with reefal limestone, thick to medium bedded whitish limestone, and thinly bedded mudstone and marl (Akay et al., 1985; Çiner et al., 2008). Despite the fact that it includes foraminifera, mollusks and echinoids, age of the unit is controversial. Akay et al. (1985) argued that the Gebiz Limestone is laterally transitional with Eskiköy Formation, and they are both Messinian in age. Glover and Robertson (1998) proposed late Tortonian age, while Poisson et al. (2003b) suggested Pliocene age. Poisson et al. (2011) assigned Messinian age for the Gebiz Limestone according to the most recently acquired nannoplankton data.

### **2.3.4 Post-Miocene Units**

Post-Miocene units include Pliocene and Quaternary deposits. Pliocene units comprise Eskiköy Formation, Yenimahalle Formation and Alakilise Formation. Quaternary units comprise Antalya Tufa and alluvial cover. Although, the post-Miocene units are out of the scope of this thesis, however, a brief information about the post-Miocene deposits is given below.

Eskiköy Formation is widely exposed the southwestern part of the Aksu basin around Antalya city center. It overlies unconformably the Aksu and Karpuzçay formations as well as Antalya Nappes, and is laterally transitional with the Yenimahalle Formation (Akay et al., 1985). Maximum thickness of the Eskiköy Formation is 400 m. The unit is characterized by poorly sorted and well rounded conglomerates at the bottom. The sequence continues upwards with sandstone and mudstone alternations (Akay et al., 1985) According to planktonic foraminifera and nannoplankton content, age of the formation is Zanclean (Poisson et al., 2011).

Yenimahalle Formation is well exposed around the Yenimahalle Village and Gebiz area. Its thickness is 250 m. It is characterized by the shallow marine deposits, marl and sandstone alternation. Yenimahalle Formation is vertically transitional with the Alakilise Formation (Poisson et al., 2003).

Alakilise Formation is composed of sandstone, siltstone and thick conglomerate alternation (Akay et al., 1985; Poisson et al., 2003). It contains foraminifera, ostracoda and molluscan fauna. Alakilise Formation was dated to Pliocene based on its molluscan fauna (Poisson et al., 2003).

Antalya Tufa is widely exposed, a series of terraces, on the western part of Aksu Basin. Its thickness is 250 m in the west, while ranges between 20-30 m in the east. Terra rossa-type soils overlies the Mesozoic platform carbonates of the Antalya complex and Beydağları Platform and tufa deposits (Glover and Robertson, 1998).

## CHAPTER 3

### PALEOBATHYMETRY

The tectonic mechanism determine the geometry and depositional environment of marine basins. In order to get better clarification of history of marine basins, paleobathymetry studies play an important role (Allen and Allen, 1990). Paleobathymetry studies concern the depositional depth estimation of marine basins. Uplift and subsidence history can be understood via the paleobathymetric evolution of the marine basins taking into account the global sea level changes (Van der Zwaan et al, 1990). As the paleodepth estimations get more precise, understanding of the history of the vertical movements of basin floors can be more comprehensive. Paleontology, based on mainly foraminifera, plays an important role in paleobathymetry estimations that cannot be fulfilled with another tool (Allen and Allen, 1990).

Fossil calcareous benthic foraminifera are very useful to reconstruct paleoenvironment due to changing abundance and diversity of the different groups in the marine deposits. In marine environments, there are many factors, such as water depth, temperature, salinity, substrate etc. that affect the life of foraminifera (Van Morkhoven et al., 1986; Loeblich and Tappan, 1988; Gupta, 1999). Water depth is studied in relation with other factors such as nutrient influx and oxygenation; and is inferred from the distribution and abundance of foraminiferal groups. Foraminifera based paleobathymetry methods are being improved with the increasing number of paleoenvironment studies focused on qualitative and quantitative analyses of foraminifera (Gibson, 1989; Van der Zwaan et al, 1990; Van Hinsbergen, 2005; Hohenegger, 2005).

Qualitative bathymetry studies are conducted with benthic foraminifera species. Each benthic foraminifera species has its own habitat and one of the controlling factor of this habitat is water depth. Each species indicates a depth interval and these can be overlapping each other, may intersect or not. This creates faunal zones consisting of benthic species and gives an opportunity to estimate depth range (Phleger, 1951; Bandy, 1953; Bandy and Arnal, 1960). The extant benthic foraminifera species can be used directly as a proxy for paleobathymetric studies; on the other hand, extinct species are only reliable within certain error margins since their paleobathymetric range is deduced from comparisons and analogy with living taxa. However, the paleodepth range of benthic fossils, which have no recent counterparts, has to be ascertained by comparing the species with living taxa. Another problem is the existence of heterobathyal species, living in different depth ranges at different location (Bandy and Chierici, 1966). Moreover, when the number of benthic species decreases, it is more difficult to obtain a precise depth range. In this case, the uncertainty of the obtained results may be hundreds of meters. Under these circumstances, quantitative studies have become more important. The planktonic foraminifera in this case, are used for paleobathymetric studies as well as their biostratigraphical application (Bandy and Chierici, 1966; Wright, 1978; Van der Zwaan et al., 1999; Kouwenhoven, 2000; Van Hinsbergen et al, 2005).

### **3.1 History of P/B and Depth Relation**

At the beginning of the 1950's, depositional depths of marine basins were reconstructed in relation to the benthic and planktonic foraminifer abundance. After Phleger (1951) mentioned this phenomenon, Grimsdale and Van Morkhoven (1955) and Smith (1955) showed that there is a systematic relation between P/B ratio and depth. They were studied samples of recent sediments and found that the proportion of the planktonic foraminifers to the total foraminifer population increases from shallow water to deep water. According to Grimsdale and Van Morkhoven (1955), while the benthic population is dominant in neritic environments, it is nearly absent at abyssal depths. They also argued that the number of planktonic increases together with water depth because planktonic foraminifera exist in the uppermost layers of the water. They explained any unexpected results, such as breaks in distributions, with slumping

and abrupt sea level change. Although they clarified the general concept, they did not propose a sensitive method for paleobathymetry by using P/B ratio.

In the following years, P/B ratios become widely used for the bathymetric analyses and different depth ranges were obtained from these analyses mentioned below. According to Wright (1977), besides depth, P/B ratios are related to distance of upwelling water masses, salinity, turbidity and distance from the shore. In spite of these depth related factors, Wright (1977) proposed an equation derived from P/B ratio to obtain the depositional depth. Van Marle et al. (1987) used Wright's (1977) regression model as a regional model, while considering modern patterns and environmental conditions (Figure 11) Van Hinte (1978) indicated that the resolution of the paleobathymetric curve depends on the age of the deposition; younger deposits may have higher resolution than older deposits. Besides quantitative calculations, he derived paleobathymetric curves based on paleodepth intervals according to faunal distribution.

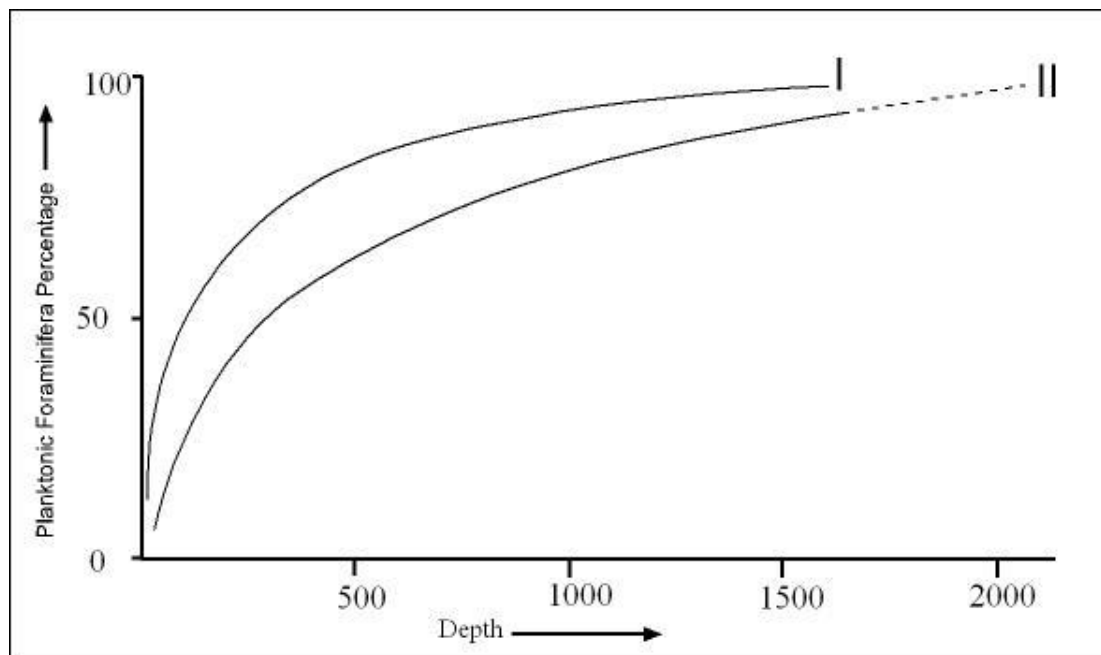


**Figure 11:** First (I) line is the regional model of the Van Marle et al. (1987) and second (II) line is the model of Wright (1977) (as cited in Van Marle et al., 1987)

According to Berger and Diester-Haass (1989), P/B ratio is influenced by three main factors that are depth, food supply and partial dissolution and these factors are also

dependent on each other. Food supply to the seafloor is from vertical flux, which depends on depth, and also lateral flux from the continental margin which depends on the distance from the shore. Organic matter on the sea floor is the main factor that affects the benthic abundance, and this is directly related to P/B ratio. They derived a productivity index depending on the depth and P/B ratio excluding effects of dissolution (see also Van der Zwaan et al. 1990). They showed that organic flux decreases proportionally with increasing depth. In other words, depth could be expressed as a function of only P/B ratio, similar to the “Wright-model” (Van der Zwaan et al., 1990).

In Equation (1), %P indicates the percentage of planktonic foraminifers in relation to the total foraminifer assemblage. Constants of the Equation (1) are very close to the equation by Wright (1977). Furthermore, again %P is preferred instead of P/B ratio. Between 0 and 1000 m water depth, P/B ratios have values between 0 and 10. Deeper than 1000 m, P/B ratio rapidly goes to infinity. To avoid this deadlock in regression analyses, the equation can be described log-linear when %P is used. (Van der Zwaan et al., 1990)

$$Depth (m) = e^{3.58718+(0.03534*\%P)} \quad \text{Equation (1)}$$

Van der Zwaan et al (1990) eliminated the unexpected or irregular data, if there is downslope contamination, reworking and dissolution. They improved the regression analyses by recalculating the %P value with discarding stress marker benthic foraminifers. While planktonic foraminifer population are generally increasing with depth, benthic species may show different trends, because some of the benthic species, namely the infaunal group, do not directly relate with the supply of the organic matter and food from the overlying water layers. These infaunal benthic species feed from the organic matter buried in sediments. Van der Zwaan et al. (1990) eliminated infaunal benthic species and obtained better regression results.

Van der Zwaan et al. (1990) compared observed depth value of the recent sample and predicted depth values based on Equation (1). Most of the values matched up with each other; however, some of the predicted depths diverged from the observed depth (Figure 12). In this case, they defined confidence limits for the model. 99% P corresponds to 1200 m, lower confidence limit of it is 860 m and upper one is 1650 m.

For 50% P, which corresponds to 430 m, lower confidence limit of it is 310 m and upper one is 590 m. Standard error is greater at the deeper estimations (Van der Zwaan et al., 1990).

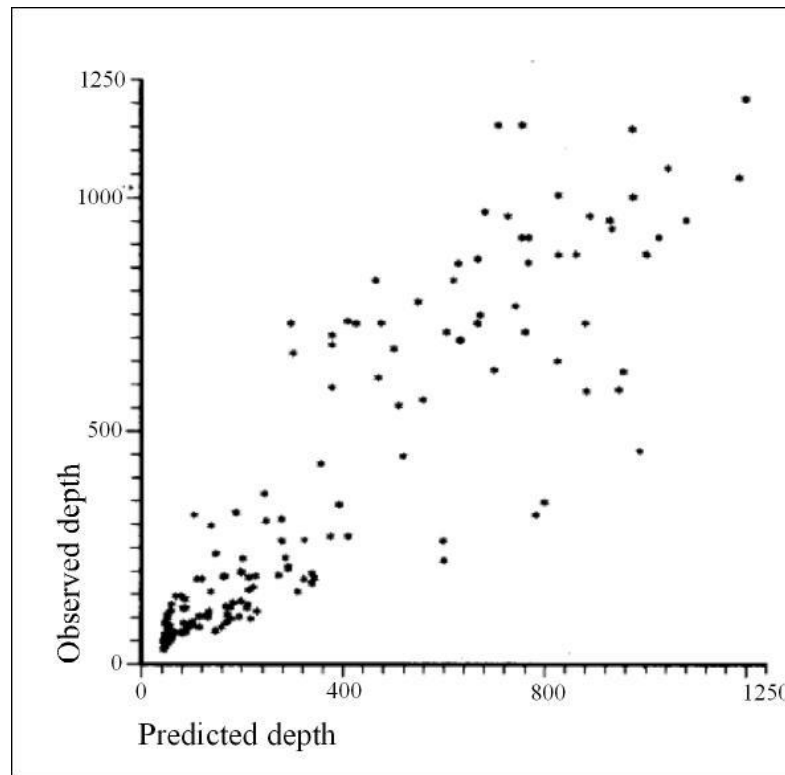


**Figure 12:** Observed versus predicted depth plots (Van der Zwaan et al., 1990)

Van Hinsbergen et al. (2005) proposed a standard methodology for the late Cenozoic using the general notion of Van der Zwaan et al. (1990). Deep infaunal benthic species were considered as stress markers, and they calculated %P value as:

$$\%P = 100 * (P / (P + B - S)) \quad \text{Equation (2)}$$

P = number of planktonic foraminifera;

B = number of benthic foraminifera;

S = number of stress markers (deep infaunal benthic species)

From the 1950's to today, the relevant studies are presented in Table 2 with authors and their claims about P/B and depth relations.

**Table 2:** Authors of studies and their claims about P/B and depth relations in a chronological order.

<b>Authors (year)</b>	<b>P/B and depth relations</b>
Phleger (1951)	Mentioned about P/B and depth relations.
Grimsdale and Van Morkhoven (1955)	Showed systematic relation with P/B and depth relations.
Smith (1955)	
Wright (1977)	Showed relation with equation $D = e^{(0.0418 * \%P) + 3.4823}$
Van Hinte (1978)	Proposed paleobathymetric resolution chart with respect to time.
Gibson (1989)	Used modern patterns of %P for Cenozoic applications.
Van der Zwaan et al (1990)	Showed relation with equation $D = e^{3.58718 + (0.03534 * \%P)}$ and improved %P calculation with review of benthic foraminifera.
Van Hinsbergen et al. (2005)	Proposed a standard methodology for late Cenozoic with using equation proposed by Van der Zwaan (1990).

Stress markers are explained in more detail in the following chapters. When we excluded stress markers from the total benthic assemblage, we have depth markers, which indicates a specific depth range, this will be explained in “taxonomic check” section. Limits of the calculation by Van der Zwaan et al. (1990) are between 36 and 1238 m according to values of %P that range from 0 to 100% (Figure 13). According to Van Morkhoven et al. (1986), the following bathymetric zones are applied:

Inner neritic (IN) = 0-30 m

Middle neritic (MN) = 30-100 m

Outer neritic (ON) = 100-200 m

Upper bathyal (UB) = 200-600 m

Middle bathyal (MB) = 600-1000 m

Lower bathyal (LB) = 1000-2000 m

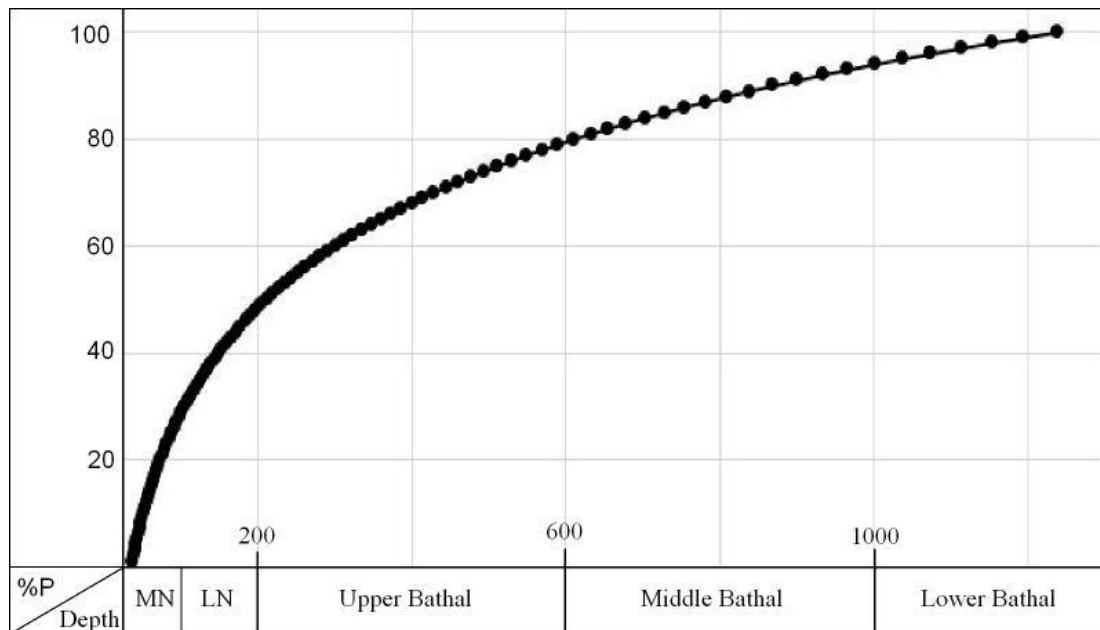


**Figure 13:** %P versus depth graphic based on Equation (1) (Van der Zwaan et al., 1990).

### 3.2 Sample Collection and Preparation

Samples were collected for paleobathmetry analyses from measured sections mentioned in Chapter 2. Samples were collected from fresh surfaces (Figure 14) and the average sampling interval is indicated below for each section.



**Figure 14:** Sample collection from (a) Turbidites from the Gömbe Basin, coded as GB, (b) from the Gömbe Basin, coded as GÖM, (c) from Aksu Basin, coded as IS.

Samples are collected in Gömbe trough two sub-sections. One of them is along the turbidities at the top and 94 samples were collected from 630 m thickness. Collected samples were coded as GB. The average sampling interval was 7 m in this section. However, due to the fact that most of the units consist of sand size material, there were not any foraminifera in the washed samples. These discarded samples are characterized by quartz and highly abundant rock fragments (Figure 15).



**Figure 15:** (a) Quartz grains (See EDS analyses APPENDIX A, Figure 25); (a) Black rock fragments (See EDS analyses in APPENDIX A, Figure 26) from GB section, GB-30; (b) Rock grains with calcite matrix (See EDS analyses APPENDIX A, Figure 24) from GÖM section, GÖM-12; (c) Rock grains with calcite matrix from Aksu (IS) section, IS-36 (See EDS analyses APPENDIX A, Figure 22; (d) Rock grains with calcite matrix from Aksu (IS) section, IS-56 (See EDS analyses Appendix A, Figure 23)

The other sub-section, below the GB section, was coded as GÖM. This section consists of an alteration of mudstone and limestone. Collected samples along this section were from mudstone. Twenty-two samples were collected from 220 m thickness. The

average sampling interval was 10 m in this section. Samples 1, 3, 14 and 15th samples were discarded from in this section, due to absence of foraminifera. Samples, 4, 5, 7, 9, 10, 13, 16, indicating anoxic environment, were discarded from the analyses as well.

In Aksu basin, samples were collected from 1620 m of section. The section starts in the core of the anticline and it is characterized by a 2 m in average mudstone and 50 cm sandstone alternation. Nearing the top of the section, grain size becomes coarser and it turns to a sandstone-conglomerate alternation. The average sampling interval was 10 m in this section, when non-exposed parts were excluded. Samples, 3, 5, 9, 12, 17, 27, 34, 35, 38, 43, 44, 48, indicates anoxic environment, and depth markers absent in them, so they were discarded. Other samples that foraminifera is absent, which were discarded.

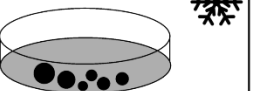
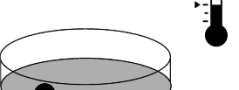
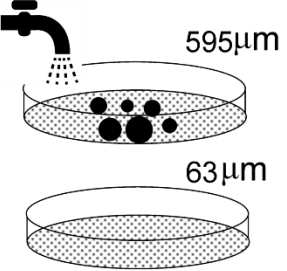
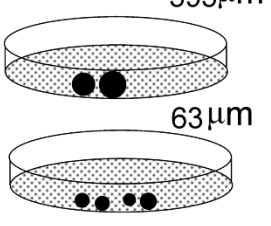
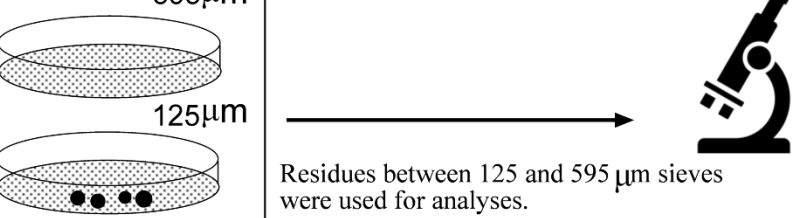
### **3.2.1 Sample Preparation**

Mixing of the samples causes contamination which can severely affect the results of the analyses. To avoid such a contamination, during both field and laboratory studies, the sampling and analyzing equipment should be washed and kept clean (Green, 2001).

Extraction of foraminifera from rocks has been is easy for loosely consolidated late Cenozoic sedimentary rocks. Generally, using tap water is a fast adequate way to extract foraminifera from the samples. In this way, the study gains speed and extraction does not take long time. However, water is not adequate for some lithified rocks, in which case some other physical or chemical methods needed to be applied. The choice of a method is dependent on the investigated material, where the main concern is to avoid damage or dissolution of the foraminifera. The best procedure is commonly found with trial and error (Green, 2001).

Kennedy and Coe (2014) proposed the freeze-thaw method comparing to standard methods using with hydrogen peroxide and other chemicals, because disaggregation with chemicals can easily cause dissolution of foraminifera. Besides, chemical safety risks are minimized with the freeze-thaw method. The method makes use of the expansion of water upon freezing. Water fills the pores of the sample, and then frozen water expands and cracks the rock. This process facilitates disintegration. Freeze-thaw method was used for the highly consolidated samples sections from Gömbe Basin.

Despite Kennedy and Coe (2014) add some steps, such as rapid heating, detergent and ultrasound stages, following steps were enough for extraction in this study.

1.		Largest of a bean size with hammer.
2.		Soaked in cold water for 24 hours until they are saturated.
3.		Put into freezer for approximately three hours.
4.		Heated in bakery oven to 40°C
5.		Put into water in average for a day
6.		Washed under tap water with 63 and 595 µm sieves
7.		For residues over on the 595 µm seive, turn back step 2. For residuals between 63 and 595 µm sieves were dried.
8.		Residues between 125 and 595 µm sieves were used for analyses.

**Figure 16:** Steps 1-7 are the freeze thaw method (Kennedy and Coe, 2014) and step 8 was applied for analyses (Van Hinsbergen et al., 2005).

Collected samples were broken into pieces of which the largest were of a bean size with a hammer, and were soaked in cold water for 24 hours, until they were saturated. Saturated samples were put into the freezer for approximately three hours. Frozen samples were kept at room temperature for thawing, then they were heated in a bakery oven to 40°C for three hours (Green, 2001). Later, the dried samples were put into water on average for a day for disintegration to take place. The samples were then washed under tap water with stacked 63 µm and 595 µm sieves. For residues left over on the 595 µm sieve, the same procedure was applied. Repeating maximum 5 times proved enough for the desired outcomes in this study. Washed residues between 63 µm and 595 µm sieves were dried (Figure 16).

In order to use 125 and 595 µm size fraction for counting, dried samples are sieved (Figure 16) and then divided in equal quantities with a microsplitter (Van Hinsbergen, 2005). Samples are spread on picking tray and counted until obtain at least 300 planktonic and benthic species (Gibson, 1989).

### **3.3 Suitability of Samples**

As mentioned before, some unexpected results, outlier data points, may occur due to paleoenvironmental conditions. These factors affect the foraminifera during life, or after death. Main reasons for the unexpected results are downslope transportation, reworking and carbonate dissolution; the samples should be checked for these factors after washing. However, at least, there have to be foraminifera in the collected samples. (Gibson, 1989; Van der Zwaan et al., 1990; Van Hinsbergen et al., 2005)

When dissolution of carbonate occurs, foraminifers are affected differently. General acceptance is that planktonic foraminifers are affected more compared to benthic species. If there is a dissolution event, it will cause a drop in the P/B results. Besides, smaller specimens are more prone to dissolution compared to larger ones (Van der Zwaan et al., 1990). This gives the same result. Moreover, dissolution resistance differs from one taxon to another in benthic species. (Neguyen and Spejler, 2014). If there is carbonate dissolution or fragmented shells dominate the sample, it will be skipped (Van Hinsbergen et al., 2005). Dissolution can partly affect the shell of foraminifera. Van Hinsbergen et al. (2005) mention that if benthic species can be

recognized and determined the sample would be adequate for analysis. *Hoeglundina elegans*, an aragonitic species, is vulnerable to selective dissolution.

Downslope transportation and reworking create crucial contamination problems resulting in displacement of species. Older individuals may be transported and reworked in younger sediments, and taxa belonging to different depth environments may be mixed (Figure 17). Reworking can be better understood with biostratigraphy studies.

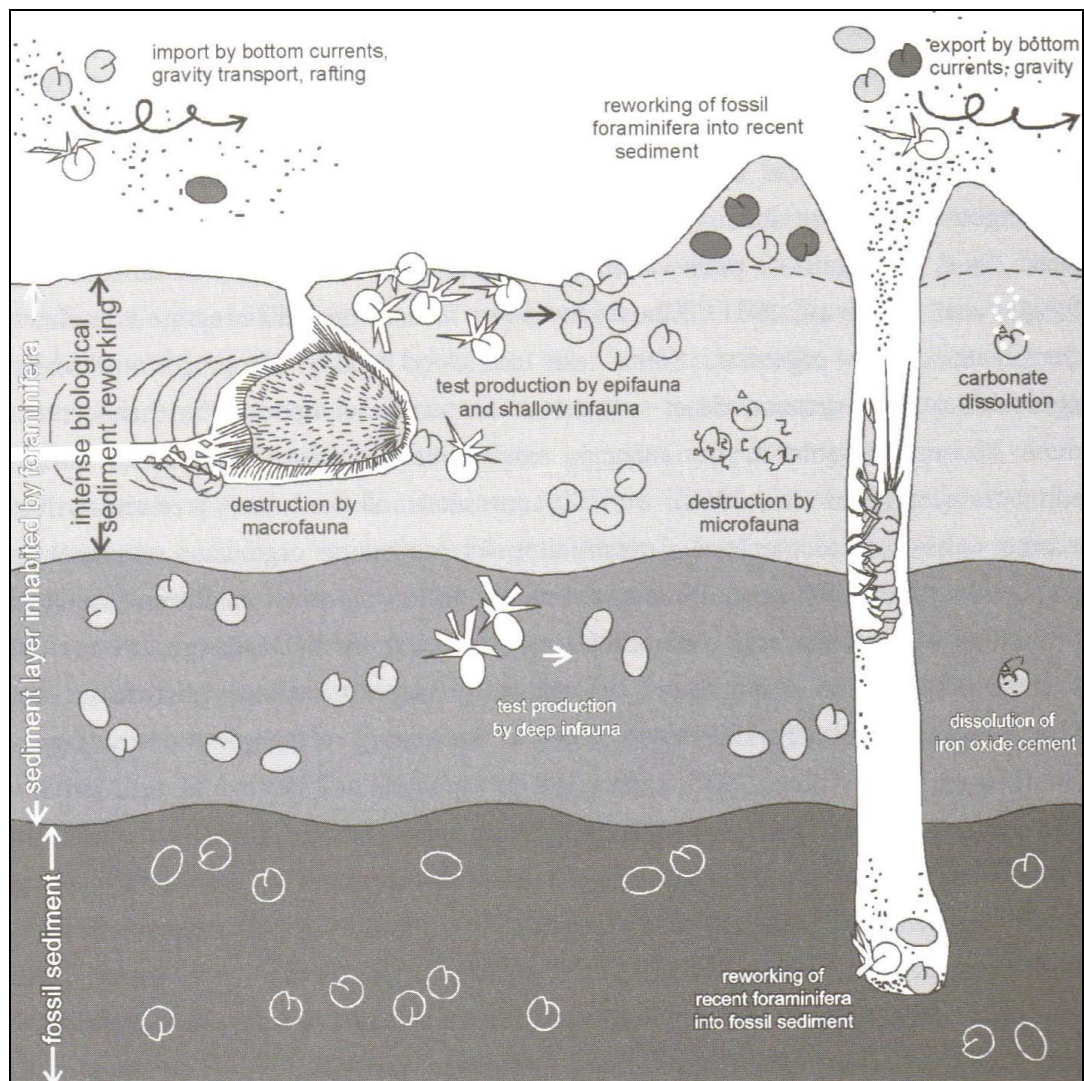


**Figure 17:** Overview of processes affecting the generation of the benthic foraminiferal assemblage (De Stigter et al., 1996)

Downslope transportation can be recognized by comparing benthic species. Shallower water benthic species may be transported to deeper parts where they are not expected to live (Bandy & Arnal, 1960). If this is dominant case for an individual sample, it is discarded. Samples, containing high amounts of quartz grains or rock fragments or size sorting of the foraminifers and sediment grains, an evidence for transportation, are also discarded (Van Hinsbergen et al., 2005). In addition, below 50 m water depth, transportation can occur in an opposite direction due to storms. In this case, taxa living in deeper settings can be seen in the shallower levels (Hohenneger, 2005; Perez-Asensio et al., 2014).

Samples, which are dominated by deep infaunal benthic species, are evidence for anoxic or dysoxic environments (Van der Zwaan et al., 1990). In addition, these environments can be recognized by low diversity of benthic species. Deep infaunal benthic species are considered stress markers, and are also excluded from the calculation (Van Hinsbergen et al., 2005).

### **3.4 Stress Markers**

Benthic species live on or in the sea floor sediment; however, depth in sediment could vary according to available food and oxygen. It was mentioned that organic flux and depth can be correlated by using planktonic foraminifer ratio to total foraminifer assemblage. However, not all of benthic species are used in this correlation. Epifaunal benthic species, living on top of the sediment, are used due to dependency on the organic flux. The rest of the benthic species, the infaunal ones live in deeper parts of the sediments. They are not primarily affected by food supply (Van der Zwaan et al., 1990; Van Hinsbergen et al., 2005; Hohennegger, 2005).

It is generally accepted that oxygen and organic flux are two factors which act together. Increasing organic flux needs more oxygen (Figure 18, Jorriksen et al., 1995) Even though abundance of benthic species may vary according to food flux; anoxic environments determine the presence/absence of these species. While it is hard to find epifaunal benthic species in anoxic environments, infaunal ones dominate and cause disturbance in P/B distribution (Van der Zwaan, 1990; Jorriksen et al., 1995; Van

der Zwaan et al., 1999; Den Dulk et al., 2000; Van Hinsbergen et al., 2005; Kouwenhoven and Van der Zwaan, 2006; Nguyen and Spejier, 2014).

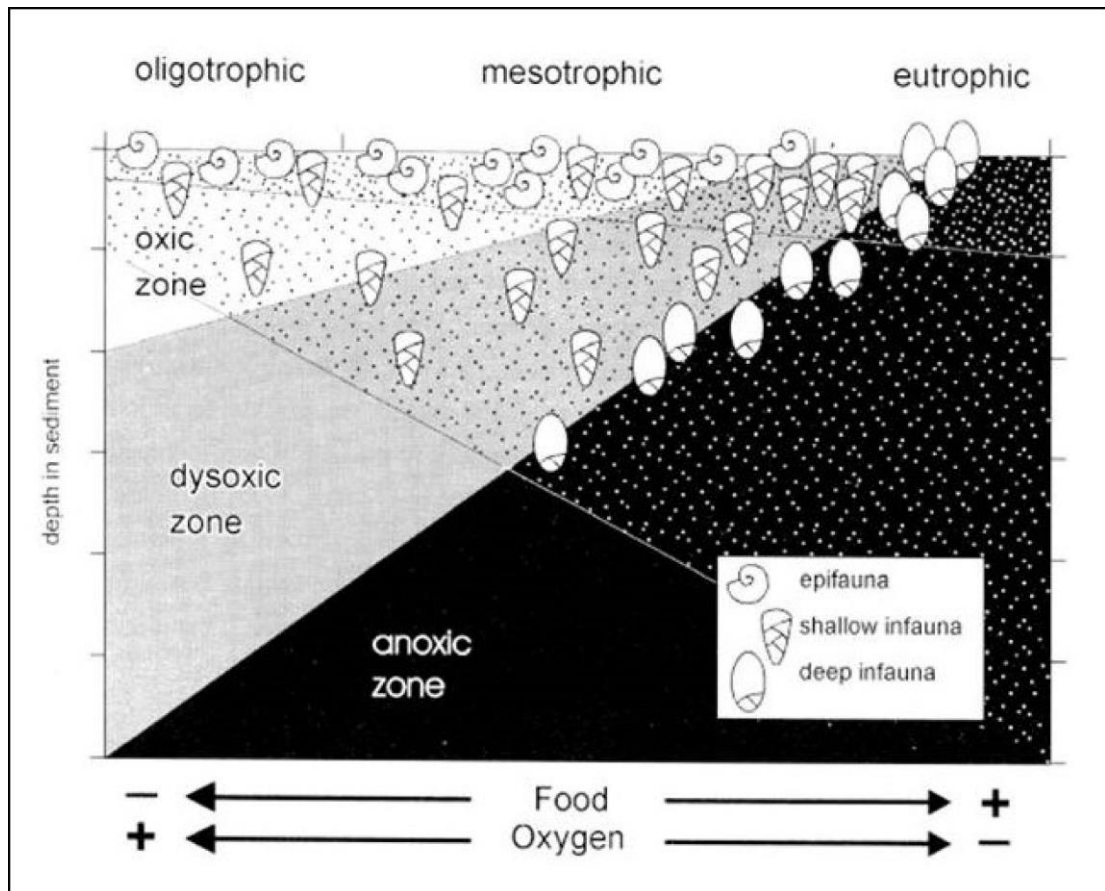


**Figure 18:** Living depth of the benthic foraminiferal in terms of food availability and oxygen concentration. (Jorissen et al., 1995; Van der Zwaan et al., 1999)

Van der Zwaan et al. (1990) discarded the benthic genera *Bulimina*, *Globobulimina*, *Bolivina*, *Uvigerina* and *Fursenkoina*. Van Hinsbergen et al. (2005) excluded some *Uvigerina* species from the stress markers and used them as depth marker; *U. semiornata*, *U. peregrina*, *U. proboscidea*, *U. hispida*; *U. semiornata*. In addition to genera *Rectuvigerina*, *Valvulineria*, *Cancris*, *Stainforthia* and *Chilostomella* were added as stress marker. Despite the fact that *Hoeglundina elegans* is an epifauna-shallow infaunal species, it is discarded, because water depth is not a factor that affects the occurrence of *Hoeglundina elegans* (Perez-Asensio, 2012).

According to previous studies *Valvulineria*, *Bulimina*, *Globobulimina*, and *Bolivina* (see Appendix C and D) species were used as stress marker. *Uvigerina* species are also used as a stress marker, because of that *Uvigerina* species tolerates the low oxygen environment (Schweizer, 2006).

### **3.5 %P and Depth Results**

The results of %P obtained from the GÖM section are used in depth equation of Van der Zwaan et al. (1990). Figure 19 shows the relation with the stratigraphic section. In this section, %P of all counted samples are greater than 95% and the calculated depth ranges between 1070 m to 1150 m (see also Appendix B for calculated values). %P and depth graphs of the stratigraphic sections from Aksu (IS) are shown in Figure 20 (see also Appendix B for calculated values). In the Aksu section, the general trend of sea level is shallowing with respect to %P, while the grain size of the sediments is coarsening upward towards the top of the section.

### **3.6 Taxonomic check**

A quantitative calculation of foraminiferal data, based on %P, should be checked with qualitative data based on benthic species. It is vital for reliability to compare the results with depth markers. As mentioned before, using benthic species in %P calculation must related specific water depth range (Figure 21). However, absence or presence of the depth markers may associated to changing depth as well as other environmental conditions (Van Hinsbergen, 2005; Perez and Asensio, 2012).

Benthic species showing a wide depth range occurrence are not useful for paleobathymetry (Perez and Asensio, 2012). Van Hinsbergen et al. (2005) show the depth range of marker species, common in the Mediterranean. *Gyroidina* species may show occurrence from outer neritic to lower bathyal depth, from 100 m to 5000 m (Perez and Asensio, 2012). *Gyroidina* species are present in both the Gömbe and Aksu sections, so, they are not useful for any correlation. Both the genus *Anomalinoidea* and genus the *Lenticulina* are not useful for paleobathymetry either, due to the fact that they are genera, not species; and have wide bathymetric ranges.

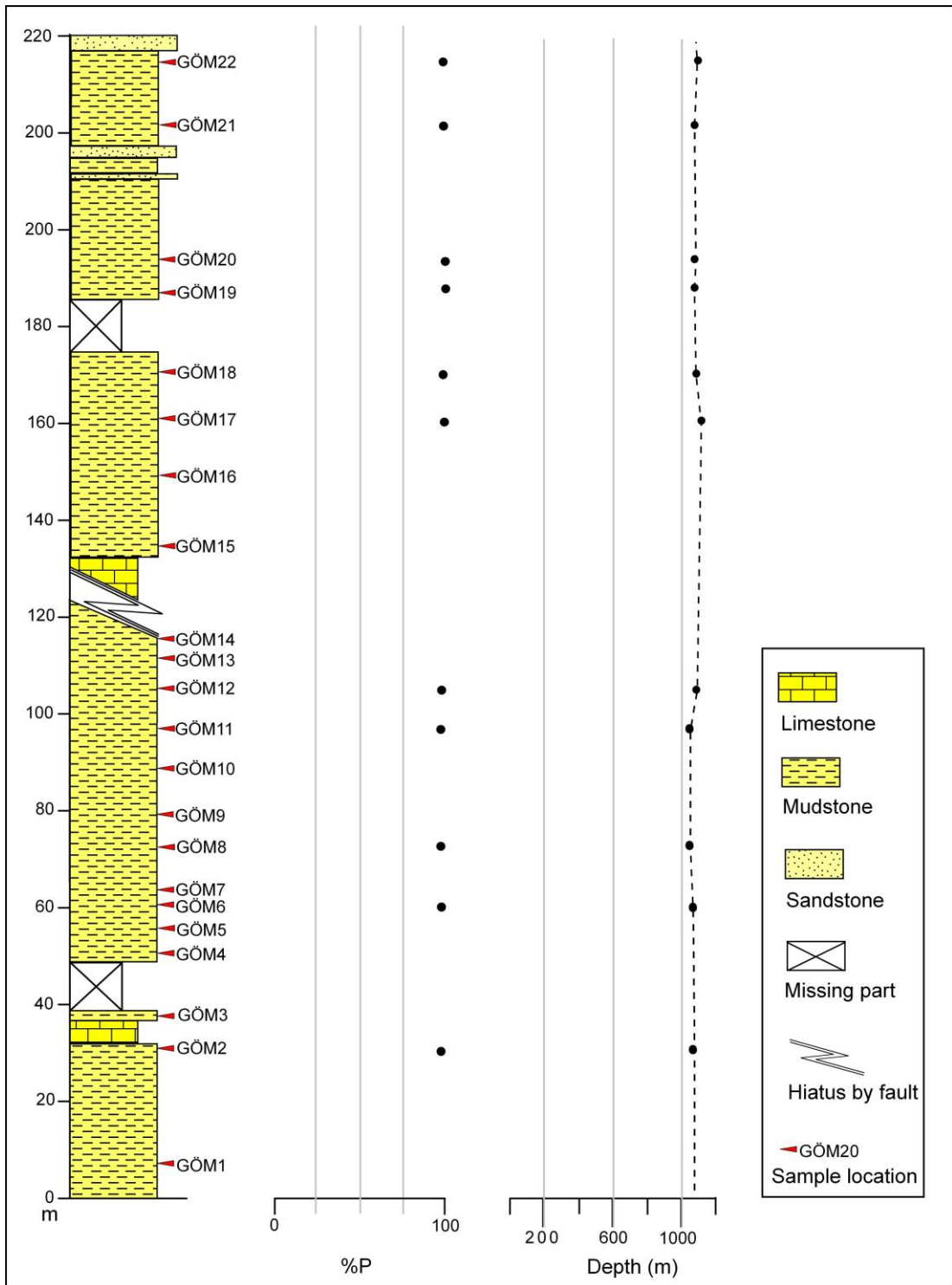


**Figure 19:** %P and depth graphics with the stratigraphic sections from GÖM section (see also Appendix B for calculated values)

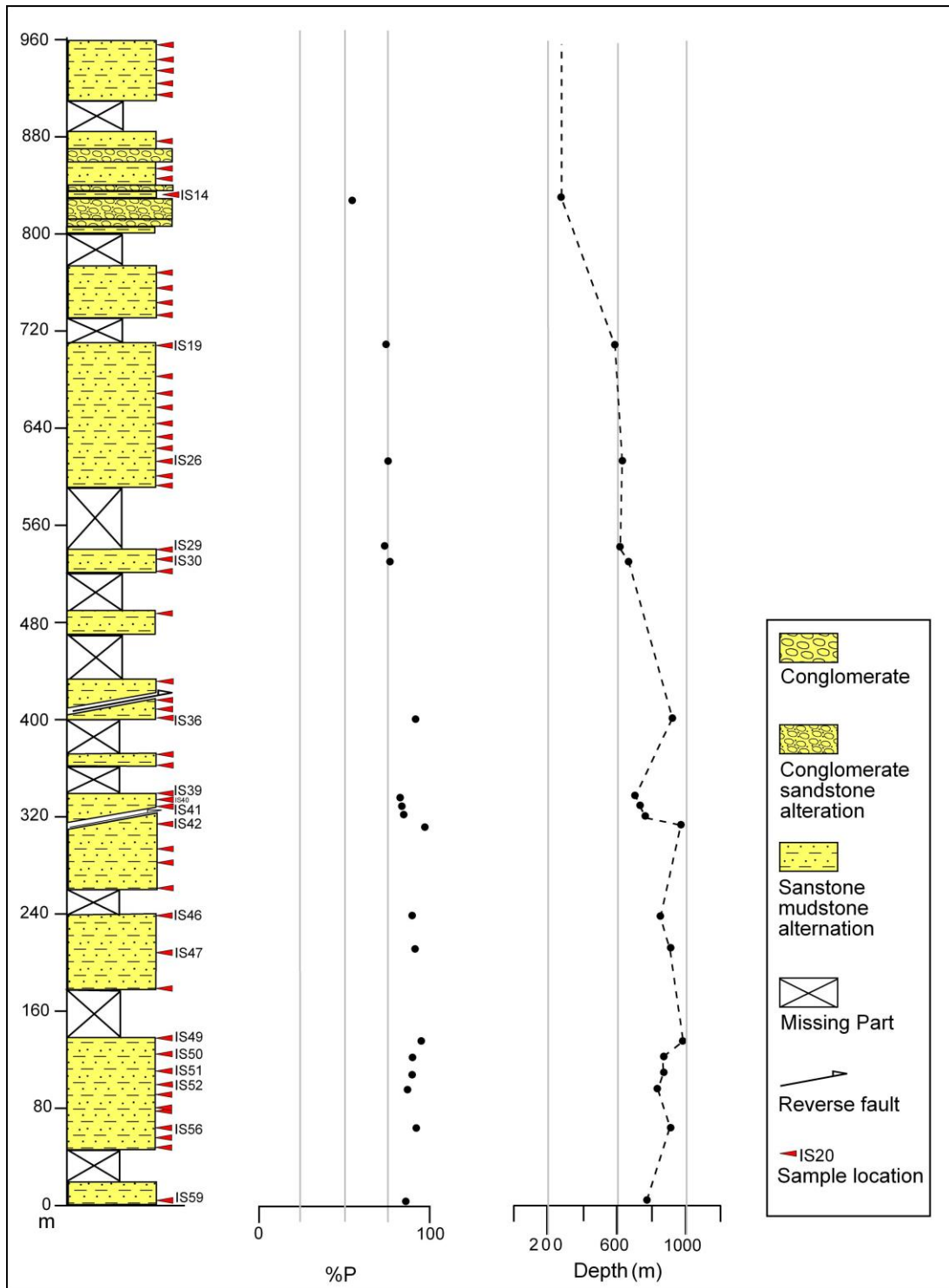


**Figure 20:** %P and depth graphics with the stratigraphic sections from IS section (see also Appendix B for calculated values)

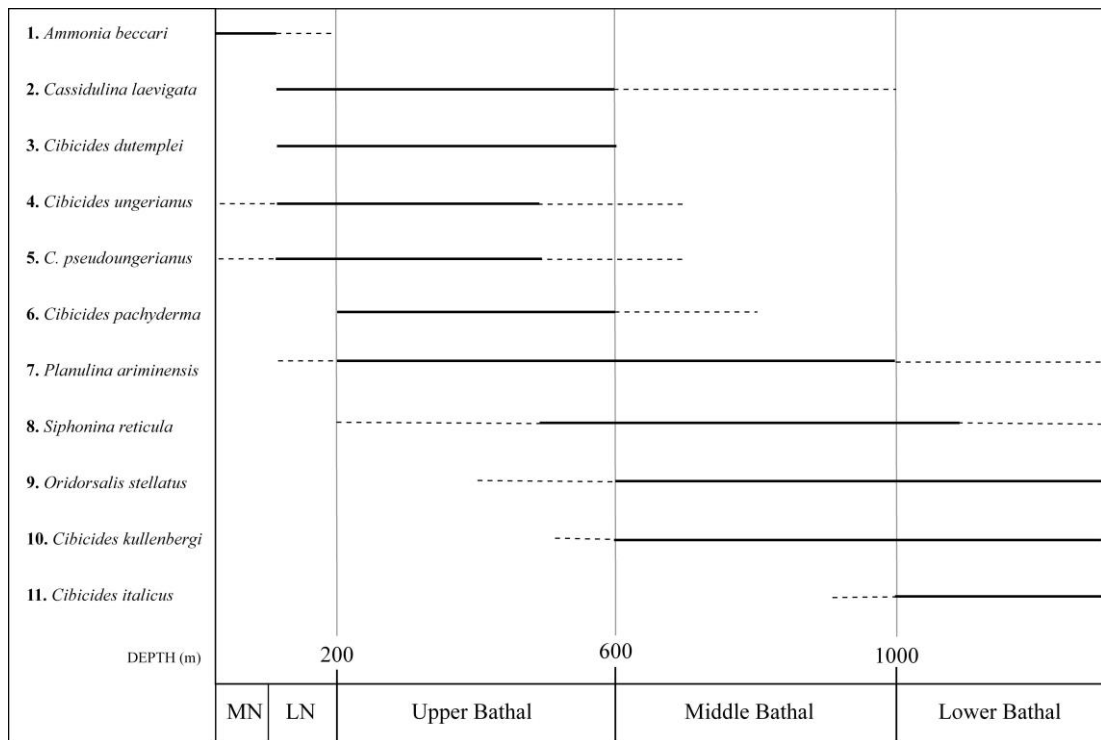


**Figure 21:** Depth range of the marker species (Modified from Van Hinsbergen et al.2005). (See also Chapter 4)

Depth results from %P are compared to depth markers and they are illustrated for both Gömbe and Aksu Basins on the Figure 22 and Figure 23, respectively. In the Gömbe section, the calculated depth is always above the thousand meters. Depth ranges that were derived from depth markers, confirm the depth from %P. Moreover, the presence of *Cibicides italicus* narrows down the range of depth, due to fact that it indicates deeper than 1000 m (Schweizer, 2006). In Aksu section, sample, coded as IS-31, is discarded due to fact that carbonate dissolution, it is not possible that depth result is less than 200 m, according to depth marker content. In spite of the fact that, samples, coded as IS-49 and IS-52, are within confidence limit, they have to be deeper compared to the depth derived from the %P, because the upper depth limit of *Cibicides italicus* is around the 1000 m.

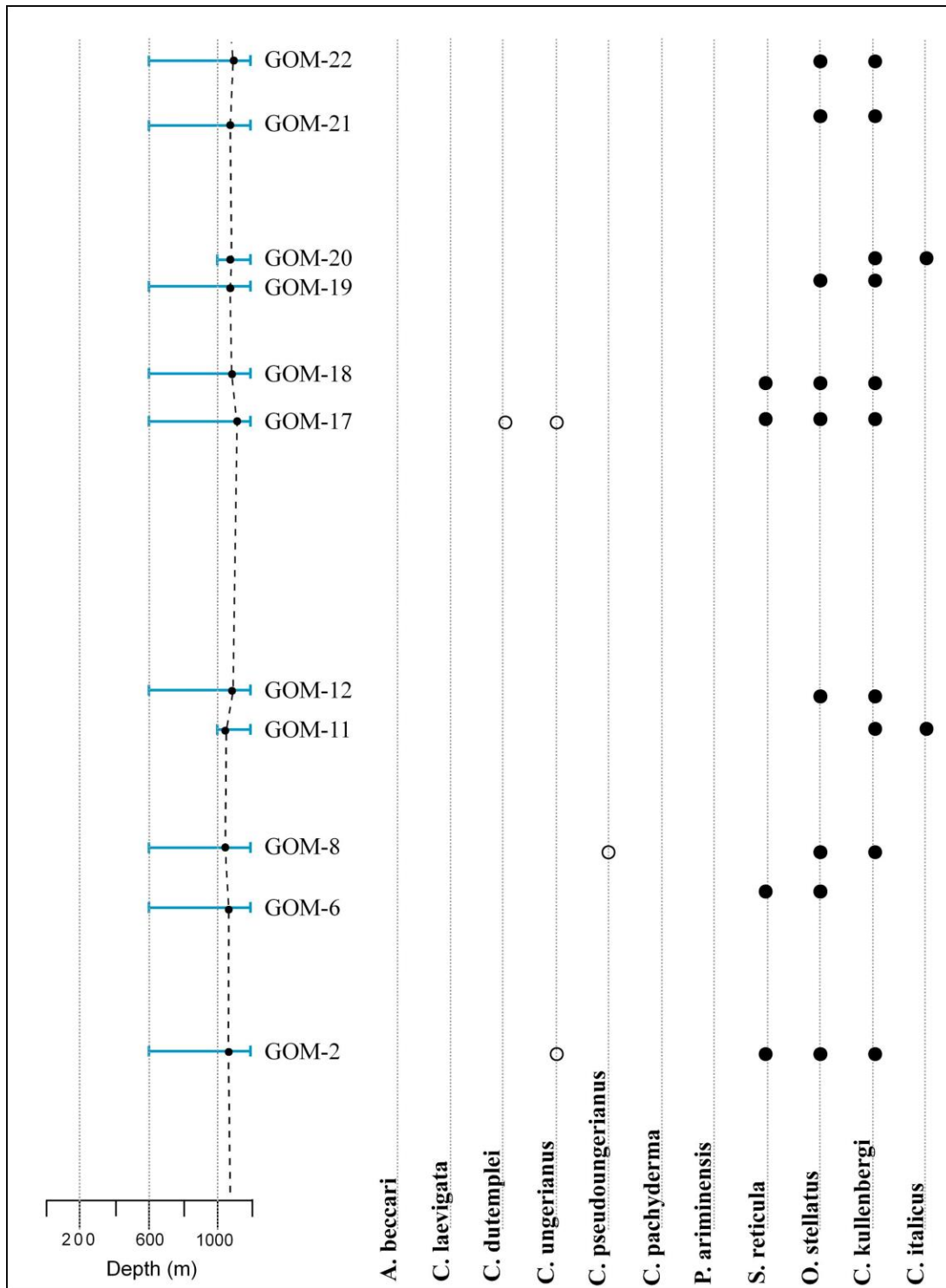


**Figure 22:** Depth ranges, indicated with blue color, according to depth markers from Gömbe Basin.

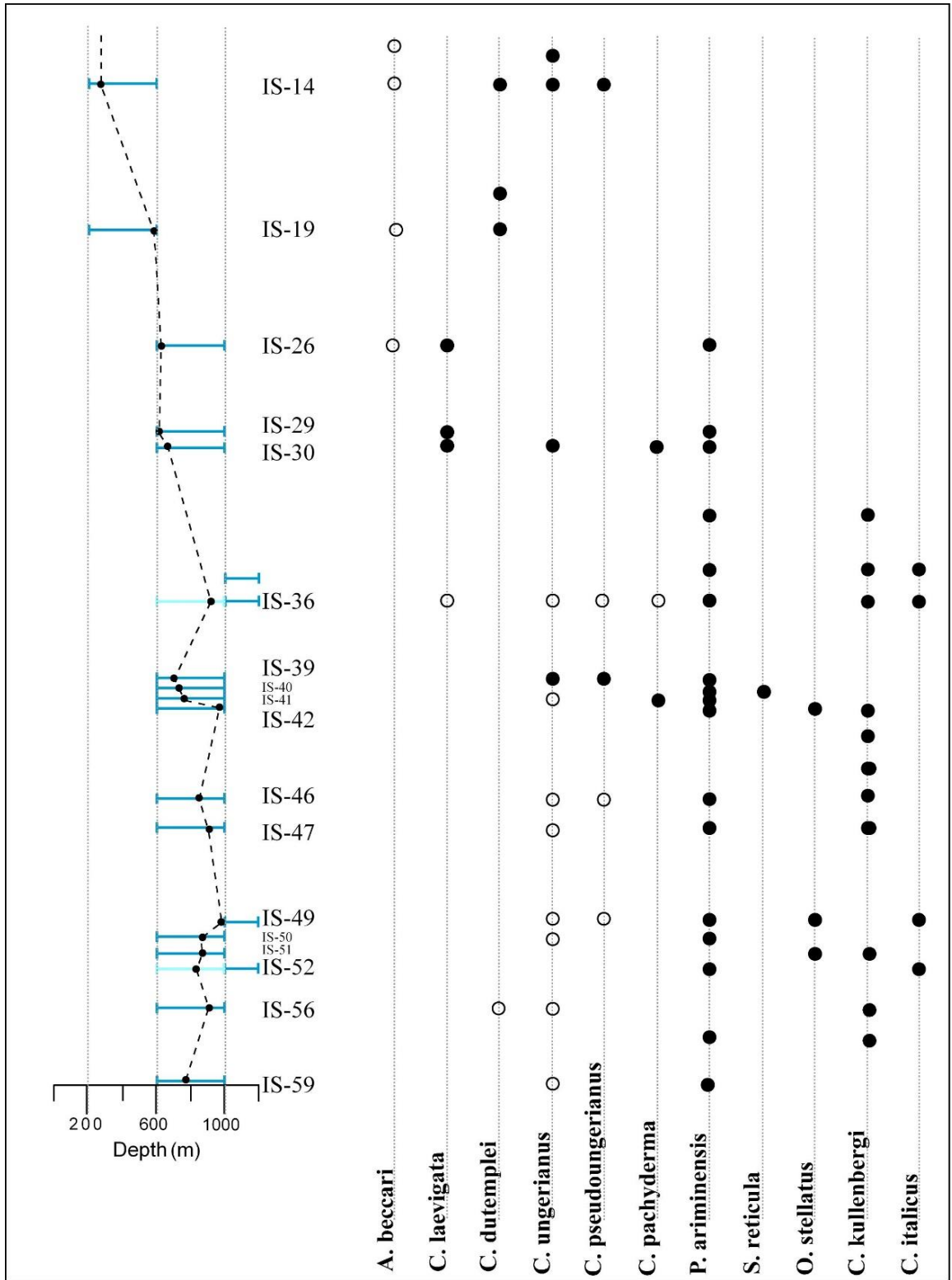


**Figure 23:** Depth ranges, indicated with blue color, according to depth markers from Aksu Basin.



## CHAPTER 4

### DISCUSSION

The Miocene evolution of SW Anatolia within the Isparta Angle was studied in the light of the paleobathymetric evolution of two sub-basins. One of them is the Gömbe sector of the Lycian Foreland Basin, on the Beydağları Platform which is tectonically overlain by the Lycian Nappes. The other is the Aksu Foreland Basin deposited in front of the Aksu Thrust.

Paleobathymetric study was conducted in order to understand the depositional environment and subsidence history of the basins. Moreover, these results provides an opportunity to better understand the thrusting mechanism of the basins and the Miocene evolution of the Isparta Angle as a whole.

In this study, paleobathymetry method, based on the percentage of planktonic foraminifera with respect to the total foraminifer assemblage, proposed by Van Hinsbergen (2005), was used. The depositional depth of the basins was derived from %P from suitable samples. Confidence limits of these quantitative results were verified and validated using specific benthic depth markers.

Resolution of quantitative paleobathymetry is based on the number of samples covering a time interval; each sample gives a depth result from %P and makes drawing “paleobathymetry curve” possible (Van Hinte, 1978). To obtain more detailed results, the numbers of samples can be increased for a given time interval (Van Hinsbergen et al., 2005). 116 and 59 samples was collected as indicated on the constructed

stratigraphic sections (Figure 5 and Figure 10). Discarding samples decreased the resolution of the study. Nevertheless, obtained paleodepth results from %P covered the section GÖM and IS.

In this study, depositional time of the basins was taken into account according to formation which they belong, based on the literature. The age of the bottom level of the Gömbe section (GÖM) is Late Burdigalian to Early Langhian (Şenel, 2004), and the age of the Aksu section (IS) is Serravalian to Tortonian (Çiner et al., 2008). The main limitation of the study is that there is not significant chronostratigraphic correlation on the measured sections. Obtained paleodepth results are interpreted in compliance with this frame.

At the top and middle of the Gömbe section (GB), the paleobathymetry could not be constructed due to absence of the foraminiferal fauna. This part is dominated by quartz and rock fragments, and well sorting was observed in some of the levels indicating current deposition. Calculated depth levels of the base of the section (GÖM) were deeper than the thousand meter and this was confirmed by the presence of *Cibicides italicus*.

Global eustatic sea level was falling as indicated in Figure 24, from 20 Ma to 13.8 Ma (Burdigalian to Langhian) in general trend (Haq et al, 1988). Supposed that there was not any global sea level change during Upper Burdigalian to Lower Langhian, sedimentation rate was almost equal to subsidence rate in the Gömbe Basin. This process was continued by higher sedimentation rate, and turbidites had been deposited until the end of Langhian during the emplacement of the Lycian Nappes on the Beydağları platform (Hayward 1984, Poisson et al., 2003).

At the bottom of the Aksu section (IS), the paleodepth was middle bathyal range. The paleodepth reached thousand meters, lower bathyal range, at some levels where the *Cibicides italicus* is present. In the middle bathyal range *Cibicides kullenbergi*, *Oridorsalis stellatus*, *Siphonina reticula*, *Planulina arminensis* co-occur. Depositional depth range changed middle bathyal to upper bathyal. Upper bathyal range contains *Planulina arminensis*, *Cibicides pachyderma*, *Cibicides ungerianus*, *Cibicides pseudoungerianus*, *Cibicides dutemplei*, *Casudulina levigata*. At the top of the section, size distribution was coarser, and the turbiditic activities increased. Depth results

could not be obtained from bottom levels. Nevertheless, it can be deduced from general trend that depositional depth went to shallower from bottom to top.

Global eustatic sea level change is indicated on Figure 24 for Aquitanian to Tortonian (Haq et al., 1988). Shallowing of the depositional depth was greater than the global eustatic sea level change. Even if global sea level change is taken into account during that time, rate of sedimentation exceeded the rate of subsidence in the middle and upper level of the Aksu Basin. Rate of subsidence, related possibly with the Aksu Thrust, get slower at the Tortonian time.

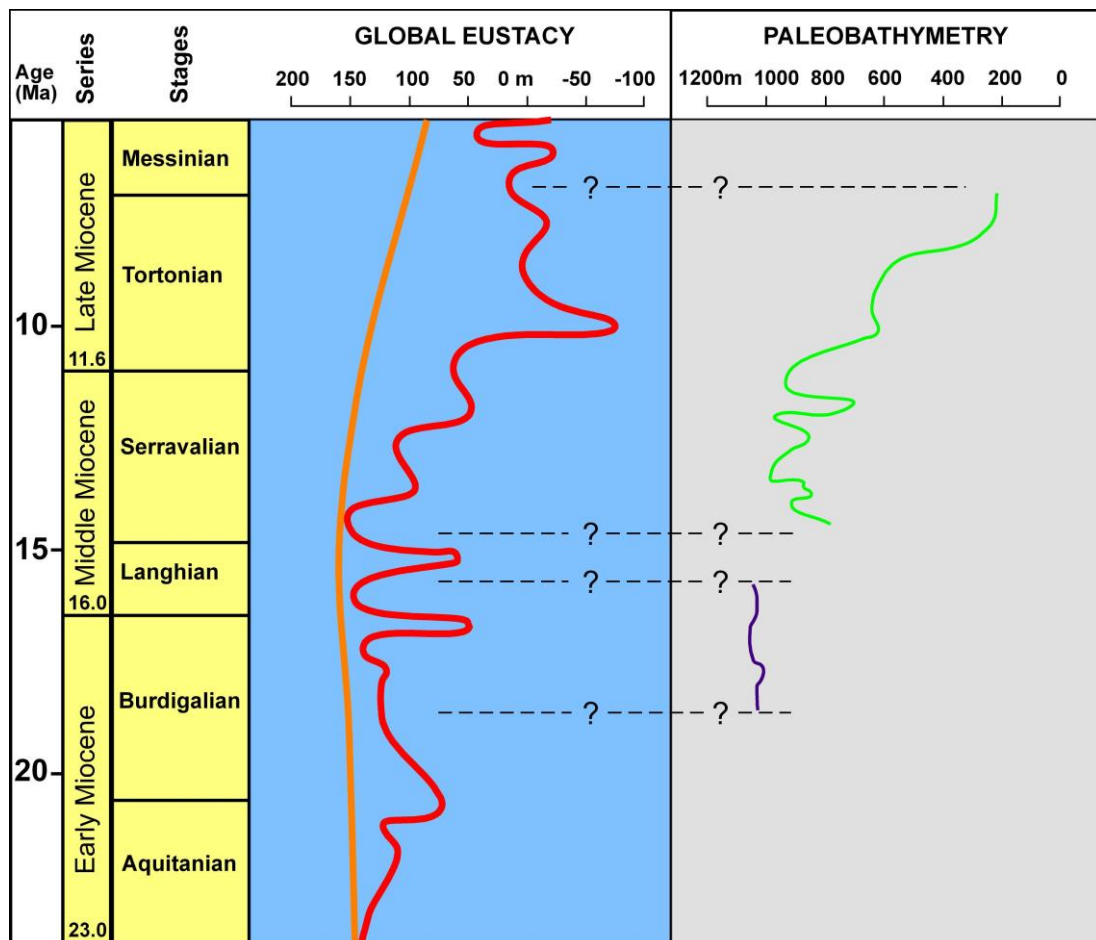


**Figure 24:** Global eustatic sea level change in Miocene (Haq et al., 1988). Red line is short term, orange line is long term sea level change (Modified from Haq et al., 1988) Paleobathymetry curves of the Gömbe (purple line) and Aksu (green line) Basins.



## CHAPTER 5

### CONCLUSIONS

The main work performed in the context of this thesis produced following conclusions;

Stratigraphy and paleobathymetry of the Gömbe indicates:

1. Depositional depths were deeper than thousand meters;
2. If the global sea level was assumed to be fixed, sedimentation rate was almost equal to subsidence rate.
3. This process was attained by high sedimentation rate by turbidites.

Stratigraphy and paleobathymetry of the Aksu basin indicates:

4. Depositional depth were shallowing as a general trend;
5. Shallowing of the depositional depth is more than the falling of the eustatic sea level during Serravallian to Tortonian;
6. Rate of sedimentation exceeded the rate of subsidence in the middle part of the Aksu Basin.
7. Subsidence rate decreased during Tortonian.



## REFERENCES

- Akay, E., & Uysal, Ş. (1988). Post-Eocene tectonics of the central Taurus Mountains. *Mineral Res. Expl. Bull*, 108, 23-34.
- Akay, E., Uysal, S., Poisson, A., Cravatte, J., & Müller, C. (1985). Antalya Neojen havzasının stratigrafisi. *TJK Bülteni*, 28(2), 105-121.
- Alçıçek, M. C., Ten Veen, J. H., & Özkul, M. (2006). Neotectonic development of the Çameli basin, southwestern Anatolia, Turkey. *Geological Society, London, Special Publications*, 260(1), 591-611.
- Alçıçek, M. C., Brogi, A., Capezzuoli, E., Liotta, D., & Meccheri, M. (2013). Superimposed basin formation during Neogene–Quaternary extensional tectonics in SW-Anatolia (Turkey): insights from the kinematics of the Dinar Fault Zone. *Tectonophysics*, 608, 713-727.
- Allen, P. A. & Allen, J. R. 1990. Basin Analysis: Principles and Applications. Blackwell Scientific Publications, Oxford, 451p.
- Aral, İ. (1989). Geology of the Menderes Massif and the Lycian Nappes south of Denizli, western Taurides.
- Bandy, O. L. (1953). Ecology and paleoecology of some California foraminifera. Part I. The frequency distribution of recent foraminifera off California. *Journal of Paleontology*, 161-182.
- Bandy, O. L., & Arnal, R. E. (1960). Concepts of foraminiferal paleoecology. *AAPG bulletin*, 44(12), 1921-1932.
- Bandy, O. L., & Chierici, M. A. (1966). Depth-temperature evaluation of selected California and Mediterranean bathyal foraminifera. *Marine Geology*, 4(4), 259-271.

- Barun, K. (1999). *Modern foraminifera* (pp. 1-6). B. K. S. Gupta (Ed.). Dordrecht: Kluwer Academic Publishers.
- Berger, W. H., & Diester-Haass, L. (1988). Paleoproductivity: the benthic/planktonic ratio in foraminifera as a productivity index. *Marine Geology*, 81(1-4), 15-25.
- Berggren, W. A., & Miller, K. G. (1989). Cenozoic bathyal and abyssal calcareous benthic foraminiferal zonation. *Micropaleontology*, 308-320.
- Blumenthal, M.M., 1963. Le système structural du Taurus sud Anatolies. Bull. Soc. Géol. Fr. (Livre à Mémoire de Professor P. Fallot, Mémoir hors-série)1, 611–662.
- Celâl, A. M., & Yilmaz, Y. (1981). Tethyan evolution of Turkey: a plate tectonic approach. *Tectonophysics*, 75(3-4), 181193203-190199241.
- Collins, A. S., & Robertson, A. H. (1998). Processes of Late Cretaceous to Late Miocene episodic thrust-sheet translation in the Lycian Taurides, SW Turkey. *Journal of the Geological Society*, 155(5), 759-772.
- Corliss, B. H. (1991). Morphology and microhabitat preferences of benthic foraminifera from the northwest Atlantic Ocean. *Marine micropaleontology*, 17(3-4), 195-236.
- Çetinkaplan, M., Pourteau, A., Candan, O., Koralay, O. E., Oberhänsli, R., Okay, A. I., ... & Şengün, F. (2016). P–T–t evolution of eclogite/blueschist facies metamorphism in Alanya Massif: time and space relations with HP event in Bitlis Massif, Turkey. *International Journal of Earth Sciences*, 105(1), 247-281.
- Çiner, A., Karabiyikoğlu, M., Monod, O., Deynoux, M., & Tuzcu, S. (2008). Late Cenozoic Sedimentary Evolution of the Antalya Basin, Southern Turkey. *Turkish Journal of Earth Sciences*, 17(1).
- De Rijk, S., Jorissen, F. J., Rohling, E. J., & Troelstra, S. R. (2000). Organic flux control on bathymetric zonation of Mediterranean benthic foraminifera. *Marine Micropaleontology*, 40(3), 151-166.

- De Stigter, H. C. (1996). Recent and fossil benthic foraminifera in the Adriatic Sea: distribution patterns in relation to organic carbon flux and oxygen concentration at the seabed. *Faculteit Aardwetenschappen*.
- Den Dulk, M., Reichart, G. J., Van Heyst, S., Zachariasse, W. J., & Van der Zwaan, G. J. (2000). Benthic foraminifera as proxies of organic matter flux and bottom water oxygenation? A case history from the northern Arabian Sea. *Palaeogeography, Palaeoclimatology, Palaeoecology*, 161(3), 337-359.
- Deynoux, M., Çiner, A., Monod, O., Karabıyıkoglu, M., Manatschal, G., & Tuzcu, S. (2005). Facies architecture and depositional evolution of alluvial fan to fan-delta complexes in the tectonically active Miocene Köprüçay Basin, Isparta Angle, Turkey. *Sedimentary Geology*, 173(1), 315-343.
- Diester-Haass, L. (1988). Sea level changes, carbonate dissolution and history of the Benguela Current in the Oligocene-Miocene off Southwest Africa (DSDP Site 362, Leg 40). *Marine Geology*, 79(3-4), 213-242.
- Dulk, M. D. (2000). *Benthic foraminiferal response to Late Quaternary variations in surface water productivity and oxygenation in the northern Arabian Sea* (Doctoral dissertation, Utrecht University).
- Dumont, J. F., Gutnic, M., Marcoux, J., Monod, O., & Poisson, A. (1972). Le Trias des Taurides occidentales (Turquie) Definition du bassin pamphylien: Un nouveau domaine à ophiolithes à la marge externe de la chaîne taurique. *Zeitschrift der Deutschen Geologischen Gesellschaft*, 385-409.
- Faccenna, C., Bellier, O., Martinod, J., Piromallo, C., & Regard, V. (2006). Slab detachment beneath eastern Anatolia: A possible cause for the formation of the North Anatolian fault. *Earth and Planetary Science Letters*, 242(1), 85-97.
- Flecker, R., Ellam, R. M., Müller, C., Poisson, A., Robertson, A. H. F., & Turner, J. (1998). Application of Sr isotope stratigraphy and sedimentary analysis to the origin and evolution of the Neogene basins in the Isparta Angle, southern Turkey. *Tectonophysics*, 298(1), 83-101.

- Flecker, R., Poisson, A., & Robertson, A. H. F. (2005). Facies and palaeogeographic evidence for the Miocene evolution of the Isparta Angle in its regional eastern Mediterranean context. *Sedimentary Geology*, 173(1), 277-314.
- Gibson, T. G. (1989). Planktonic benthonic foraminiferal ratios: modern patterns and Tertiary applicability. *Marine Micropaleontology*, 15(1-2), 29-52.
- Glover, C. P., & Robertson, A. H. (1998). Role of regional extension and uplift in the Plio-Pleistocene evolution of the Aksu Basin, SW Turkey. *Journal of the Geological Society*, 155(2), 365-387.
- Green, O. R., (2001). A Manual of Practical Laboratory and Field Techniques in Palaeobiology. Kluwer Academic Publishers, Dordrecht.
- Grimsdale, T. F., & Van Morkhoven, F. P. C. M. (1955, January). 4. The Ratio between Pelagic and Benthonic Foraminifera as a Means of Estimating Depth of Deposition of. *In 4th World Petroleum Congress*. World Petroleum Congress.
- Gupta, A. K. (1994). Taxonomy and bathymetric distribution of Holocene deep-sea benthic foraminifera in the Indian Ocean and the Red Sea. *Micropaleontology*, 351-367.
- Hall, J., Aksu, A. E., King, H., Gogacz, A., Yaltrak, C., & Çifçi, G. (2014). Miocene–Recent evolution of the western Antalya Basin and its linkage with the Isparta Angle, eastern Mediterranean. *Marine Geology*, 349, 1-23.
- Haq, B. U., Hardenbol, J., & Vail, P. R. (1987). Chronology of fluctuating sea levels since the Triassic. *Science*, 235(4793), 1156-1167.
- Hayward, A. B., & Robertson, A. H. F. (1982). Direction of ophiolite emplacement inferred from Cretaceous and Tertiary sediments of an adjacent autochthon, the Bey Dağları, southwest Turkey. *Geological Society of America Bulletin*, 93(1), 68-75.
- Hayward, A. B. (1984). Miocene clastic sedimentation related to the emplacement of the Lycian Nappes and the Antalya Complex, SW Turkey. *Geological Society, London, Special Publications*, 17(1), 287-300.

- Hohenegger, J. (2005). Estimation of environmental paleogradient values based on presence/absence data: a case study using benthic foraminifera for paleodepth estimation. *Palaeogeography, Palaeoclimatology, Palaeoecology*, 217(1), 115-130.
- Hohenegger, J., Andersen, N., Baldi, K., Ćorić, S., Pervesler, P., Rupp, C., & Wagreich, M. (2008). Paleoenvironment of the Early Badenian (Middle Miocene) in the southern Vienna Basin (Austria)—multivariate analysis of the Baden-Sooss section. *Geologica Carpathica*, 59, 461-487.
- Hüsing, S. K., Zachariasse, W. J., Van Hinsbergen, D. J., Krijgsman, W., Inceöz, M., Harzhauser, M., ... & Kroh, A. (2009). Oligocene–Miocene basin evolution in SE Anatolia, Turkey: constraints on the closure of the eastern Tethys gateway. *Geological Society, London, Special Publications*, 311(1), 107-132.
- Iaccarino, S. M., Cita, M. B., Gaboardi, S., & Gruppini, G. M. (1999). 15. High-Resolution Biostratigraphy at the Miocene/Pliocene boundary in Holes 974b and 975b, Western Mediterranean1. *In Proceedings of the Ocean Drilling Program: Scientific Results* (Vol. 161, p. 197).
- İslamoğlu, Y. (2001). The molluscan fauna and stratigraphy of Antalya Miocene basin (West-Central Taurids, SW Turkey). *Bulletin of the Mineral Research and Exploration*, 123(124), 27-58.
- İslamoğlu, Y., & Taner, G. (2002). Molluscan fauna and stratigraphy of the Uçarsu and Kasaba formations at Kasaba Miocene basin (western Taurides, SW Turkey). *Bulletin of Mineral Research and Exploration*, 125, 31-57.
- İşler, F. I., Aksu, A. E., Hall, J., Calon, T. J., & Yaşar, D. (2005). Neogene development of the Antalya Basin, Eastern Mediterranean: An active forearc basin adjacent to an arc junction. *Marine geology*, 221(1), 299-330.
- Jonkers, H. A. (1984). *Pliocene benthonic foraminifera from homogeneous and laminated marls on Crete* (Doctoral dissertation, Utrecht University).

- Jorissen, F. J. (1987). The distribution of benthic foraminifera in the Adriatic Sea. *Marine Micropaleontology*, 12, 21-48.
- Jorissen, F. J. (1988). *Benthic foraminifera from the Adriatic Sea: principles of phenotypic variation* (Doctoral dissertation, Utrecht University).
- Jorissen, F. J., de Stigter, H. C., & Widmark, J. G. (1995). A conceptual model explaining benthic foraminiferal microhabitats. *Marine micropaleontology*, 26(1-4), 3-15.
- Karabıyıkoglu, M., Çiner, A., Monod, O., Deynoux, M., Tuzcu, S., & Örcen, S. (2000). Tectonosedimentary evolution of the Miocene Manavgat Basin, western Taurides, Turkey. *In Tectonics and magmatism in Turkey and the surrounding area* (Vol. 173, pp. 271-294). Geological Society of London Special Publication.
- Karabıyıkoglu, M., Tuzcu, S., Çiner, A., Deynoux, M., Örcen, S., & Hakyemez, A. (2005). Facies and environmental setting of the Miocene coral reefs in the late-orogenic fill of the Antalya Basin, western Taurides, Turkey: implications for tectonic control and sea-level changes. *Sedimentary geology*, 173(1), 345-371.
- Kennedy, A. E., & Coe, A. L. (2014). Development of the freeze–thaw processing technique for disaggregation of indurated mudrocks and enhanced recovery of calcareous microfossils. *Journal of Micropalaeontology*, 2013-020.
- Kissel, C., Averbuch, O., de Lamotte, D. F., Monod, O., & Allerton, S. (1993). First paleomagnetic evidence for a post-Eocene clockwise rotation of the Western Taurides thrust belt east of the Isparta reentrant (Southwestern Turkey). *Earth and Planetary Science Letters*, 117(1-2), 1-14.
- Koç, A., van Hinsbergen, D. J., Kaymakci, N., & Langereis, C. G. (2016). Late Neogene oroclinal bending in the central Taurides: A record of terminal eastward subduction in southern Turkey?. *Earth and Planetary Science Letters*, 434, 75-90.

- Kouwenhoven, T. J. (2000). *Survival under stress: benthic foraminiferal patterns and Cenozoic biotic crises*. Faculteit Aardwetenschappen.
- Kouwenhoven, T. J., & Van der Zwaan, G. J. (2006). A reconstruction of late Miocene Mediterranean circulation patterns using benthic foraminifera. *Palaeogeography, Palaeoclimatology, Palaeoecology*, 238(1), 373-385.
- Lefevre, R. 1967. Un nouvel element de la geologie du Taurus lycien: les nappes d'Antalya (Turquie). C.r. Seances Acad. Sci. Paris 265, 1365-1368.
- Loeblich, A. R. Jr. and Tappan, H., 1988, Foraminiferal genera and their classification, *Von Nostrand Reinhold Company*, New York, 2v, 970 p
- Mackintosh, P. W., & Robertson, A. H. (2009). Structural and sedimentary evidence from the northern margin of the Tauride platform in south central Turkey used to test alternative models of Tethys during Early Mesozoic time. *Tectonophysics*, 473(1), 149-172.
- Meijers, M. J., van Hinsbergen, D. J., Dekkers, M. J., Altner, D., Kaymakçı, N., & Langereis, C. G. (2011). Pervasive Palaeogene remagnetization of the central Taurides fold-and-thrust belt (southern Turkey) and implications for rotations in the Isparta Angle. *Geophysical Journal International*, 184(3), 1090-1112.
- Milker, Y., & Schmiedl, G. (2012). A taxonomic guide to modern benthic shelf foraminifera of the western Mediterranean Sea. *Palaeontologia electronica*, 15(2), 1-134.
- Morris, A., & Robertson, A. H. F. (1993). Miocene remagnetisation of carbonate platform and Antalya Complex units within the Isparta Angle, SW Turkey. *Tectonophysics*, 220(1-4), 243-266.
- Nguyen, T. M. P., & Speijer, R. P. (2014). A new procedure to assess dissolution based on experiments on Pliocene–Quaternary foraminifera (ODP Leg 160, Eratosthenes Seamount, Eastern Mediterranean). *Marine Micropaleontology*, 106, 22-39.

- Okay, A. I., Zattin, M., & Cavazza, W. (2010). Apatite fission-track data for the Miocene Arabia-Eurasia collision. *Geology*, 38(1), 35-38.
- Önalın, M. (1979), Elmalı-Kaş (Antalya) arasındaki bölgenin jeolojisi: *ÜFF Monografileri, PhD Thesis*, 29, 131 s, İstanbul
- Özgül, N. (1976). Toroslar'm bazı temel jeoloji özellikleri. *Bulletin of the Geological Society of Turkey*, 19, 65-78.
- Özgül, N., (1984). Stratigraphy and tectonic evolution of the central Taurus. In: Tekeli, O., Göncüođlu, M.C. (Eds.), *Geology of the Taurus Belt. MTA*, Ankara, pp.77–90.
- Panieri, G., Camerlenghi, A., Conti, S., Pini, G. A., & Cacho, I. (2009). Methane seepages recorded in benthic foraminifera from Miocene seep carbonates, Northern Apennines (Italy). *Palaeogeography, Palaeoclimatology, Palaeoecology*, 284(3), 271-282.
- Pérez-Asensio, J. N., Aguirre, J., Schmiedl, G., & Civis, J. (2012). Messinian paleoenvironmental evolution in the lower Guadalquivir Basin (SW Spain) based on benthic foraminifera. *Palaeogeography, Palaeoclimatology, Palaeoecology*, 326, 135-151.
- Phleger, F. B. (1951). *Foraminifera distribution in some sediment samples from the Canadian and Greenland Arctic*. Scripps Institution of Oceanography of California.
- Poisson, A. 1977, Recherches géologiques dans les Taurides occidentales (Turquie). These, Université de Paris-Sud Faculte des Sciences d'Orsay, 795p.
- Poisson, A., Orszag-Sperber, F., Kosun, E., Bassetti, M. A., Müller, C., Wernli, R., & Rouchy, J. M. (2011). The Late Cenozoic evolution of the Aksu basin (Isparta Angle; SW Turkey). New insights. *Bulletin de la Société Géologique de France*, 182(2), 133-148.
- Poisson, A., Yađmurlu, F., Bozcu, M., & Şentürk, M. (2003a). New insights on the tectonic setting and evolution around the apex of the Isparta Angle (SW Turkey). *Geological Journal*, 38(3-4), 257-282.

- Poisson, A., Wernli, R., Sağular, E. K., & Temiz, H. (2003b). New data concerning the age of the Aksu Thrust in the south of the Aksu valley, Isparta Angle (SW Turkey): consequences for the Antalya Basin and the Eastern Mediterranean. *Geological Journal*, 38(3-4), 311-327.
- Ricou, L. E., Argyriadis, I., & Marcoux, J. E. A. N. (1975). L'Axe Calcaire du Taurus, un alignement de fenêtres arabo-africaines sous des nappes radiolaritiques, ophiolitiques et métamorphiques. *Bulletin de la Société géologique de France*, 7(6), 1024-1044.
- Ricou, L. E., Marcoux, J., & Poisson, A. (1979). L'allochtonie des Bey Dagları orientaux; reconstruction paléogéographique des Taurides occidentales. *Bulletin de la Société Géologique de France*, 7(2), 125-133.
- Robertson, A. H. F., & Woodcock, N. H. (1982). Sedimentary history of the south-western segment of the Mesozoic–Tertiary Antalya continental margin, south-western Turkey. *Eclogae Geologicae Helveticae*, 75(3), 517-562.
- Rouchy, J. M., Caruso, A., Pierre, C., Blanc-Valleron, M. M., & Bassetti, M. A. (2007). The end of the Messinian salinity crisis: evidences from the Chelif Basin (Algeria). *Palaeogeography, Palaeoclimatology, Palaeoecology*, 254(3), 386-417.
- Sagular, E. K. (2009). Fossil didemnid ascidian spicule records in the Plio-Quaternary marine clastics of the Antalya Basin (Eastern Mediterranean) and their stratigraphic calibration to new microfossil data. *Geosciences Journal*, 13(2), 121-131.
- Sagular, E. K., & Çoban, H. (2009). Antalya Neojen havzasındaki tefra ara tabakalı denizel kırıntıların nannofosillere dayanan kronostratigrafisi. *Yerbilimleri Dergisi*, 30(2), 145-167.
- Schweizer, M. (2006). *Evolution and molecular phylogeny of Cibicides and Uvigerina (Rotaliida, Foraminifera)* (Vol. 261). Utrecht University.
- Schweizer, M., Pawlowski, J., Kouwenhoven, T. J., Guiard, J., & van der Zwaan, B. (2008). Molecular phylogeny of Rotaliida (Foraminifera) based on

- complete small subunit rDNA sequences. *Marine Micropaleontology*, 66(3), 233-246.
- Schweizer, M., Pawlowski, J., Kouwenhoven, T., & van der Zwaan, B. (2009). Molecular phylogeny of common cibicidids and related Rotaliida (Foraminifera) based on small subunit rDNA sequences. *The Journal of Foraminiferal Research*, 39(4), 300-315.
- Smitho Jr, F. D. (1955). Planktonic foraminifera as indicators of depositional environment. *Micropaleontology*, 147-151.
- Sprovieri, R., & Hasegawa, S. (1990). Plio-Pleistocene benthic foraminifer stratigraphic distribution in the deep-sea record of the Tyrrhenian Sea (ODP Leg 107). In *Proceedings of the Ocean Drilling Program, Scientific Results* (Vol. 107, pp. 429-459). College Station, TX (Ocean Drilling Program).
- Şenel, M. (2004). Stratigraphic and structural features of the Yeşilbarak Nappe in Western Taurus range and its comparison with the similar units in SE Anatolia and North Cyprus. *Bulletin Of The Mineral Research and Exploration*, 128(128).
- Şengör, A. M. C., Yılmaz, Y., & Sungurlu, O. (1984). Tectonics of the Mediterranean Cimmerides: nature and evolution of the western termination of Palaeo-Tethys. *Geological Society, London, Special Publications*, 17(1), 77-112.
- Şengör, A. M. C., Özeren, S., Genç, T., & Zor, E. (2003). East Anatolian high plateau as a mantle-supported, north-south shortened domal structure. *Geophysical Research Letters*, 30(24).
- Ten Veen, J. T., Boulton, S. J., & Alçiçek, M. C. (2009). From palaeotectonics to neotectonics in the Neotethys realm: The importance of kinematic decoupling and inherited structural grain in SW Anatolia (Turkey). *Tectonophysics*, 473(1), 261-281.

- Ucl.ac.uk. (2018). Foraminifera. [online] Available at: <http://www.ucl.ac.uk/GeolSci/micropal/foram.html> [Accessed 18 Jan. 2018].
- Üner, S., Özsayın, E., Kutluay, A., & Dirik, K. (2015). Polyphase tectonic evolution of the Aksu Basin, Isparta Angle (Southern Turkey). *Geologica Carpathica*, 66(2), 157-169.
- Van der Zwaan, G. J. (1982). *Paleoecology of late Miocene Mediterranean foraminifera* (Doctoral dissertation, Utrecht University).
- Van der Zwaan, G. J., Duijnste, I. A. P., Den Dulk, M., Ernst, S. R., Jannink, N. T., & Kouwenhoven, T. J. (1999). Benthic foraminifers: proxies or problems?: a review of paleocological concepts. *Earth-Science Reviews*, 46(1), 213-236.
- Van der Zwaan, G. J., Jorissen, F. J., & De Stigter, H. C. (1990). The depth dependency of planktonic/benthic foraminiferal ratios: constraints and applications. *Marine Geology*, 95(1), 1-16.
- Van Hinsbergen, D. J. J., Kouwenhoven, T. J., & Van der Zwaan, G. J. (2005). Paleobathymetry in the backstripping procedure: Correction for oxygenation effects on depth estimates. *Palaeogeography, Palaeoclimatology, Palaeoecology*, 221(3), 245-265.
- Van Hinsbergen, D. J., Dekkers, M. J., & Koc, A. (2010). Testing Miocene remagnetization of Bey Dağları: Timing and amount of Neogene rotations in SW Turkey. *Turkish Journal of Earth Sciences*, 19(2), 123-156.
- Van Hinte, J. E. (1978). Geohistory analysis--application of micropaleontology in exploration geology. *AAPG Bulletin*, 62(2), 201-222.
- Van Marle, L. J., Van Hinte, J. E., & Nederbragt, A. J. (1987). Plankton percentage of the foraminiferal fauna in seafloor samples from the Australian-Irian Jaya continental margin, eastern Indonesia. *Marine Geology*, 77(1), 151-156.

- Van Morkhoven, F. P., Berggren, W. A., Edwards, A. S., & Oertli, H. J. (1986). *Cenozoic cosmopolitan deep-water benthic foraminifera* (Vol. 11). Elf Aquitaine.
- Verhallen, P. J. (1991). *Late Pliocene to Early Pleistocene Mediterranean mud-dwelling foraminifera: influence of a changing environment on community structure and evolution* (Doctoral dissertation, Utrecht University).
- Woodcock, N. H., & Robertson, A. H. F. (1982). Wrench and thrust tectonics along a Mesozoic–Cenozoic continental margin: Antalya Complex, SW Turkey. *Journal of the Geological Society*, 139(2), 147-163.
- Woodruff, F., & Douglas, R. G. (1981). Response of deep-sea benthic foraminifera to Miocene paleoclimatic events, DSDP Site 289. *Marine Micropaleontology*, 6(5-6), 617-632.
- Wright, R. (1978). 41. Neogene Paleobathymetry Of The Mediterranean Based On Benthic Foraminifers From Dsdp Leg 42a. (Abstract)
- Wright, R. G. (1977, January). Planktonic-Benthonic Ratio In Foraminifera As Paleobathymetric Tool-Quantitative-Evaluation. In *Aapg Bulletin-American Association Of Petroleum Geologists* (Vol. 61, No. 5, Pp. 842-842). 1444 S Boulder Ave, Po Box 979, Tulsa, Ok 74101: Amer Assoc Petroleum Geologist.

## **APPENDIX A**

### **EDS ANALYSES RESULTS OF SEVERAL GRAINS**

1. Rock grains with calcite matrix from AK-36, Figure 13 (c)
2. Rock grains with calcite matrix from AK-56, Figure 13 (d)
3. Rock grains with calcite matrix from GÖM-12, Figure 13 (b)
4. Black rock fragments from GB-30, Figure 13 (a)
5. Quartz grain from GB-30, Figure 13 (b)

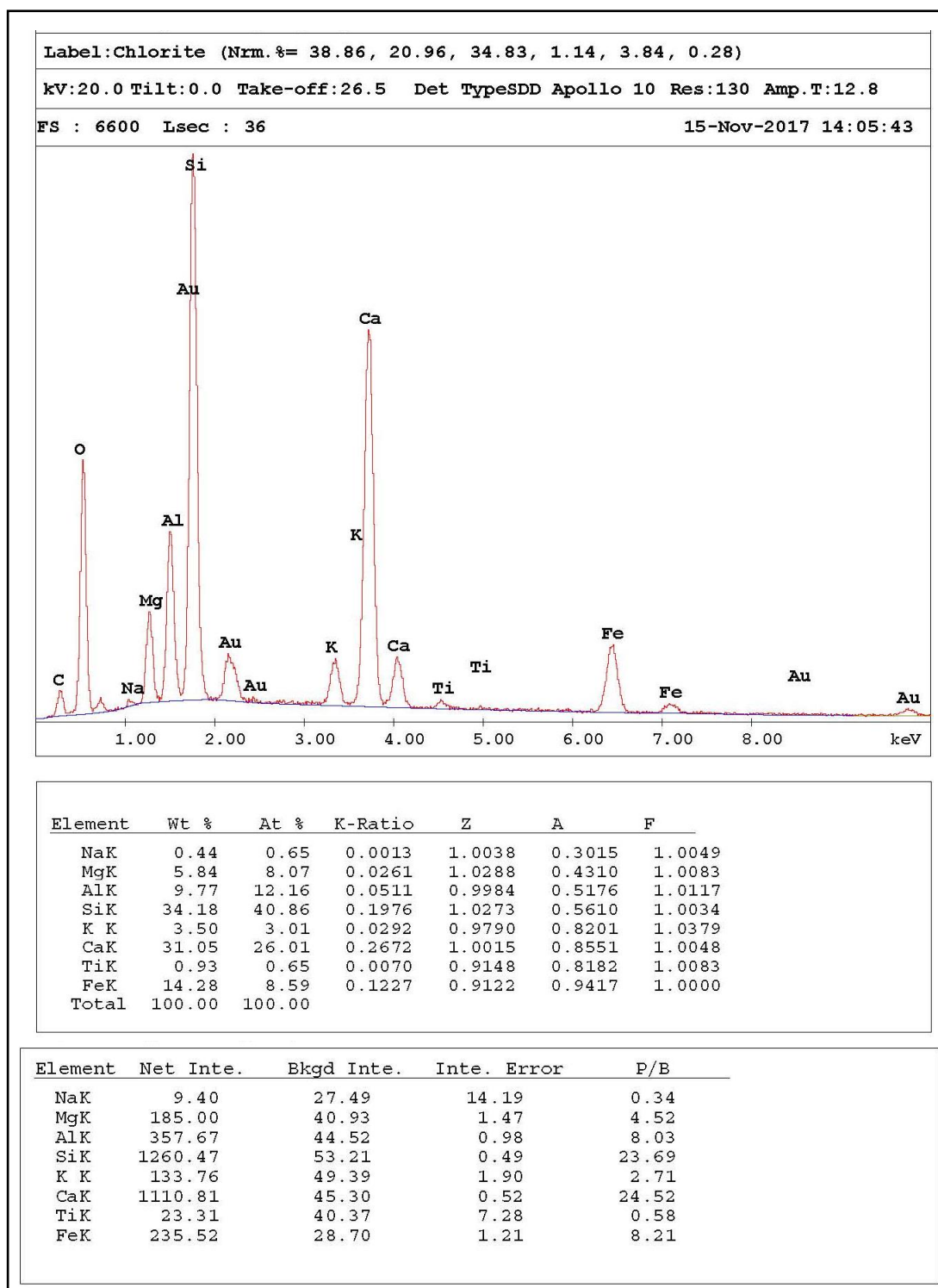


Figure 25: Rock grains with calcite matrix from AK-36, Figure 13 (c)

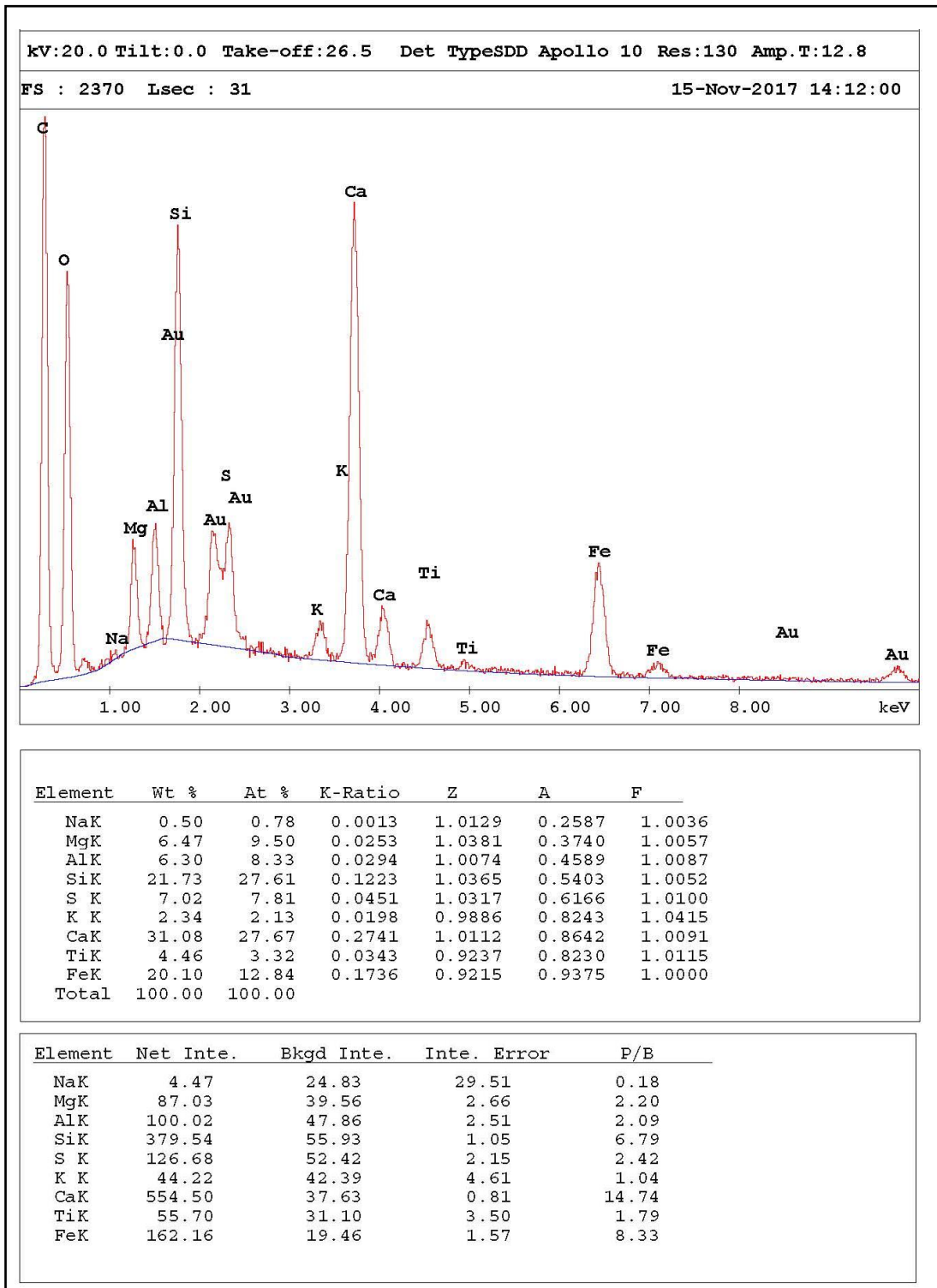


Figure 26: Rock grains with calcite matrix from AK-56, Figure 13 (d)

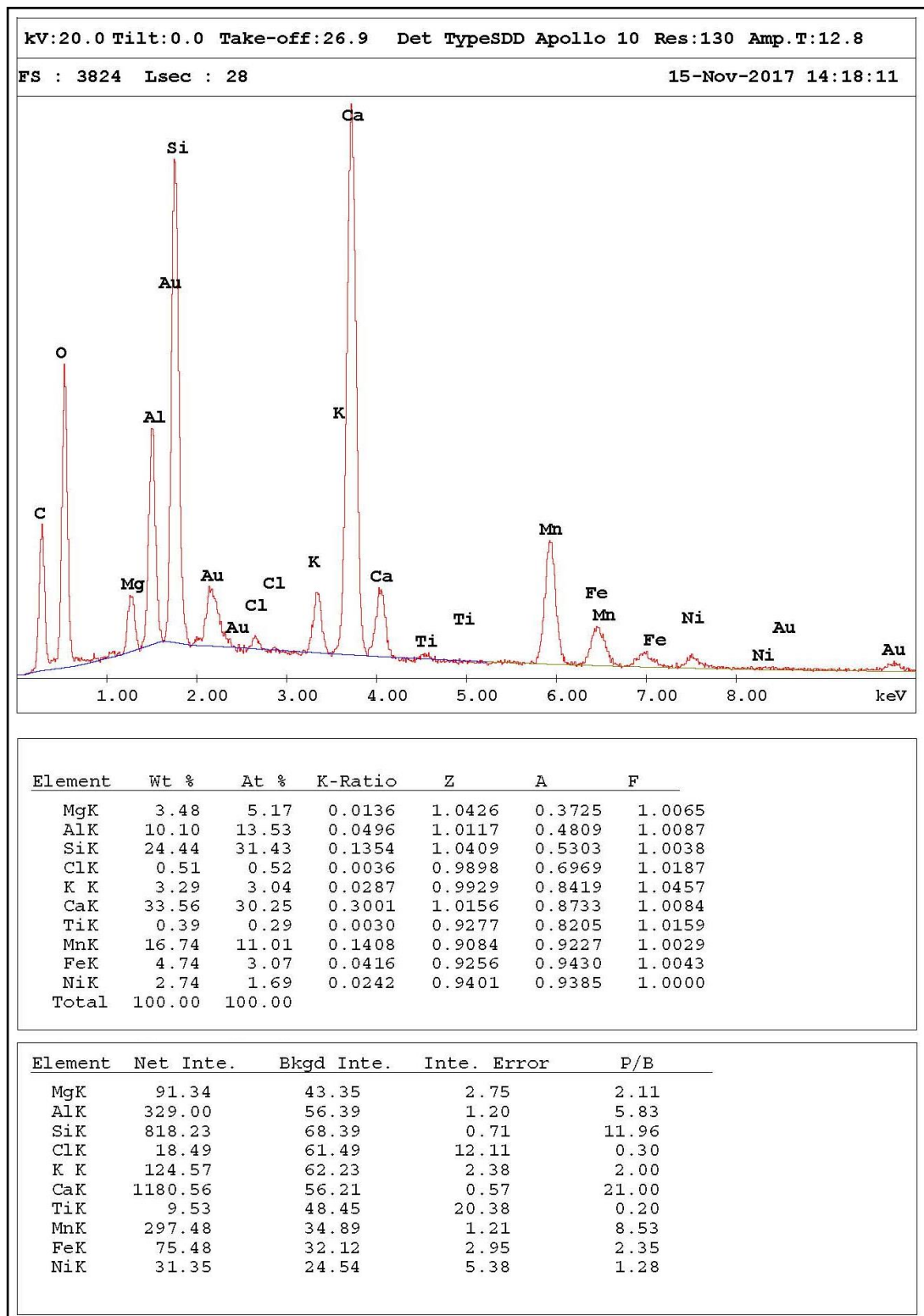


Figure 27: Rock grains with calcite matrix from GÖM-12, Figure 13 (b)

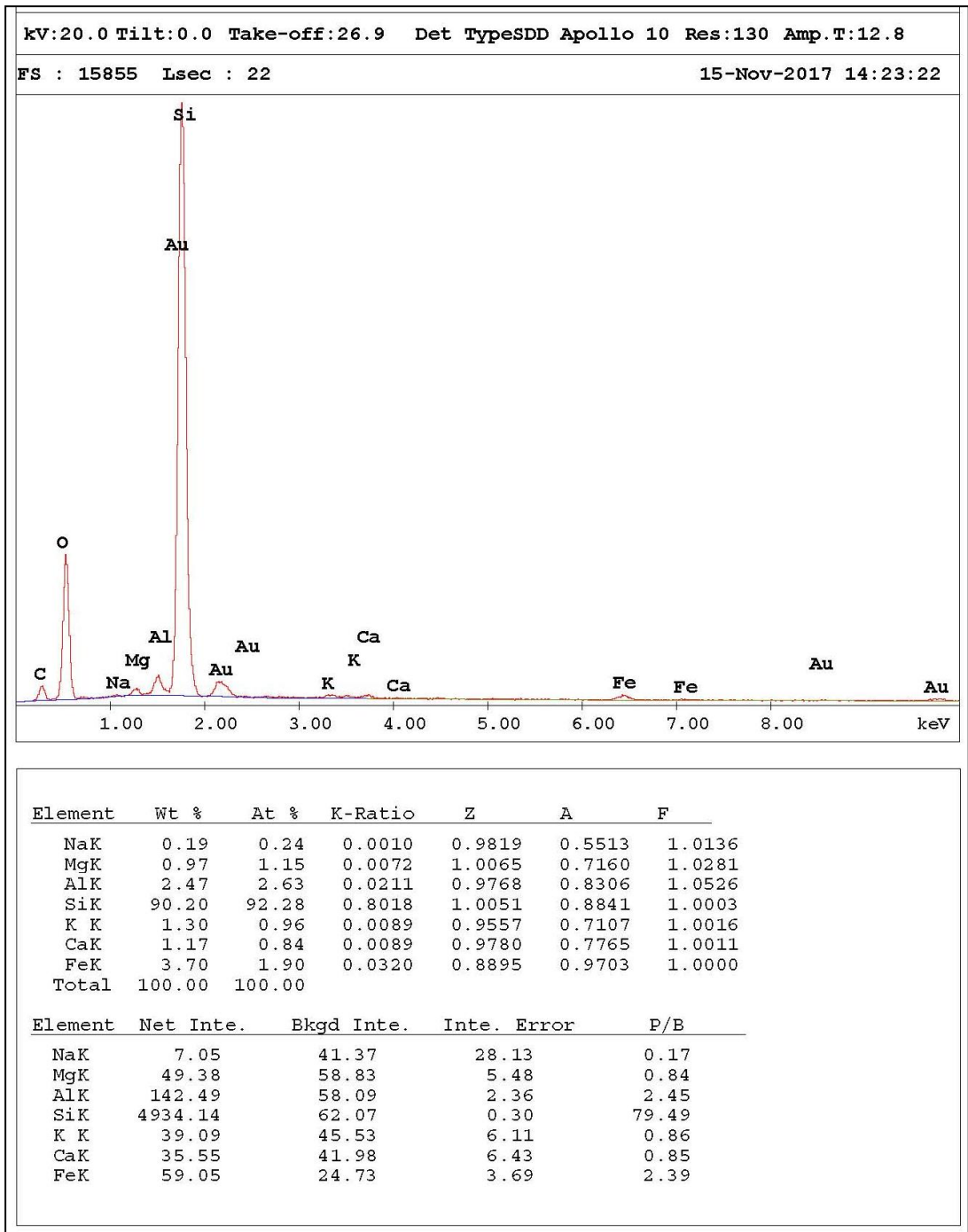
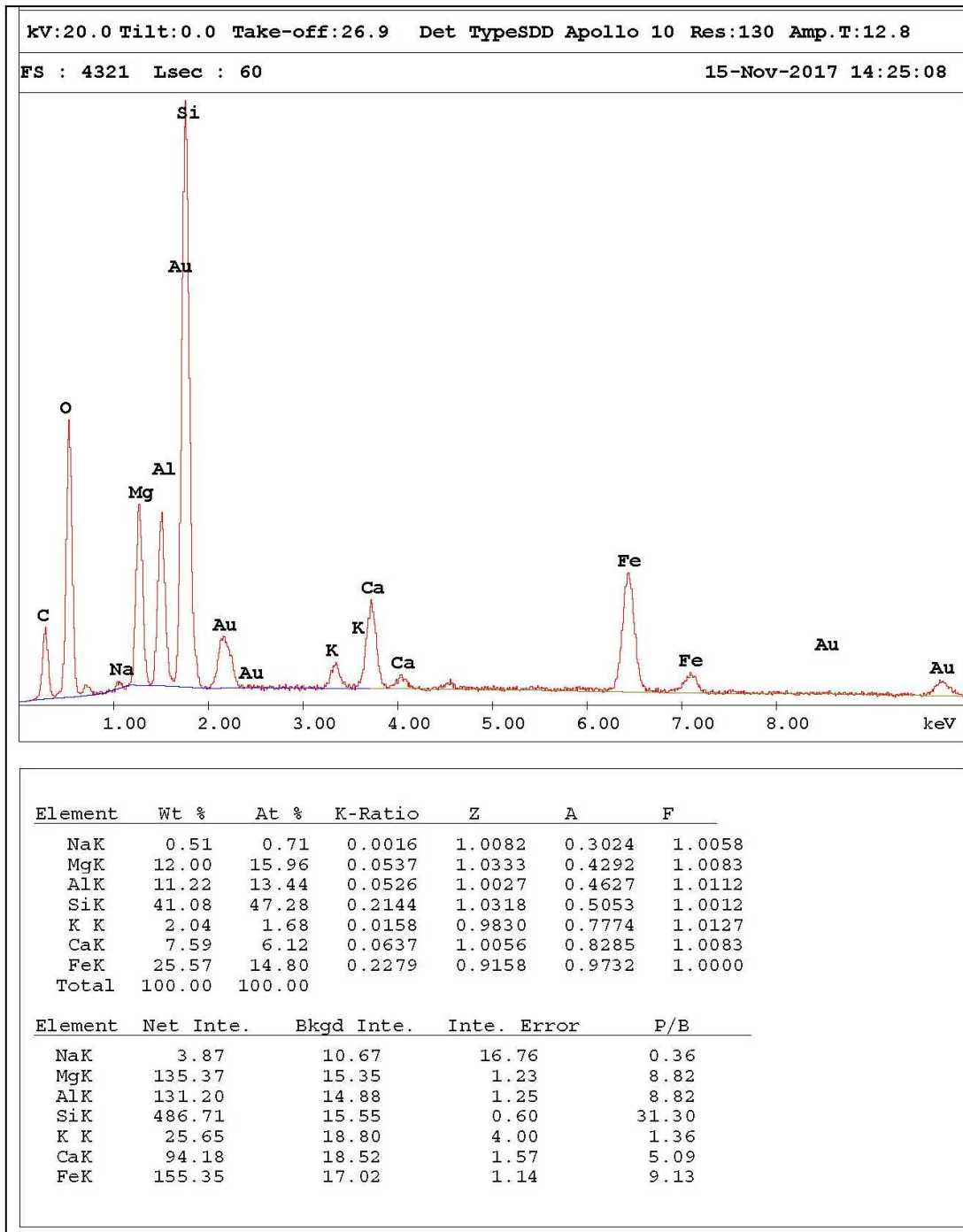


Figure 28: Black rock fragments from GB-30, Figure (a)



**Figure 29:** Quartz grain from GB-30, Figure (a)

## APPENDIX B

### QUANTITATIVE DATA ANALYSES

**Table 3:** Number of planktonic and benthic foraminifera in Gömbe section with %P and calculated depth based on Equation (1)

Sample code	1 <sup>st</sup> counting		2 <sup>st</sup> counting		Average %P	D (m)
	#Planktonic foraminifera	#Benthic foraminifera	#Planktonic foraminifera	#Benthic foraminifera		
<b>göm-2</b>	316	12	314	12	96	<b>1087</b>
<b>göm-6</b>	350	15	346	15	96	<b>1069</b>
<b>göm-11</b>	326	15	326	17	95	<b>1049</b>
<b>göm-12</b>	473	16	479	17	97	<b>1095</b>
<b>göm-17</b>	765	13	752	13	98	<b>1166</b>
<b>göm-18</b>	502	18	507	18	97	<b>1096</b>
<b>göm-19</b>	470	9	473	9	98	<b>1158</b>
<b>göm-20</b>	233	5	233	5	98	<b>1149</b>
<b>göm-21</b>	589	27	590	27	96	<b>1060</b>
<b>göm-22</b>	424	16	430	16	96	<b>1089</b>

**Table 4:** Number of planktonic and benthic foraminifera in Aksu section with %P and calculated depth based on Equation (1)

Sample code	1 <sup>st</sup> counting		2 <sup>st</sup> counting		Average %P	D (m)
	#Planktonic foraminifera	#Benthic foraminifera	#Planktonic foraminifera	#Benthic foraminifera		
is-14	312	235	315	237	57	271
is-19	372	99	388	99	79	598
is-29	332	84	332	84	80	606
is-30	306	67	305	67	82	656
is-31	110	177	110	178	38	140
is-36	656	46	678	46	94	986
is-39	297	67	312	66	83	686
is-40	263	48	263	52	85	717
is-41	299	51	303	51	86	742
is-42	421	28	420	28	94	993
is-46	484	58	479	58	88	822
is-47	479	42	475	42	92	931
is-49	574	37	562	37	93	997
is-50	326	39	326	39	89	849
is-51	592	64	600	64	90	879
is-52	322	43	328	43	88	819
is-56	318	33	326	33	91	891
is-59	276	47	283	47	86	744

## APPENDIX C

### TAXONOMIC NOTES

In order to obtain %P for paleobathymetric reconstructions of the studied basins, a micropaleontological study has been carried out on the benthic foraminifera at species level. Before the calculation of %P, the observed forms were identified and representative ones were photographed and plates were prepared. Plates 1-4 are light microscope pictures, Plates 5-8 are SEM pictures.

The classification is based on morphology of the foraminifera: test shape, suture type, aperture type and ornamentation. are used as taxonomic parameters.

In this chapter, a brief description of the examined forms is given according to literature (see below). Moreover, synonymy lists, which are not the complete lists but are put together from the recent and accessible literature, are provided.

Loeblich and Tappan (1988) was used as the main reference for the generic classification. Moreover, the catalog of Van Morkhoven et al. (1986) was used as the main reference for benthic foraminifer species and their paleobathymetric ranges. More recent studies were taken into account as indicated below.

Chamber arrangement and aperture style are two important morphological features for classification of foraminifers. Principle type of chamber arrangement and aperture style are shown in Figure 30 and Figure 31.

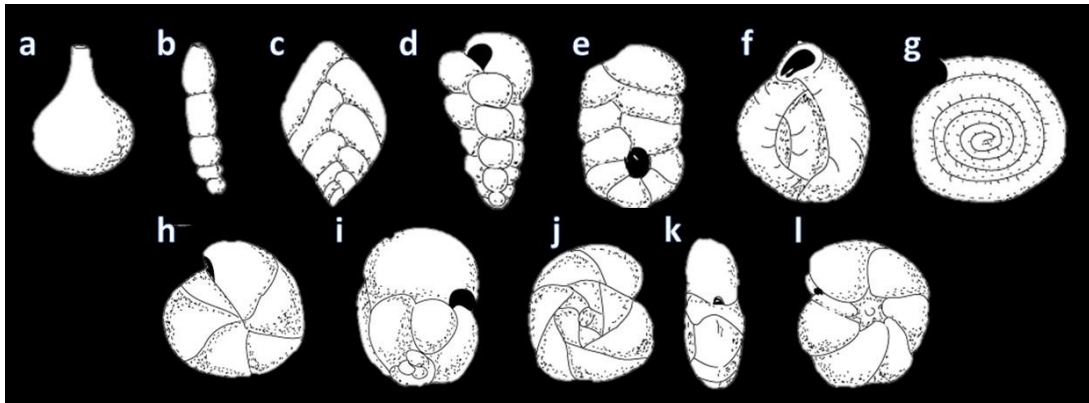


**Figure 30:** Principles types of chamber arrangement. a. single chambered; b. uniserial; c. biserial; d. triserial; e. palnispiral to biserial; f. milioline; g. planispiral evolute; h. planispiral involute; i. streptospiral; j-k-l. trochospiral (Spiral view; side view; umbilical view) (Modified from Loeblich and Tappan, 1964 as cited in Ucl.ac.uk, 2018).

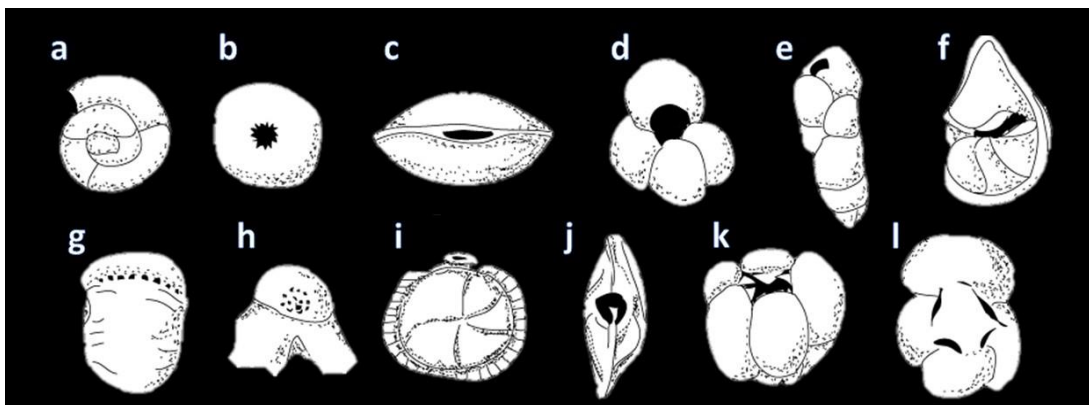


**Figure 31:** Principles types of aperture. a. open end of tube; b. terminal radiate; c. terminal slit; d. umbilical; e. loop shaped; f. interiomarginal; g. interiomarginal multiple; h. areal crbrate; i. with phialine lip; j. with bifid tooth; k. with umbilical teeth; with umbilical bulla (Modified from Loeblich and Tappan, 1964 as cited in Ucl.ac.uk, 2018).

FAMILY BOLIVINIDAE GLAESSNER, 1937

Genus *Bolivina* d'Orbigny, 1839

Type species: *Bolivina plicata* d'Orbigny, 1839

Pl. 4, Fig. 5-7; Pl. 8, Fig. 5-8

**Description:** Test is elongate and ovoid to triangular in outline; broad and biserial chambers; lowest margin of the chambers is retrograde and overlap the previous chambers; wall is calcareous, hyaline and perforate; narrow loop aperture; one margin of the aperture bordered by rim, other one is bordered toothplate (Loeblich and Tappan, 1988).

**Stratigraphy:** Upper Cretaceous to Recent (Loeblich and Tappan, 1988)

FAMILY VAGINULINIDAE REUSS, 1860

Genus *Lenticulina* Lamarck, 1804

Type species: *Lenticulina rotulatus* d'Orbigny, 1804

Pl. 3, Fig. 3

**Description:** Planispiral and lenticular test; chambers are broad and low, slowly increase; last one or two chambers are uncoiled; sutures are curved; aperture radiate and slitlike at the peripheral angle; wall is calcareous and hyaline (Loeblich and Tappan, 1988).

**Stratigraphy:** Triassic to Recent (Loeblich and Tappan, 1988)

FAMILY ROTALIIOAE EHRENBERG, 1839

Genus *Ammonia* Brünnich, 1772

Type species: *Nautilus beccari* Linnaeus, 1758

*Ammonia beccarii* Linnaeus, 1758

Pl. 7, Fig. 2

[for further synonymy before 1988 see Loeblich and Tappan]

1988. *Nautilus beccarii* Linnaeus, Loeblich and Tappan, pl. 479, fig. 2, 3

1988. *Ammonia beccarii* Linnaeus, Jorissen, pl. 2, figs. 5, pl. 5-6.

2000. *Ammonia beccarii* Linnaeus, Den Dulk, pl. 10, figs. 1.

**Description:** Genus *Ammonia* has biconvex with low trochospiral test; wall is calcareous and perforated; interiomarginal extraumbilical arch aperture (Loeblich and Tappan, 1988). *Ammonia beccarii* has nodulated ornamentation on the both side; moreover, sutures are seen like sculptured at the last whorl on the spiral side; Genus *Ammonia beccarii* also differentiated by this feature to other *Ammonia* species (Jorissen, 1988).

**Stratigraphy:** Late Miocene to Recent (Jorissen, 1988).

**Paleobathymetry:** Neritic (Jorissen, 1988).

FAMILY ANOMALINIDAE CUSHMAN, 1927

Genus *Anomalinoides* Brotzen, 1942

Type species: *Anomalinoides plummerae* Brotzen, 1942

Pl. 7, Fig. 5

**Description:** Trochospiral; chambers inflated and sutures are curved on spiral side; sutures are depressed and slightly curved on umbilical side; wall is calcareous, coarsely perforate; aperture is low interiomarginal arch which extends both side with bordered lip (Loeblich and Tappan, 1988).

**Stratigraphy:** Late Cretaceous to Recent (Loeblich and Tappan, 1988)

FAMILY BULIMINIDAE JONES, 1875

Genus *Bulimina* d'Orbigny, 1826

Type species: *Bulimina margarita* d'Orbigny, 1826

Pl. 4, Fig. 8-9; Pl. 4, Fig. 9-10

**Description:** Test is ovate; triserial; maybe later ones are uniserially arranged; depressed and oblique sutures; the wall is calcareous and perforate; aperture is loop shaped on the base of last chamber with rim and tooth plate (Loeblich and Tappan, 1988).

**Stratigraphy:** Upper Cretaceous to Recent (Loeblich and Tappan, 1988).

Genus *Globobulimina* Cushman, 1927

Type species: *Globobulimina pacifica* Cushman, 1927

Pl. 8, Fig. 11-14

**Description:** Genus *Globobulimina* is differentiated from genus *Bulimina* by chamber size which is rapidly increasing and strongly overlapping each other; last chamber completely overlap the preceding ones; loop shaped apertures provided by tooth plate (Loeblich and Tappan, 1988)

**Stratigraphy:** Late Paleocene to Recent (Loeblich and Tappan, 1988).

FAMILY CASSIDULINIDAE D'ORBIGNY, 1839

Genus *Cassidulina* d'Orbigny, 1826

Type species: *Cassidulina laevigata* d'Orbigny, 1826

*Cassidulina laevigata* d'Orbigny, 1826

Pl. 3, Fig. 4; Pl. 7, Fig. 1

1988. *Cassidulina laevigata* d'Orbigny, Loeblich and Tappan, pl. 555, fig. 1-8

1988. *Cassidulina laevigata* d'Orbigny, Jorissen, pl. 1, fig. 8.

1994. *Cassidulina laevigata* d'Orbigny; Gupta, pl. 2, fig. 11.

2000. *Cassidulina laevigata* d'Orbigny; Kouwenhoven, p. 193, pl. 9, fig. 11.

2012. *Cassidulina laevigata* d'Orbigny; Perez and Asensio, fig. 6-N.

**Description:** Hyaline and perforated calcareous wall; surface is smooth and polish; test is slightly elongated; biserial and planisiral enrolling; elongated slit aperture (Loeblich and Tappan, 1988).

**Stratigraphy:** Late Eocene to Recent (Loeblich and Tappan, 1988).

**Paleobathymetry:** Neritic to upper bathal (Kouwenhoven, 2000).

FAMILY CIBICIDIDAE CUSHMAN, 1927

Genus *Cibicides* de Monfort, 1808

Type Species: *Cibicides refulgens* de Monfort, 1808

**Description:** According to Loeblich and Tappan (1988), the genus *Cibicides* has a calcareous and perforate wall. The coiling type is trochospiral with a concave evolute spiral side and a convex involute umbilical side. Low interiomarginal aperture; planoconvex.

Loeblich and Tappan (1988) used as a criterion that being planoconvexity for differentiating between the genera *Cibicides* de Montfort and 1808 from genus *Cibicoides* Thalmann, 1939. Morkhoven et al. (1986) also used the genus *Cibicoides* instead of genus *Cibicides* for biconvex morphotypes. Verhallen (1991) disapproved convexity as a criterion for generic separation. Gupta (1994) postulated that convexity is related to environmental conditions and morphological changes can co-occur with environmental change within a single species. Schweizer (2009) confirmed this notion with molecular results. Schweizer (2009) used the shape of the axial profile, the shape of the sutures, the porosity and the thickness of the wall as morphological criteria. These criteria are followed in this study for distinction of *Cibicides* species. *Cibicides dutemplei*, *C. italicus*, *C. kullenbergi*, *C. pachyderma*, *C. pseudoungerianus*, *C. ungerianus* are described below together with their paleobathymetric ranges.

*Cibicides dutemplei* d'Orbigny , 1846

Pl. 1, Fig. 2; Pl. 5, Fig. 2

**Selected synonymy** [for further synonymy before 1986 see Morkhoven et al. (1986)]

1986. *Cibicoides dutemplei* d'Orbigny; Van Morkhoven et al., pp. 112-113, pl. 35, figs. 1-2.

1994. *Cibicides mexicanus* Nuttall; Gupta, pl. 5, fig. 6.

2000. *Cibicides dutemplei* d'Orbigny; Den Dulk, pl. 7, fig. 2a-b.

2000. *Cibicides dutemplei* d'Orbigny; Kouwenhoven, pl. 2, fig. 2a-c.

2006. *Cibicides dutemplei* d'Orbigny; Schweizer, pl. 12, fig. a.

**Description:** The test of *Cibicides dutemplei* is slightly biconvex; the sutures are imperforate and they border the chambers on the umbilical side; the porosity, which is coarse, can be seen on the spiral side; the wall of *Cibicides dutemplei* is thick and it has generally large size (Schweizer, 2009).

**Stratigraphy:** Early Miocene to Pliocene (Morkhoven et al., 1986).

**Paleobathymetry:** Outer neritic to upper bathyal (Morkhoven et al., 1986).

*Cibicides italicus* Di Napoli Alliata, 1952

Pl. 2, Fig. 3; Pl. 6, Fig. 3

2000. *Cibicides italicus* Di Napoli Alliata; Kouwenhoven, pl. 3, fig. 2a-c.

2006. *Cibicides italicus* Rzehak; Schweizer, pl. 3, fig. a-k.

2009. *Cibicides italicus* Rzehak; Panieri et al., pl. 1, fig. 8, 8a.

**Description:** Planoconvex test; the sutures, which are flush and glassy, can be seen on the spiral side; the porosity, which is coarse, can be seen on the spiral side; the wall of *Cibicides italicus* is glassy and thick (Schweizer, 2006).

**Stratigraphy:** Late Miocene to early Pliocene (Schweizer, 2006).

**Paleobathymetry:** Lower bathyal to abyssal (Schweizer, 2006).

*Cibicides kullenbergi* Parker, 1953

Pl. 2, Fig. 1; Pl. 6, Fig. 1

1991 *Cibicoides kullenbergi* Parker; Corliss, pl. 1, fig. 6, 8, 9.

1994. *Cibicides kullenbergi* Parker; Gupta, pl. 5, fig. 5.
2000. *Cibicides kullenbergi* Parker; Den Dulk, pl. 6, fig. 4a-c.
2000. *Cibicides kullenbergi* Parker; Kouwenhoven, pl. 1, fig. 4a-c.
2006. *Cibicides kullenbergi* Rzehak; Schweizer, pl. 4, fig. a-m.
2009. *Cibicides kullenbergi* Rzehak; Panieri et al., pl. 1, fig. 6, 6a.

**Description:** Biconvex test; additional calcite is observed on the spiral side; the sutures can be seen on the umbilical side, but not on the spiral side due to covering by extra calcite, plug like structure can be seen; the porosity, which is coarse, can be seen on the spiral side; the wall of *Cibicides kullenbergi* is white and thick; it has large size (Schweizer, 2006).

**Stratigraphy:** Late Oligocene to Recent (Schweizer, 2006).

**Paleobathymetry:** Bathyal and abyssal (Schweizer, 2006).

*Cibicides pachyderma* Rzehak, 1886

Pl. 2, Fig. 2; Pl. 6, Fig. 2

[for further synonymy before 1986 see Morkhoven et al. (1986)]

1986. *Cibicidoides pachyderma* Rzehak; Van Morkhoven et al., pp. 68-70, pl. 22, fig. 1a-c.
2000. *Cibicides pachyderma* Rzehak; Kouwenhoven, pl. 2, fig. 1a-c.
2006. *Cibicides pachyderma* Rzehak; Schweizer, pl. 6, fig. a-p.
2007. *Cibicides pachyderma* Rzehak; Rouchy et al., pl. 2, fig. 14-15.
2009. *Cibicides pachyderma* Rzehak; Panieri et al., pl. 1, fig. 7, 7a.

**Description:** Biconvex test; the sutures are imperforate on the umbilical side, also depressed and glassy; and flushed on the spiral side; the porosity, which is coarse, can be seen on the spiral side; the wall of *Cibicides pachyderma* is opaque-white and it has small size (Schweizer, 2006).

**Stratigraphy:** Early Oligocene to Recent (Schweizer, 2006).

**Paleobathymetry:** Upper bathyal (Schweizer, 2006).

*Cibicides pseudoungerianus* Chusman, 1922

Pl. 1, Fig. 4; Pl. 5, Fig. 4

1991. *Cibicides pseudoungerianus* Cushman; Verhallen, pp. 129-136, pl. 16, fig.1-4.

2000. *Cibicides pseudoungerianus* Cushman; Den Dulk, pl. 6, fig. 3a-c.

2000. *Cibicides pseudoungerianus* Cushman; Kouwenhoven, pl. 1, fig. 3a-c.

2006. *Cibicides pseudoungerianus* Cushman; Schweizer, pl. 7, fig. a-p.

**Description:** Biconvex test; the sutures can be seen on umbilical side and the last whorl on spiral side; because there is thick supplementary calcite on the spiral side; as mentioned before, the chamber of *Cibicides ungerianus* can be seen on the spiral side and it is differentiated from *Cibicides pseudoungerianus* by this feature; moreover, on the spiral side, the porosity can be seen coarse; the wall of *Cibicides ungerianus* has a thick and it has medium size (Schweizer, 2006).

**Stratigraphy:** Early Oligocene to Recent (Schweizer, 2006).

**Paleobathymetry:** Neritic to upper bathyal (Schweizer, 2006).

*Cibicides ungerianus* d'Orbigny, 1846

Pl. 1, Fig. 3; Pl. 5, Fig. 3

1991. *Cibicides ungerianus* d'Orbigny; Verhallen, p. 129, pl. 16, figs. 5-9.

2000. *Cibicides ungerianus* d'Orbigny; Den Dulk, pl. 6, fig. 1a-c.

2000. *Cibicides ungerianus* d'Orbigny; Kouwenhoven, pl. 1, fig. 2a-c.

2006. *Cibicides ungerianus* d'Orbigny; Schweizer, pl. 10, fig. a-l.

2007. *Cibicides ungerianus* d'Orbigny; Rouchy et al., pl. 2, fig. 16.

**Description:** Ventro-convex to biconvex; the sutures can be seen on both spiral and umbilical side; *Cibicides ungerianus* is differentiated from *Cibicides pseudoungerianus* according to visibility of the chambers on the spiral side; the porosity is coarse; porosity at the last chamber on the umbilical side is coarser than the spiral side; the wall of *Cibicides ungerianus* is thin and hyaline; it can be seen large size (Schweizer, 2009).

**Stratigraphy:** Miocene to Recent (Schweizer, 2006).

**Paleobathymetry:** Neritic to upper bathyal (Schweizer, 2006).

#### FAMILY GAVELINELLIDAE HOFKER, 1956

Genus *Gyroidina* d'Orbigny, 1826

Type species: *Gyroidina orbicularis* d'Orbigny, 1826

Pl. 3, Fig. 1; Pl. 7, Fig. 4

**Description:** The test is throchospiral; spiral side is evolute and flattened or slightly convex, chamber size gradually increasing, early whorls covered by calcite; umbilical side is convex, sutures are curved; aperture is low interiomarginal slit.

**Stratigraphy:** Many species placing in *Gyroidina* have synonyms in *Gyroidinoides* and *Hansenisca* (Jones 2014). The stratigraphic range of *Gyroidina sp.* is Cretaceous to Recent (Loeblich and Tappan, 1988; Jones 2014).

FAMILY EPISTOMINIDAE WEDEKIND, 1937

Genus *Hoeglundina* Brotzen, 1948

Type species: *Rotalia elegans* d'Orbigny, 1826

*Hoeglundina elegans*

Pl. 3, Fig.2

[for further synonymy before 1986 see Morkhoven et al. (1986)]

1986. *Hoeglundina elegans* d'Orbigny; Van Morkhoven et al., pp. 99, pl.29, fig. 1,2.

1988. *Hoeglundina elegans* d'Orbigny, Loeblich and Tappan, pl. 478, fig. 1-5

1994. *Hoeglundina elegans* d'Orbigny; Bolli et al., pl. 55, fig. 6-9

**Description:** Test is biconvex; early trochospiral coiling, later planispiral and evolute; wall is aragonitic, perforate and surface is very smooth (Loeblich and Tappan, 1988). Chambers are triangular and straight on umbilical side, while rectangular and curved on spiral side; primary aperture is small (as cited in Van Morkhoven et al, 1986, Loeblich and Tappan, 1988).

**Stratigraphy:** Late Eocene to Pliostocene (Van Morkhoven et al, 1986).

FAMILY ORIDORSALIDAE LOEBLICH AND TAPPAN, 1984

Genus *Oridorsalis* Andersen, 1961

Type species: *Oridorsalis westi* Andersen, 1961

*Oridorsalis stellatus* Silvestri, 1898

Pl. 7, Fig. 3

1984. *Oridorsalis stellatus* Silvestri; Jonkers, p. 165, pl. 5, fig 4a, b.

1990. *Oridorsalis stellatus* Silvestri; Sprovieri and Hasegawa, p. 456, pl. 2, fig 1-3.

1999. *Oridorsalis stellatus* Silvestri; Iaccarino et al., p. 214, pl. 1, fig 5,6

2000. *Oridorsalis stellatus* Silvestri; Kouwenhoven, p. 187, pl. 6, figs. 2.

**Description:** Test of *Oridorsalis stellatus* is biconvex; it is trochospiral coiling and four to five chambers are seen in the final whorl on the spiral side; periphery is round and broad; aperture type is interiomarginal slit (Jonkers, 1984). Genus *Oridorsalis stellatus* is morphologically very close to genus *Oridorsalis umbonatus*, some of difference caused by environmental change (Kouwenhoven, 2000).

**Stratigraphy:** Oligocene to Recent (Bolli et al., 1994; Jones, 1994).

**Paleobathymetry:** Middle abyssal and more (Kouwenhoven, 2000).

FAMILY PLANULINIDAE BERMUDEZ, 1952

Genus *Planulina* d'Orbigny, 1826

Type species: *Planulina ariminensis* d'Orbigny, 1826

*Planulina ariminensis*

Pl. 1, Fig. 1; Pl. 5, Fig. 1

[for further synonymy before 1986 see Morkhoven et al. (1986)]

1986. *Planulina ariminensis* d'Orbigny; Van Morkhoven et al., pp. 38, pl.10, fig. 1-4.

2000. *Planulina ariminensis* d'Orbigny; Kouwenhoven, p. 189, pl. 7, fig. 4.

2007. *Planulina ariminensis* d'Orbigny; Rouchy et al., pl. 3, fig. 2.

2012. *Planulina ariminensis* d'Orbigny; Milker and Schmiedl, fig. 24. 3,4.

**Description:** *Planulina ariminensis* has a perforated calcareous wall; outline of the test is generally circular and test is compressed and keeled; it is low trochospiral; evolute on the spiral side and slightly evolute on the umbilical side; it is characterized by that imperforate and thick sutures are bordered low and broad chambers; aperture type of *Planulina ariminensis* is an equatorial and interiomarginal slit which extends to umbilical side; lip borders to aperture (Van Morkhoven et al., 1986; Loeblich and Tappan, 1988)

**Stratigraphy:** Late Miocene to Pleistocene (Van Morkhoven et al., 1986).

**Paleobathymetry:** Outer neritic to 800m. (Van Morkhoven et al., 1986).

#### FAMILY SIPHONINIDAE CUSHMAN, 1927

Genus *Siphonina* Reuss, 1850

Type species: *Siphonina fimbriata* Reuss, 1850

= *Rotalina reticula* Czjzek, 1848

*Siphonina reticula* Czjzek, 1848

Pl. 2, Fig. 4; Pl. 6, Fig. 4

2000. *Siphonina reticula* Czjzek; Kouwenhoven, p. 187, pl. 6, figs. 3.

2007. *Siphonina reticula* Czjzek; Rouchy et al., pl. 3, fig. 8,9.

2009. *Siphonina reticula* Czjzek; Panieri et al., pl. 1, fig. 5.

2012. *Siphonina reticula* Czjzek; Milker and Schmiedl, fig. 23. 24-26.

**Description:** *Siphonina reticula* perforated calcareous wall; test is trochospiral and biconvex, but convexity of sides are not equal to each other; surface is smooth on both sides and sutures are thick on the spiral side while depressed on the umbilical side; lenticular test is keeled at the periphery; its aperture on the short neck, which is bordered by lip, characterizes *Siphonina reticula* (Milker and Schmiedl, 2012).

**Stratigraphy:** Miocene to Recent (Kouwenhoven, 2000).

**Paleobathymetry:** 500 m and more. (Kouwenhoven, 2000).

#### FAMILY UVIGERINIDAE HAECKEL, 1894

Genus *Uvigerina* d'Orbigny, 1826

Type species: *Uvigerina pygmaea* d'Orbigny, 1826

Pl. 4, Fig. 1-4; Pl. 8, Fig. 1-4

**Description:** According to Loeblich and Tappan (1988), genus *Uvigerina* has calcareous and perforate wall. Test of *Uvigerina* is elongate and triserial. Surface of the test can be costae or spine. Genus *Uvigerina* is characterized by its aperture on a neck. Generally, aperture is bordered by phialine lip and tooth-plate can be recognized inside of the aperture in detailed view (Schweizer, 2006).

**Stratigraphy:** The stratigraphic range of *Uvigerina sp.* is Late Eocene to Recent (Loeblich and Tappan, 1988).

FAMILY BAGGINIDAE CUSHMAN, 1927

Genus *Valvulineria* Cushman, 1926

Type species: *Valvulineria californica* Cushman, 1926

Pl. 8, Fig. 15-16

**Description:** Test is rounded; chambers are trochospirally arranged; chamber size gradually increases; spiral side flattened, umbilicus side is depressed; sutures are curved; wall is calcareous and perforate; aperture is an interiomarginal, extraumbilical arch (Loeblich and Tappan, 1988)..

**Stratigraphy:** The stratigraphic range of *Valvulineria sp.* is Paleocene to Recent (Loeblich and Tappan, 1988).

## **APPENDIX D**

### **PLATES AND EXPLANATIONS**

## PLATE 1

1. *Planulina ariminensis* d'Orbigny

(umbilical/side/spiral view of the same individual, IS-36 )

2. *Cibicides dutemplei* d'Orbigny

(spiral/side/umbilical view of the same individual, IS-19)

3. *Cibicides ungerianus* d'Orbigny

(spiral/side/umbilical view of the same individual, IS-39 )

4. *Cibicides pseudoungerianus* Chusman

(umbilical/side/spiral view of the same individual, IS-39)

Plate 1: ULM images with scale bar indicating 100  $\mu$ m



## PLATE 2

1. *Cibicides kullenbergi* Parker

(umbilical/side/spiral view of the same individual, IS-42)

2. *Cibicides pachyderma* Rzehak

(umbilical/side/spiral view of the same individual, IS-41 )

3. *Cicides italicus* Di Napoli

(umbilical/side/spiral view of the same individual, IS-52)

4. *Siphonina reticula* Czjzek (IS-40)

Plate 2: ULM images with scale bar indicating 100  $\mu\text{m}$

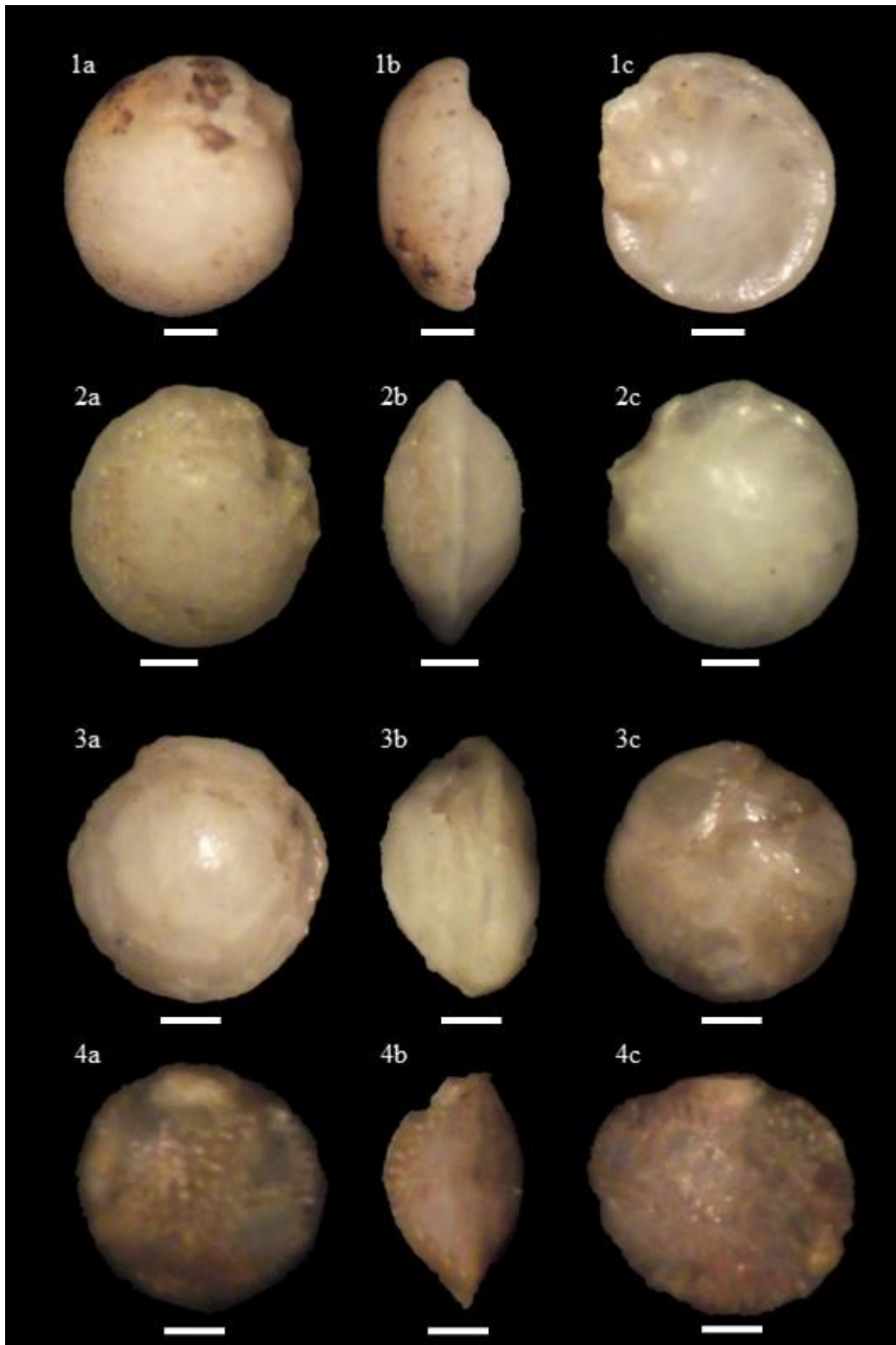


### PLATE 3

1. *Gyroidina* spp.  
(spiral/side/umbilical view of the same individual, IS-31)
  
2. *Hoeglundina elegans*  
(spiral/side/umbilical view of the same individual, GOM-17)
  
3. *Lenticulina* sp. (GOM-2)
  
4. *Cassidulina laevigata* d'Orbigny (IS-52)

Plate 3: ULM images with scale bar indicating 100  $\mu$ m

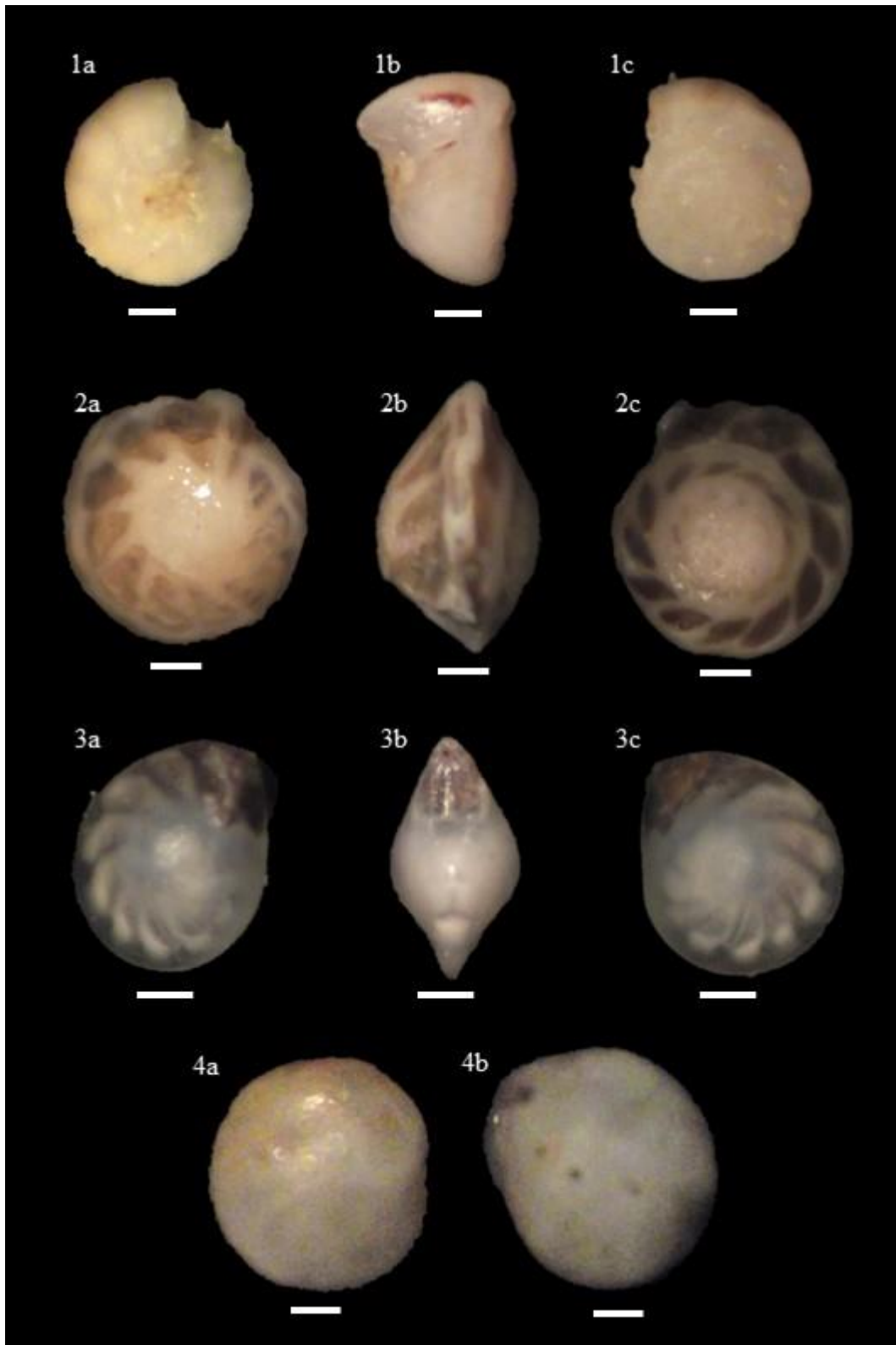


## PLATE 4

1-4. *Uvigerina* sp. (IS-14; IS-19; GOM-2; GOM-17)

5-7. *Bolivina* sp. (IS-36; IS-36; IS-39)

8-9. *Bulimina* spp. (IS-36; IS-36)

Plate 4: ULM images with scale bar indicating 100  $\mu$ m



## PLATE 5

1. *Planulina ariminensis* d'Orbigny

(umbilical, IS-41; side, IS-39; spiral, IS-36)

2. *Cibicides dutemplei* d'Orbigny

(spiral, IS-14; side, IS-14; umbilical, IS-19)

3. *Cibicides ungerianus* d'Orbigny

(spiral, IS-46; side, IS-46; umbilical, IS-39 )

4. *Cibicides pseudoungerianus* Chusman

(spiral, IS-46; side, IS-39; umbilical, IS-39)

Plate 5: SEM images with scale bar indicating 100  $\mu\text{m}$

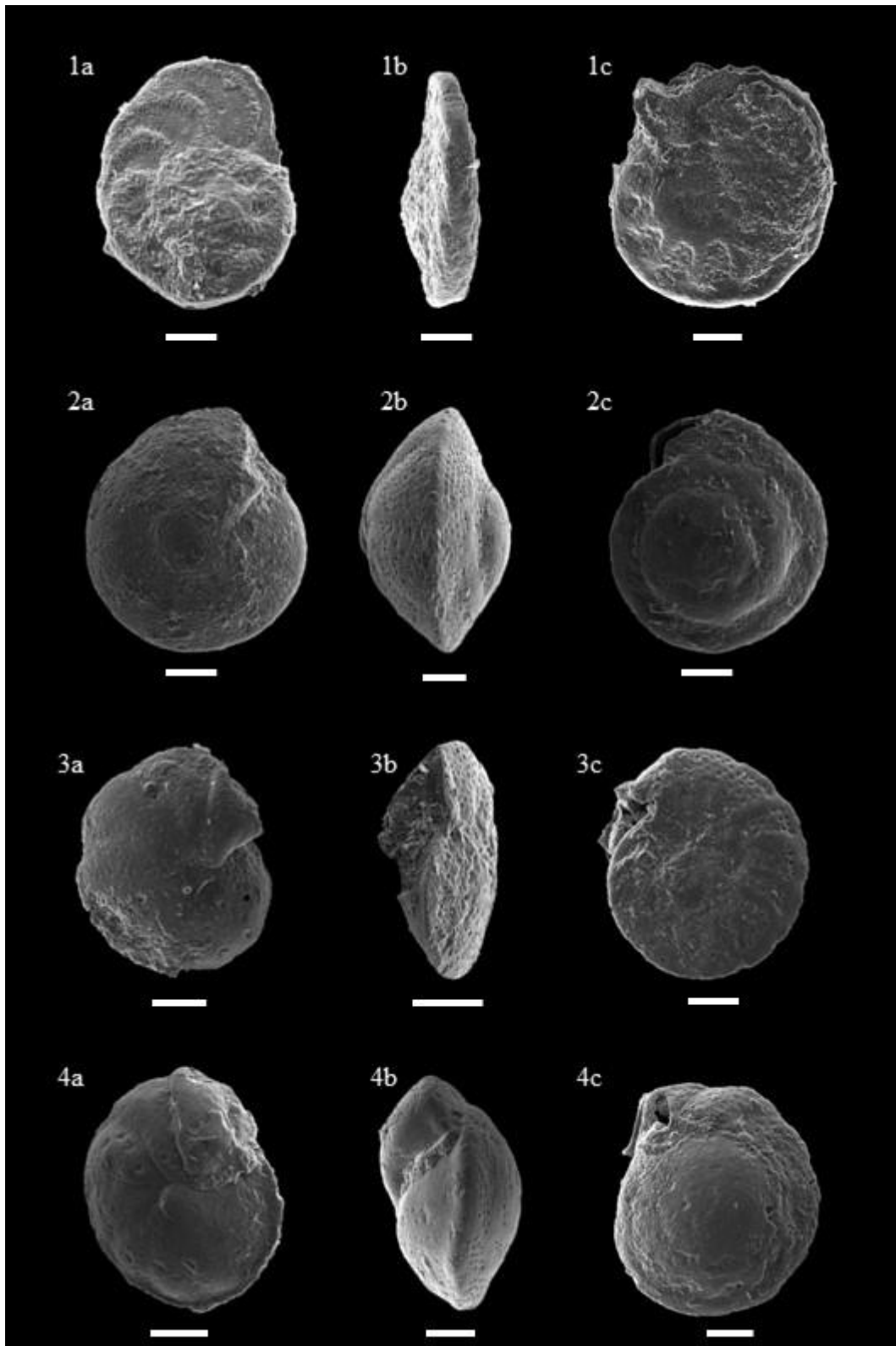


## PLATE 6

1. *Cibicides kullenbergi* Parker

(umbilical, IS-56, side, IS-42; spiral, IS-56)

2. *Cibicides pachyderma* Rzehak

(umbilical, IS-40 /side, IS-41/spiral, IS-40)

3. *Cicides italicus* Di Napoli

(umbilical, IS-52; side, GOM-17; spiral, GOM-17)

4. *Siphonina reticula* Czjzek (GOM-18; IS-40)

Plate 6: SEM images with scale bar indicating 100  $\mu\text{m}$

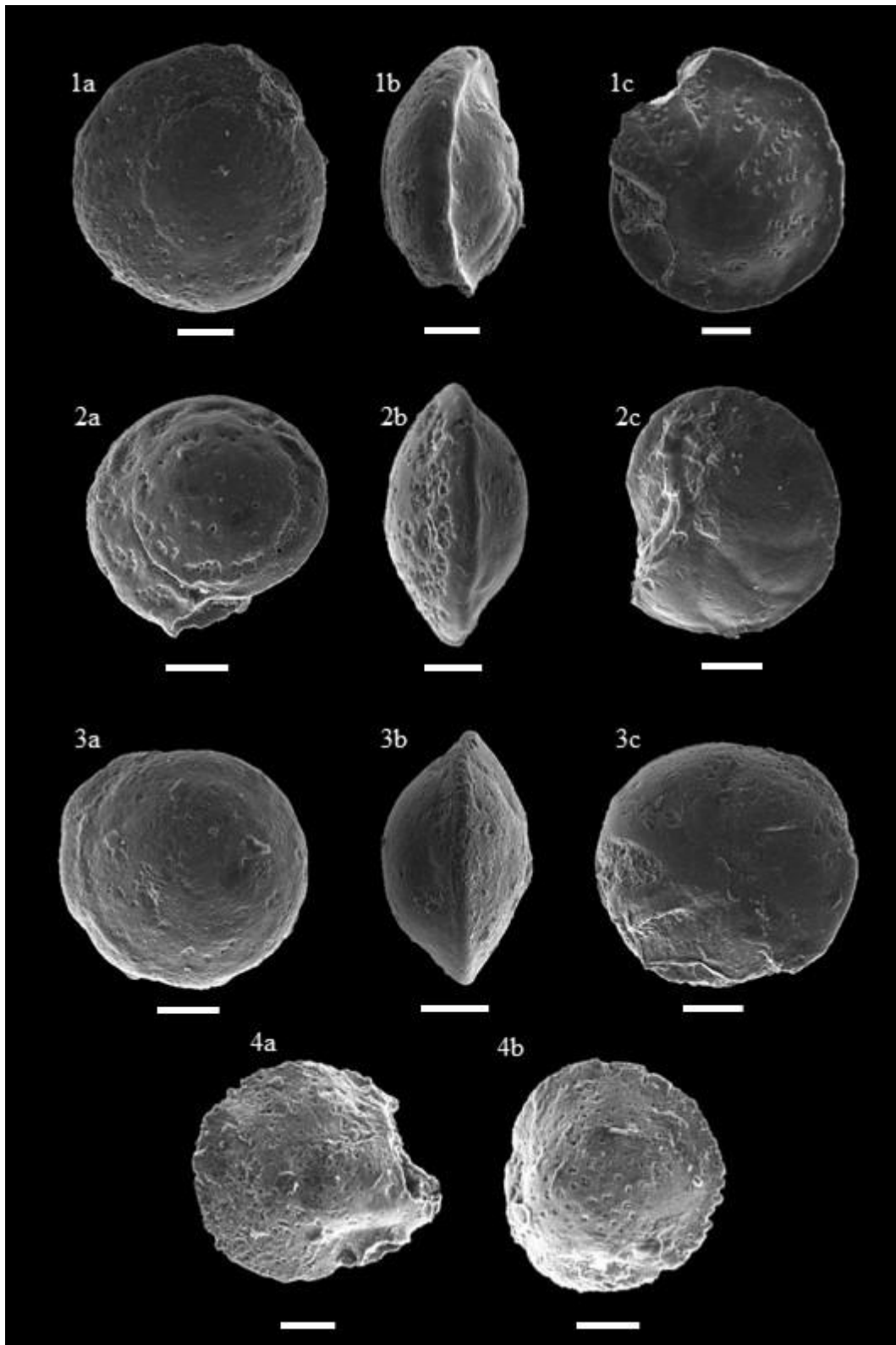


## PLATE 7

1. *Cassidulina laevigata* d'Orbigny (IS-52; IS-52; IS-51)
2. *Ammonia beccarii* Linnaeus (IS-14)
3. *Oridorsalis stellatus* Silvestri (spiral, IS-42; umbilical, IS-49)
4. *Gyroidina* sp. (IS-31; IS-31; IS-19)
5. *Anomalinoides* sp. (spiral, IS-49; side, IS-49; umbilical, IS-49)

Plate 7: SEM images with scale bar indicating 100  $\mu\text{m}$

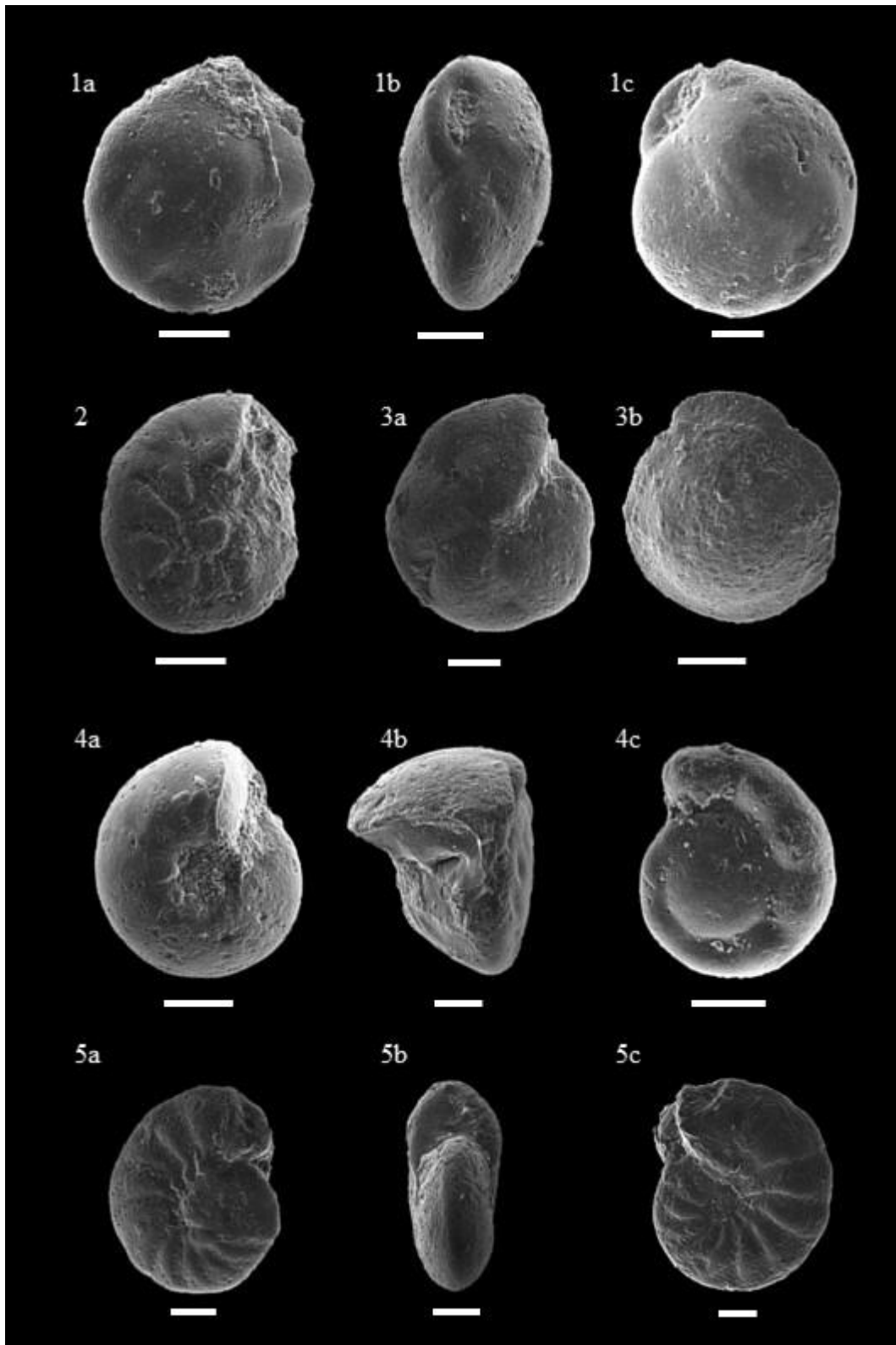


## PLATE 8

1-4. *Uvigerina* sp. (IS-14; IS-19; GOM-2; GOM-17)

5-8. *Bolivina* sp. (IS-36; IS-36; GOM-17- IS-39)

9-10 *Bulimina* spp. (IS-46; IS-49)

11-14. *Globobulimina* spp. (IS-46; IS-49)

15. *Valvulineria* sp (umbilical view, IS-36)

16. *Valvulineria* sp (spiral view, IS-36)

Plate 8: SEM images with scale bar indicating 100  $\mu\text{m}$

